Improving Loss Estimation for Woodframe Buildings

Volume 1: Report

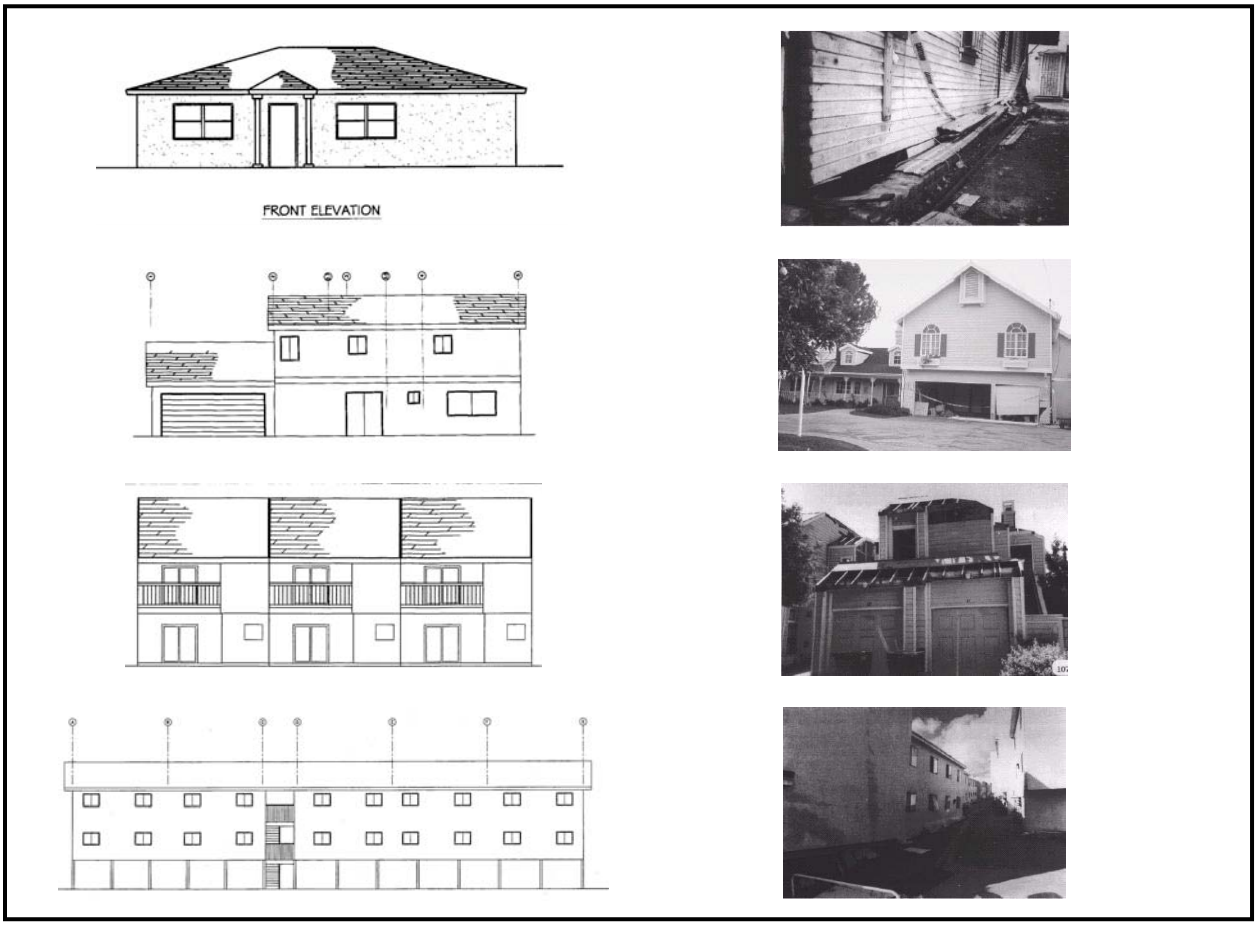

CUREE-Caltech Woodframe Project

Element 4, Economic Aspects

May 2002

Improving Loss Estimation for Woodframe Buildings
Volume 1: Report

Final Report of Tasks 4.1 and 4.5 of the CUREE-Caltech Woodframe Project

May 2002

By K.A. Porter, J.L. Beck, H.A. Seligson, C.R. Scawthorn, L.T. Tobin, R. Young, and T. Boyd

Published by the Consortium of Universities for Research in Earthquake Engineering, Richmond, CA

Report sponsored by the Federal Emergency Management Agency and the California Governor's Office of Emergency Services. Administered by the Consortium of Universities for Research in Earthquake Engineering for the California Institute of Technology.

Cover photographs by Ben Schmid, Los Angeles Department of Building and Safety, and Bob Powell, are used with permission from the Earthquake Engineering Research Institute.

Improving Loss Estimation for Woodframe Buildings

Keith A. Porter and James L. Beck
California Institute of Technology, Pasadena, California

Hope A. Seligson and Charles R. Scawthorn
EQE International, Oakland, California

L. Thomas Tobin
Tobin & Associates, Mill Valley, California

Ray Young and Tom Boyd
Young & Associates, Los Angeles, California

Abstract

This report documents Tasks 4.1 and 4.5 of the CUREE-Caltech Woodframe Project. It presents a theoretical and empirical methodology for creating probabilistic relationships between seismic shaking severity and physical damage and loss for buildings in general, and for woodframe buildings in particular. The methodology, called assembly-based vulnerability (ABV), is illustrated for 19 specific woodframe buildings of varying ages, sizes, configuration, quality of construction, and retrofit and redesign conditions. The study employs variations on four basic floorplans, called index buildings. These include a small house and a large house, a townhouse and an apartment building. The resulting seismic vulnerability functions give the probability distribution of repair cost as a function of instrumental ground-motion severity. These vulnerability functions are useful by themselves, and are also transformed to seismic fragility functions compatible with the HAZUS software.

The methods and data employed here use well-accepted structural engineering techniques, laboratory test data and computer programs produced by Element 1 of the CUREE-Caltech Woodframe Project, other recently published research, and standard construction cost-estimating methods. While based on such well established principles, this report represents a substantially new contribution to the field of earthquake loss estimation. Its methodology is notable in that it calculates detailed structural response using nonlinear time-history structural analysis as opposed to the simplifying assumptions required by nonlinear pushover methods. It models physical damage at the level of individual building assemblies such as individual windows, segments of wall, etc., for which detailed laboratory testing is available, as opposed to two or three broad component categories that cannot be directly tested. And it explicitly models uncertainty in ground motion, structural response, component damageability, and contractor costs. Consequently, a very detailed, verifiable, probabilistic picture of physical performance and repair cost is produced, capable of informing a variety of decisions regarding seismic retrofit, code development, code enforcement, performance-based design for above-code applications, and insurance practices.

Executive Summary

Introduction

Housing in the United States is mostly woodframe, which has proven in recent earthquakes to be subject to unacceptable damage. Practical seismic risk-mitigation measures are available. Possible measures include stricter, more frequent inspections to ensure high-quality construction; adding foundation bolts and structural sheathing to unbraced unbolted cripple walls; adding structural sheathing to increase the strength and stiffness of new construction above that required by current codes; and installing new shearwalls or moment frames at soft stories such as tuck-under parking in apartment buildings.

The challenge to implementing these measures is in deciding which ones are cost-justified. Their up-front costs are readily estimated by construction contractors, but to assess their benefit requires knowledge of how the home will perform in a future earthquake with and without the measure. This in turn requires three pieces of information: (1) the seismic hazard, i.e., how frequently earthquakes will occur and how severe will be their motions), (2) the as-is seismic vulnerability of a building, i.e., how severe will be the damage and loss to the building, as a function of ground-motion severity, and (3) the building's what-if seismic vulnerability, i.e., the relationship between loss and ground-motion severity *with* the mitigation measure.

Thanks to efforts by the US Geological Survey, the California Geological Survey, and others, seismic hazard information is readily available for the entire country; it is the other two pieces of information that are lacking. The problem is that seismic vulnerability functions from historical loss data typically lack the resolution to distinguish between detailed as-is and what-if conditions. Also, most other currently available methods rely heavily on expert opinion, which can be seen as weakening the conclusions of studies that rely on them. The methodology employed by HAZUS suffers somewhat from both shortcomings. Although it is an advanced approach that employs structural analysis and extensive empirical data, it is category-based, cannot distinguish the effects of detailed mitigation measures, and relies to a significant extent on expert opinion. For the present study, which seeks to assess the seismic vulnerability of 19 particular woodframe dwellings, a new methodology was necessary.

Selection of Methodology

The approach employed here is called assembly-based vulnerability (ABV). It uses well-accepted principles of structural modeling, nonlinear time-history structural analysis, component reliability information from laboratory tests, and standard construction cost-estimation principles. These analytical elements are combined in a probabilistic

framework to reflect important uncertainties in the loss estimate, including uncertainties in ground motion, structural characteristics, component damageability, and construction and repair costs. The ABV framework is straightforward and conceptually similar to methodologies developed in various forms since the 1960s, including that of HAZUS, but novel in its degree of detail, avoidance of expert opinion, and manner and extent to which it treats uncertainty.

Summary of Methodology

ABV is implemented using a process called Monte Carlo simulation. It works as follows. First, the building is modeled as a unique collection of standard assemblies, each of which is a collection of building materials constructed into a recognizable component, such as a gypsum wallboard partition, a floor diaphragm, a shearwall, etc.

A structural model of the building is created that reflects best-estimate mass, damping, and force-deformation characteristics. Uncertainties in each parameter are quantified, and a number of simulations of the model are created, reflecting the probability distribution of each structural parameter. An historical or simulated ground-motion recording is selected at random from a number of available records and scaled to a level of shaking severity of interest, with due consideration of scaling limits. The ground motions proposed for the SAC Steel Project are used here and scaled based on the damped elastic spectral acceleration at the building's small-amplitude fundamental period of vibration (S_a). The ground motion is paired with one of the simulated structural-analysis models, and a nonlinear time-history structural analysis is performed to estimate the deformations, accelerations, and other engineering parameters of the structure's response to the ground motion.

These structural responses are then used to simulate damage to each assembly in the building. This works as follows. Each damageable assembly in the building is associated with a set of fragility functions, which are relationships that provide the probability that the assembly will be damaged in some predefined way, as a function of structural response. These fragility functions are highly specific, for example distinguishing between the damageability of walls that differ in finish, framing, sheathing, or fastening. Test data developed for the CUREE-Caltech Woodframe Project, as well as other experimental information, are used to create these fragility functions. For each simulation, the structural response to which each assembly is subjected is input to the fragility function, giving a failure probability. A damage state is then simulated in a manner consistent with the calculated failure probability. This produces a simulated damage state for every assembly in the building, i.e., a snapshot of the building's damaged state: which windows are cracked, which walls need repair, etc.

Construction costs to repair these damaged assemblies are estimated using standard construction cost-estimation principles by a professional cost estimator. Uncertainty on these costs is accounted for. The total repair cost is calculated by summing the number

of damaged assemblies of each type times the cost per repair. Uncertain contractor overhead and profit is added, resulting in a single simulation of total repair cost at a given level of seismic shaking severity.

Thus, each ABV simulation produces a snapshot of the ground motion, the forces and deformations in every structural element, the damage to every assembly, and the cost charged by the contractor perform the repairs on an assembly-by-assembly basis. The process is repeated many times at the given level of shaking severity, S_a, to estimate a probability distribution of cost given S_a, and then repeated at many levels of S_a to compile the probabilistic seismic vulnerability function.

The vulnerability function resulting from the ABV analysis is convolved with the seismic hazard to determine expected annualized loss, which is then used to calculate the present value of future earthquake losses, for a given planning period and discount rate. This process is repeated to calculate the present value of future losses under as-is and a variety of what-if, risk-mitigation, measures. The reduction in present value of future loss from as-is to what-if conditions is the benefit of the risk-mitigation measure. This process is illustrated using the seismic hazard for a single location, but one could readily repeat it for any location using the seismic vulnerability functions presented here along with the seismic hazard from the US Geological Survey or others.

There are some other useful products of the ABV analysis. One can quantify the uncertainty in the damage factor (defined as the repair cost divided by the building replacement cost) as a function of shaking severity or versus the expected value of the damage factor. One can examine the contribution to overall loss by assembly type, or floor, or any grouping of interest. One can relate loss to structural response, for example, expressing it as a function of interstory drift, and quantify the probability of reaching or exceeding performance levels that are defined in terms of physical damage.

Conclusions and Recommendations

The ABV methodology is employed to evaluate the vulnerability of 19 woodframe buildings to ground shaking. (Ground failures such as landsliding and liquefaction are not considered, nor are other secondary effects such as water damage from broken pipes.) The study produced probabilistic seismic vulnerability functions for each building, treating important sources of uncertainty and producing HAZUS-compatible fragility functions. The seismic vulnerability functions generally agree with past earthquake experience documented by previous investigators of the 1971 San Fernando, 1983 Coalinga, and 1994 Northridge Earthquakes.

The study finds that construction quality makes a significant difference in seismic vulnerability, typically changing loss by 50% or more relative to the typical case. Five of seven mitigation measures examined make a significant difference in future damage. Bracing cripple walls, designing stiffness and strength to above-code levels, and adding

steel frames or structural sheathing to soft stories all reduce seismic vulnerability by up to an order of magnitude or more at certain levels of strong shaking. No significant reduction in seismic vulnerability was detected for two of the redesign measures, namely, adding structural sheathing to spandrel beams ("waist walls") and designing based on an assumption of a rigid diaphragm. The five effective loss-reduction measures can reduce loss on the order of 5% to 25% of the building replacement cost, depending on shaking severity.

It is found that the loss given a particular level of shaking severity can often but not always be approximated by a lognormal probability distribution, with a logarithmic standard deviation between 0.6 and 1.4. Uncertainty in loss more strongly correlates with mean damage than with shaking severity. It is found that line-of-sight costs (the painting of an entire room or wall when only a portion of the room or wall is damaged) are substantial, contributing up to half the total repair costs at a given level of shaking. The costs associated with window breakage is very small.

A thorough probabilistic risk study was not a part of this study. Such study would consider the likelihood of various levels of shaking severity as well as seismic vulnerability, for a wide range of geographic locations. However, a sample of such as study is performed for each these buildings, considering the seismic hazard at a single site.

In the sample risk study, it is found that the construction quality of these buildings can affect the present value of future losses by a factor of two or more, relative to the typical-quality case. The future annualized repair cost (i.e., the constant yearly payment equivalent to the uncertain future repair costs) varies from less than $10 per year for the most rugged building, to more than $500 per year for the most vulnerable. Expressed in present-value terms, these uncertain future costs equate with an up-front, one-time cost varying from less than $100 to more than $20,000. These are substantial differences that could realistically affect a home-buyer's purchasing decision if he or she were aware of and trusted the cost estimate.

This hypothetical home-buyer might also think twice about buying or not retrofitting a house if he or she believed that the probability of its collapsing from its foundation and consequently being red-tagged were nearly 1 in 5 during the coming 10 years (as is the case with the poor-quality variant of the small house), and more than 50% in a realistic planning scenario.

Besides influencing home-buyers' purchasing and retrofit decisions, the results developed here could offer a quantifiable basis for performance-based design and code development; quantification of the effects of various insurance claims-adjustment practices; similar quantification of the effects of various levels of building inspection and code enforcement; and identification of the most important contributors to uncertainty.

The detailed methodology and vulnerability functions developed in this study are a significant step forward in the practice of loss estimation and risk management, and can serve as a foundation upon which to build a diverse set of detailed and scientifically robust probabilistic seismic vulnerability functions. Despite these advances, more research remains to be done to capture the variety and complexity of common woodframe building types in California and other seismically active regions. We offer the following recommendations for action and future research. HAZUS can be used together with the methods and results of this study to facilitate many of the recommended activities.

1. *Support risk-mitigation incentives* by earthquake insurers, governments, and nongovernmental organizations. Risk information developed here and in the following recommended studies can inform decisions to adopt such incentives, and to enhance their efficacy.

2. *Examine additional index buildings* such as Craftsman, Eichler, and Victorian houses, houses on slopes, school and commercial buildings, and woodframe construction characteristic of other seismically active regions. Examine more-complex buildings with features such as split-level construction, brick chimneys, reentrant corners, soil or foundation problems, etc. Define categories of woodframe buildings and analyze a significant number of examples of each category, in order to create category-based seismic vulnerability functions from rigorous, detailed, building-specific engineering analysis.

3. *Perform probabilistic seismic risk assessments* to determine the benefit of the risk-mitigation measures considered here, for all regions of the United States that have substantial seismic hazard. Results of such a study can be used to inform risk-management decisions by home buyers, homeowners, and other stakeholders.

4. *Study the installation quality and force-deformation-damage behavior of existing construction*. Little empirical data exist on the material strength and construction quality of various building elements such as stucco walls, shearwall nailing, etc., outside of the laboratory. It would be worthwhile to compile data on these characteristics as they exist in the field, e.g., through destructive testing of portions of buildings that are being renovated or demolished.

5. *Examine risk-communication issues* of how best to present the information developed here to inform owners' and other stakeholders' risk-mitigation decisions. Determine what styles and formats of risk information are most readily understood and used by homeowners, legislators, and others to manage risk.

6. *Create red-tag fragility functions* consistent with ATC-20 safety-inspection protocols. Emergency planners can use these to estimate temporary housing and other emergency-response needs in future earthquakes, for all regions where the ATC-20 procedures are used.

7. *Examine code-enforcement issues* to determine the effort required to ensure that new construction achieves the performance of the high-quality variants examined here. Building departments could use this information to determine the appropriate nature and frequency of inspection efforts.

8. *Quantify the effects of claims-adjustment practice,* to determine how the engineering vulnerability functions produced here should be adjusted to estimate insurance claims. Insurers such as the California Earthquake Authority could use this information to manage their risk.

9. *Validate inexpensive inspection protocols* that rely heavily on judgment such as FEMA 154 (a.k.a. ATC-21) and ATC-50. This information could be used to support the use of these risk-management tools.

10. *Validate drift limits in performance-based design guidelines* such as FEMA 273. Such guidelines rely on drift limits to simplify analysis and design. A probabilistic assessment of these limits could enhance their value.

11. *Identify the most important sources of uncertainty* to determine how to simplify loss analyses without substantially underestimating overall uncertainty.

12. *Revisit the present analyses to account for research in progress,* including tests of wall fragility and new three-dimensional structural analysis tools.

13. *Refine post-earthquake loss-data collection efforts*, to inform the creation of assembly fragility functions (damage as a function of structural deformation), repair-cost distributions, and whole-building seismic vulnerability functions.

Table of Contents

Volume 1: Report

Volume 2: Appendices

Index of Figures

Index of Tables

Chapter 1. Introduction

Objectives of the Present Study

This report presents a theoretical and empirical approach to improving loss-estimation methods for buildings in general, and woodframe buildings in particular. Its purpose is to develop seismic vulnerability functions for 19 distinct woodframe buildings of varying ages, sizes, configuration, quality of construction, and retrofit conditions. These vulnerability functions give a relationship between earthquake shaking intensity and the cost to repair the earthquake-induced damage. They are created using the latest scientific information, while relying on well-accepted structural engineering techniques, verifiable laboratory test data, and standard construction contracting principles. They account for major sources of uncertainty.

These buildings and their seismic retrofits were selected and designed by the managers of the CUREE-Caltech Woodframe Project Element 3 (Building Codes and Standards), whose objectives were both to provide insight into the performance of a diverse range of buildings, and to inform decisions regarding the design of new buildings and the seismic retrofit of existing ones. A major goal of this project was to avoid the extensive reliance on expert opinion required by existing category-based (model-building) loss-estimation methodologies.

The present study takes advantage of the laboratory test data and computer programs for structural analysis produced by Element 1 of the CUREE-Caltech Woodframe Project, as well as other recently published research. The vulnerability functions explicitly account for major sources of uncertainty, including variability in ground motion for a specified level of shaking severity, variability in structural characteristics (uncertain mass, damping, and stiffness), and variability in component fragility and in construction costs. The vulnerability functions reflect the performance and repair costs of all damageable building assemblies, structural and nonstructural alike. Finally, the methodology employed is transparent, in that its data and mathematical algorithms are presented in detail.

The seismic vulnerability functions produced in here give the probability distribution of repair cost as a function of ground-motion severity. They are also translated into a form compatible with HAZUS (Federal Emergency Management Agency, 1999). HAZUS, developed by FEMA and the National Institute of Building Sciences (NIBS), is a standardized, nationally applicable earthquake loss-estimation methodology, implemented through PC-based geographic information system software. The fragility functions in HAZUS provide the probability of a building entering particular damage states as a function of ground-shaking severity. In the present study (unlike in HAZUS), damage is calculated at the level of individual building assemblies, e.g., individual windows, segments of wall, etc., producing a very detailed probabilistic picture of

physical performance and repair cost. This feature has at least three important implications:

1. One can calculate insurance recovery in cases where different coverage limits or deductibles apply to different building components.
2. The relative contribution to total cost from individual building components can be used to identify those components whose seismic performance most needs improvement.
3. Since red-tagging in many cases is tied to evidence of physical distress of particular building components, the study results could be used to indicate the probability that the buildings would be unoccupiable after an earthquake, although this aspect is not explored in depth in the present study.

In summary, the objectives of the present study are threefold:

1. To produce seismic vulnerability functions for a variety of woodframe buildings.
2. To employ and illustrate a rigorous methodology that uses the latest, well-accepted engineering techniques and test data, explicitly accounting for major sources of uncertainty.
3. To present these vulnerability functions in the formats most useful for application to risk-management decision-making. In this study, three formats are provided: damage factor (repair cost as a fraction of replacement cost) versus spectral acceleration, damage factor versus peak ground acceleration, and in the form of damage-state fragility functions appropriate for use in HAZUS. Other formats are possible, depending on users' interests.

These objectives were framed with a variety of potential users in mind, including owners, tenants, buyers, sellers, lenders, insurers, building code developers, emergency planners, and the consultants who serve them. The potential applications are equally varied, but emphasis is placed on facilitating risk-management and risk-mitigation decision-making.

The authors have attempted to make this report accessible to non-technical readers, engineering students, construction contractors, and others who may be unfamiliar with statistics and reliability methods, by providing simplified explanations of technical terms and principles, and by minimizing the use of mathematics in the main body of the report. Supporting math is provided in appendices to this report, in Volume 2.

Caution Regarding the Use of Study Results

It is important to emphasize the intention of this project, and to caution the reader regarding the interpretation of its results. This project is a combined academic and professional exercise in estimating future earthquake damage to 19 moderately simple,

specific woodframe buildings, not a loss study for all California or other woodframe structures. There are three major differences between such studies.

1. **Selection of index buildings.** The 19 buildings examined here are not intended to represent an exhaustive sampling of all woodframe structures in California, nor to stand for entire categories of woodframe buildings. Rather, they are intended to be indicative of some of the diversity of woodframe structures, and to illustrate how the methodology can be used to expand the existing library of building vulnerability functions. Macroscopic loss estimates, such as those for insurance purposes, would require an examination of a wider variety of common woodframe construction, such as older Craftsman or Victorian homes, Eichler houses, and homes with wood or brick veneer. Some of these types have substantially different, more vulnerable lateral force-resisting systems. Victorian homes, for example, tend to lack both the structural sheathing and stucco finish of the index buildings examined here, and might therefore be far more vulnerable to earthquake damage. In addition, the presence of brick veneer can add a costly element to earthquake damage.
2. **Simplicity of index buildings.** The index buildings examined here tend to be simpler than real structures. Real homes often have brick chimneys, reentrant corners, vertical setbacks, soil or foundation problems, and other irregularities that tend to increase the amount of actual physical damage. Note however that each index building is designed in detail and its materials are well defined.
3. **Loss adjustment practice.** The cost to repair actual earthquake-induced physical damage is not the same as the likely cost associated with an insurance claim. Pre-existing cracks that were not noticed before an earthquake are often attributed to the earthquake, and submitted as part of the claim. Insurers tend to round up their payments to reduce the potential for costly appeals or litigation, particularly in large earthquakes, such as the 1994 Northridge Earthquake. And adjusters and others examining superficial damage can mistake it for more costly underlying structural damage, and pay accordingly. The result is that estimates of repair cost for loss-adjustment purposes would tend to exceed the cost of repairing only earthquake-induced damage.

The reader is therefore cautioned to consider the objectives of this study and the context in which its results are applied.

Organization of the Report

This report presents an overview of the methodology employed to develop the vulnerability functions. It presents the test data, cost estimates, and other technical information used to develop these vulnerability functions.

This chapter has introduced the objectives of the present study within the context of the larger CUREE-Caltech Woodframe Project. Chapter 2 provides an overview of existing loss-estimation methodologies. Chapter 3 summarizes the assembly-based vulnerability (ABV) methodology used in the present study, with an overview of its principles, methods, and data employed. Chapter 4 presents the four index buildings and their variants and seismic retrofit measures that together constitute the 19 study buildings examined here. Chapter 5 presents the vulnerability functions and HAZUS fragility functions for each building. Chapter 6 provides a sample risk study, examining the probabilistic benefits of the various quality levels, retrofit, and redesign measures in terms of economic performance and probability of being red tagged. Chapter 7 summarizes conclusions and lists recommendations. References are contained in Chapter 8. A glossary of terms appears in Chapter 9.

Volume 2 of this report contains seven appendices with supporting information: (A) a detailed literature review of related aspects of loss estimation, (B) drawings of the index buildings, (C) details of the structural modeling, (D) a journal article discussing the ABV methodology, (E) examination of the fragility of various damageable components in the index buildings, (F) a detailed estimate of the cost to construct each index building and to repair building damage, and (G) the ABV-based mean vulnerability functions in tabular form.

Acknowledgments

This research was funded by the Federal Emergency Management Agency (Mike Mahoney, Project Officer), and by the California Governor's Office of Emergency Services (Andy Petrow, Project Officer). Drs. Andre Filiatrault, Bryan Folz, and Hiroshi Isoda of the University of California at San Diego prepared materials essential to the structural analysis performed at Caltech. Index buildings were designed by Kelly Cobeen (GFDS Engineers), John Coil (Coil and Welsh/Thornton and Thomasetti), Jim Russell (Building Codes Consultant), and Ray Young (Young and Associates). The designers also provided descriptions of the index buildings; their text is included in this report and is gratefully acknowledged.

Building variants were created in consultation with David L. McCormick and John Shipp of ABS Consulting (formerly EQE International). Mr. McCormick also provided valuable assistance developing building-component damage models. Dr. Kenneth Campbell (ABS Consulting) provided advice regarding the ground motions to be used in the analysis. Mr. Tom Boyd (Young and Associates) produced the unit-cost estimates for the repair of damaged components, as well as estimating the replacement cost of the index buildings and the cost of the seismic retrofit and redesign measures.

Dr. Stephanie King provided statistics and analyses of field-investigation data from the Northridge Earthquake. Prof. Goetz Schierle (University of Southern California), Prof.

Rob Chai (University of California, Davis), Prof. Gerry Pardoen and Mr. Eric Freund (both of the University of California, Irvine) kindly provided pre-publication research data from their tasks of the CUREE-Caltech Woodframe Project. Mr. Ben Schmidt provided valuable advice used in the development of component fragility data. Ms. Vanessa Camelo (California Institute of Technology) assisted in several aspects of the research.

Many researchers and practitioners donated their time to participate in a Woodframe Project workshop in May 2001, and provided valuable feedback on interim results. Kelly Cobeen, Bill Graf, Onder Kustu, and Steven Maragakis provided reviews and offered valuable criticism and suggestions for improving the draft report. Robert Reitherman in particular is to be thanked for his extraordinarily thorough editorial review. The authors gratefully acknowledge the contribution of all these individuals.

Chapter 2. Review of Existing Vulnerability Methodologies

Use of Seismic Vulnerability Functions

This chapter summarizes existing methodologies for creating seismic vulnerability functions. The review presented here is brief, and summarizes only some of the relevant studies examined for the present project, with emphasis on overall methodologies. A detailed review is presented in Appendix A, summarizing topics such as research on losses from the 1994 Northridge Earthquake; effects of building characteristics on seismic performance; selection and modeling of ground motion records; nonlinear time-history structural analysis of woodframe buildings; and damageability of building components.

Seismic vulnerability functions are an essential component for managing earthquake risk. Seismic risk management involves tradeoffs between the potential loss due to an earthquake, and the costs of reducing this potential loss. These trade-offs are usually balanced in a benefit-cost or other decision framework, as follows.

- **Determine the earthquake hazard.** Seismologists, geologists, and geotechnical engineers study the seismic faults of a region of interest, in order to understand the active earthquake sources, their potential size, frequency, and location. For a given future earthquake location and magnitude, one can estimate the severity of ground shaking at a particular building site. Severity can be measured a variety of ways: in qualitative terms such as using the Modified Mercalli Intensity (MMI) scale; or using quantitative measures recorded by instruments, such as peak ground acceleration (PGA) or acceleration response spectum (S_a). (These and other terms are defined in the glossary of this report.)

- **Estimate building damage.** One uses the estimate of site shaking as input to a seismic vulnerability function, which estimates the degree of damage to a building located at that site, given the shaking severity that the earthquake causes at the site. It is usually convenient to express this degree of damage as the cost to repair the damage as a fraction of the replacement cost of the building. The ratio of the repair cost to the replacement cost is called the damage factor. A seismic vulnerability function can be deterministic—giving a single value of the damage factor for a given value of shaking severity—or probabilistic, i.e., giving an uncertain damage factor as output, such as with a mean value and a measure of uncertainty. Using the output of a seismic vulnerability function, one multiplies the damage factor by the replacement cost of the building in question, to estimate the cost to repair the building, if that earthquake occurs.

- **Compare as-is and what-if loss to estimate the benefit of a risk-mitigation measure.** Estimate losses again for what-if conditions, where the what-if is the building with a seismic retrofit, a new building code, an above-code design, or

with higher quality of construction. The reduction of what-if from as-is losses gives a measure of the benefit of the mitigation measure. Compare the benefit with the cost to determine whether the mitigation measure is economically justified.

There are other justifications for seismic retrofits and code changes and other ways to estimate earthquake losses, but the approach sketched here is nonetheless valuable for prudent risk management. Central to it is a set of vulnerability functions in which the analyst and decision-makers have some degree of confidence. The development of these vulnerability functions has consequently been the object of much research.

Methods of Creating Seismic Vulnerability Functions

A crucial element in the foregoing approach is the seismic vulnerability function. There are several ways to create seismic vulnerability functions. They can be empirically based (i.e., created using historical damage data), created using expert opinion, or constructed using engineering principles by considering the characteristics of the parts that comprise the building and using available experimental data and analytical methods. A seismic vulnerability function can be intended to reflect a particular building or created with the objective that it depict a broad category of buildings, such as all buildings of a particular height range and construction material. Important examples of each approach are detailed shortly, but it is first worthwhile to note the general principles involved in creating seismic vulnerability functions by various means, and the advantages and disadvantages of each approach.

Statistical Approach

In the statistical approach, one gathers available historical damage data, such as insurance company claims or building department surveys from past earthquakes. The data indicate the degree of damage and the severity of ground motion, and most often include a construction category. The data are collected by individual building, but usually are published only in aggregate form for reasons of confidentiality. Degree of damage is usually measured by the damage factor. One then groups the data by building category and shaking severity, and plots the data on a chart of damage factor versus severity. A smooth curve or set of curves fit to the data for a building category gives the seismic vulnerability function.

Table 2-1 shows some of the advantages and disadvantages of this approach. The method is highly defensible because it is based on actual damage data. (The problem of assuring the accuracy of the data is another question that will not be addressed here.) The downside is that the empirical method is inherently category-based, i.e., it cannot reflect any details of a particular building beyond the category, because the buildings in the group are typically unique in age, configuration, materials, etc. Because it is category-based, the vulnerability function is blind to these details, and cannot reflect regional or

temporal differences in construction, except through the use of new categories and additional data. Nor can it provide information on the vulnerability of buildings with new configurations, procedures or materials that were not represented in the historic earthquake damage. Consequently, it is problematic to evaluate the future benefit of proposed code changes or seismic retrofits.

Table 2-1:
Methods of Creating Seismic Vulnerability Functions

Method	Advantages	Disadvantages
Statistical	Empirical basis	Detail, regional, time differences ignored. Provides little information on new measures.
Expert opinion	Versatile	Difficult to judge new measures; difficult to verify.
Engineering	Versatile Verifiable Continual improvement Building-specific	Difficult to use for macroscopic loss estimation. Assessing new assemblies is laborious.

Martel (1964) and U.S. Coast and Geodetic Survey (1969) represent two early efforts to correlate building damage and shaking severity for woodframe dwellings. A number of other studies have developed relationships between ground motion and building damage (as discussed in Appendix A). These studies employ a data from past earthquake losses to these types of buildings, showing the loss and an estimate of the shaking that the buildings experienced. Figure 2-1 illustrates the type of motion-damage relationships developed in these studies. This figure depicts loss data plotted against elastic spectral displacement for 189 midrise buildings in Sendai, Japan, affected by the June 12, 1978 Miyagiken-oki Earthquake (Scawthorn *et al.*, 1981). Loss is expressed as repair cost as percent of replacement cost. Spectral displacement is evaluated at the pre-earthquake period of the building (average of horizontal directions). Scawthorn's regression analysis produces a mean seismic vulnerability function—a smooth curve fit to the data—of $y = 1.26x^{0.7}$, with a correlation coefficient $r = 0.48$ (not shown).

Expert Opinion

Even if existing historical data are inadequate, it is possible to create a vulnerability function using expert opinion. Formal methods exist to elicit expert opinion by a group of experts. In a procedure called a Delphi Process, an expert or group of experts is asked to judge an uncertain outcome, conditioned on well-defined inputs. The opinions of multiple experts can be used as data to create a probability distribution on the uncertain outcome. If the distribution is unacceptably broad, the experts can be brought together to

discuss their reasoning, and re-polled. One can account for the experts varying degrees of knowledge by having them self-rate their expertise. The judgments can then be segregated by self-rating. In one procedure, the judgments of those who self-rate their expertise as poor can be discounted, and the probability distribution on the outcome is created considering the remaining judgments (see, e.g., Dalkey *et al.*, 1970). In another approach, all the opinions can be used, but weighted by self-rating.

Figure 2-1:
Vulnerability of Japanese 3 to 12-story Reinforced-Concrete and Steel-Reinforced Concrete Composite Construction (Scawthorn, 1981)

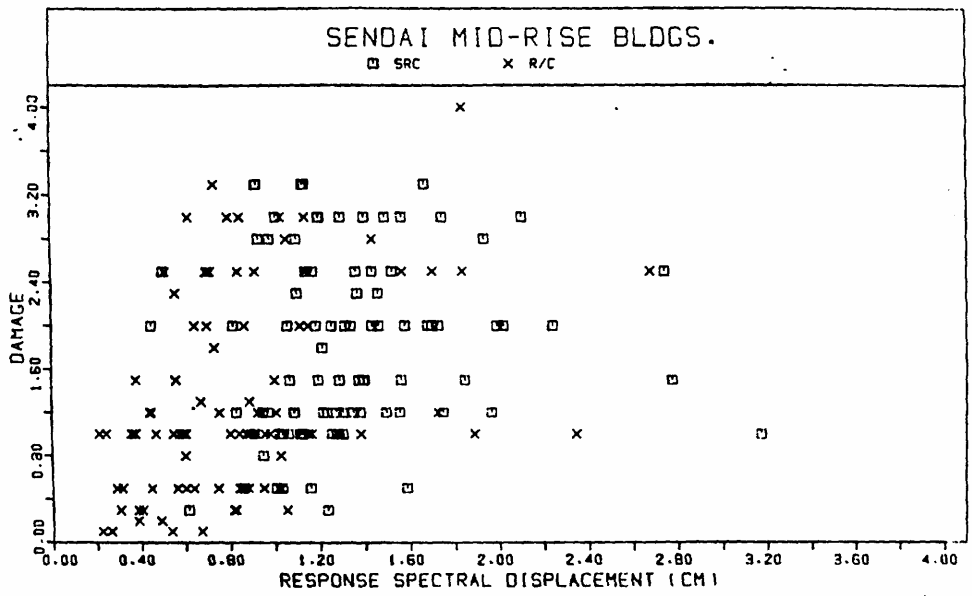

As applied to creating seismic vulnerability functions, the expert or experts are asked to judge the damage factor for a particular building or category of buildings, conditioned on shaking severity. They can be asked for low, best, and high estimates, and the process repeated for each building or category, and each level of severity. A self-rating system can be used to combine the experts' judgment into a single set of seismic vulnerability functions.

The advantage of this approach is that it does not require costly or unavailable damage data, and is very versatile, as long as experts can be found who are willing to judge the outcome of interest. It can be building-specific or category-based. Difficulties can arise when asking experts to judge new conditions of which they have no experience. They might refuse to offer their judgment, or the resulting disagreement can produce an unacceptably broad distribution. Furthermore, the use of expert opinion can be seen to weaken an argument, because it lacks a scientific (testable) basis.

One early application of expert opinion to earthquake vulnerability is found in Freeman (1932), who offers his judgment regarding future insurance losses by structure type and soil conditions, for all buildings throughout a region affected by a very large earthquake. More recently, the authors of ATC-13 (Applied Technology Council, 1985) find that inadequate empirical data existed to create a reliable and exhaustive set of seismic vulnerability functions. The authors overcome this difficulty by relying on expert opinion. Using a Delphi Process with weighting by experts' self-rating, as described above, they gather the judgments of 58 earthquake engineering academics and practitioners, who estimated the damage factor for 40 categories of California buildings as a function of MMI. Typically between four and nine experts provide opinions on a given type of model structure type. Figure 2-2 presents a sample of the experts' judgments for lowrise woodframe buildings. The symbols correspond to opinions from different experts.

Figure 2-2:
ATC-13 (1985) Expert Responses for Motion-Damage Relationships.

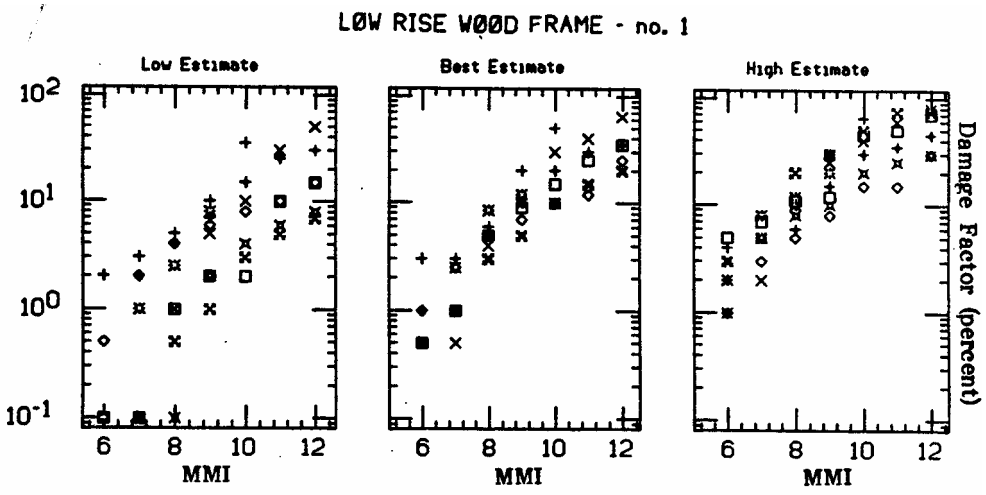

The study employs these opinions to create discrete probability distributions on damage factor for each MMI level of VI or greater. Seven damage intervals are used, each associated with a semantic damage state, from 1-None to 7-Destroyed. Several types of building and content loss are evaluated: building repair cost, content repair cost, and loss-of-use duration. (Human casualties are also addressed by the study, based on prior research and the judgment of the authors.) The approach is intended for macroscopic (i.e., societal) loss estimation, and does not account for a building's unique detailed design. All woodframe construction is characterized by a single seismic vulnerability function.

Engineering Approaches

An engineering approach to creating seismic vulnerability functions uses structural analysis to estimate the response of a building to an earthquake in terms of forces and displacements. The structural analysis can take any of four general forms: linear or nonlinear, pseudostatic or dynamic, as illustrated in Table 2-2.

Table 2-2:
Options for Structural Analysis

	Pseudostatic	**Dynamic**
Linear	1	2
Nonlinear	3	4

The nontechnical reader can understand the table as follows. The simplest approach to structural analysis for earthquake excitation is to idealize the earthquake as if it imposed stationary (static) forces, similar to the way the self-weight of a building and its contents impose forces on the structural members. In a real earthquake, the earthquake excitation and building responses change greatly over short periods of time (they are dynamic), and their moment-to-moment behavior is of interest. Typically, at significant shaking levels a building's deformation and the forces to which its members are subjected exceed the levels at which the members can spring back without damage (one aspect of nonlinearity). Thus, the nontechnical reader can intuitively see why option 4 in Table 2-2, nonlinear dynamic analysis, can estimate the building's response to strong earthquake excitation more accurately than do the other three options. The greater accuracy comes at a cost: the level of computational effort and specialized knowledge required increases from options 1 through 4.

Once the structural response is calculated, the likely damage to the building components can be estimated, using laboratory tests or other data on the damageability of the various structural and nonstructural components comprising a building. Given an estimate of component damage, one can estimate the repair cost using standard construction cost estimation techniques.

Such an approach is proposed by Steinbrugge *et al.* (1969) and Czarnecki (1973). It was employed by Scawthorn *et al.* (1981) and Scawthorn (1982) for loss estimation and for examination of optimum building code design levels for Japanese buildings. It is further developed and implemented using component test data by researchers at John A. Blume Associates in the 1980s: Scholl and Kustu (1981), Kustu *et al.* (1982), and Kustu (1986), present a methodology to develop theoretical motion-damage relationships based on detailed structural analysis of highrise buildings, followed by an assessment of damage to a variety of aggregated components based on structural response. The structural analysis

produces an estimate of the deformation of the building using nonlinear dynamic analyses (grid cell 4 in Table 2-2). The damage ratio for each component is evaluated for each floor and multiplied by the value of each component. Damage to the whole building is obtained by adding up the damage to its modules or pieces.

The HAZUS software (National Institute of Building Sciences *et al.*, 1997, 1999) also employs such an approach for a large number of building categories. The structural analysis step is performed using the capacity spectrum method (Mahaney *et al.*, 1993), a nonlinear pseudostatic approach (grid cell 3 in Table 2-2). Component damage is calculated for three aggregated component types: structural, nonstructural drift-sensitive, and nonstructural acceleration-sensitive. Repair costs are calculated based on damage to these aggregated components, combined with a fraction of building value represented by each group. Fragility functions for these components are created using a combination of engineering analysis, laboratory and other empirical component data, and the expert opinion of several structural engineers, considering a typical case for each building category. The fraction of overall value represented by each component is also based on a typical value for each general building category.

The assembly-based vulnerability (ABV) method represents a more-detailed engineering approach that is particularly useful in the present application. ABV was developed by one of us (Porter) and is described in Beck *et al.* (1999), Porter (2000), Porter *et al.* (2001a and b), and Beck *et al.* (2002). It uses nonlinear time-history structural analysis (grid cell 4 in Table 2-2), and offers three novel features.

1. **Detailed taxonomy.** Instead of using aggregated components (e.g., all nonstructural drift-sensitive components)**,** a categorization system is used to distinguish between building components at a highly detailed level. In the present application, this detailed taxonomy allows one to differentiate between woodframe shearwalls and stucco walls, thin versus thick structural sheathing, wood studs versus metal studs, walls versus windows, etc. A wall of glass is different from a wall of stucco and wallboard, even though both are nonstructural drift-sensitive components. It is a particular desideratum of the present study to be able to tell these two apart, and to more generally to compare structures that have the same general structure type, but differ in particulars of design or retrofit. Treatment of damage at this level of detail is crucial if one wishes to describe the physical performance of a facility in terms of, for example, fraction of windows broken, degree and extent of damage to interior walls, etc., which is another requisite of the present study.
2. **Uncertainty and correlation.** Each parameter in the analysis can be modeled as an uncertain variable with a probability distribution established from empirical data. The analysis is formulated in terms of conditionally independent variables, which eliminates the need to impose correlation coefficients would have to be assumed or applied from tests of different facilities. Careful treatment of uncertainty is crucial when the analysis results must be expressed in terms of the

probability of a facility being in one physical damage state or another, of when the probability of the repair cost exceeding a certain amount is required, as in the present case.

3. **Avoidance on expert opinion; verifiability.** The ABV approach allows one to make a clear association between the damageability of a component and particular laboratory tests of force-deformation and damageability behavior, as is desired in the present study. Because the analysis is performed at level detailed enough that each variable can be established from verifiable, empirical data, there is little need to rely on expert opinion, which can be seen to weaken the conclusions of a study.

Selection of Analysis Method for the Present Study

It is this last approach that is used in the present study. In summary, there are at least five reasons for selecting ABV: its building-specific nature, use of nonlinear time-history structural analysis, treatment of uncertainty, avoidance of expert opinion, and evaluation of damage at an assembly-by-assembly basis. We use this opportunity to introduce two new features to ABV: line-of-sight costs and uncertain contractor overhead and profit.

Chapter 3. Project Methodology

Introduction

The correlation of damage or loss with seismic ground-motion severity is defined as a *vulnerability function*. Figure 3-1 provides a schematic illustration of a seismic vulnerability function. It can reflect the performance of an individual structure or a class of structures.

Figure 3-1:
Probabilistic Seismic Vulnerability Function

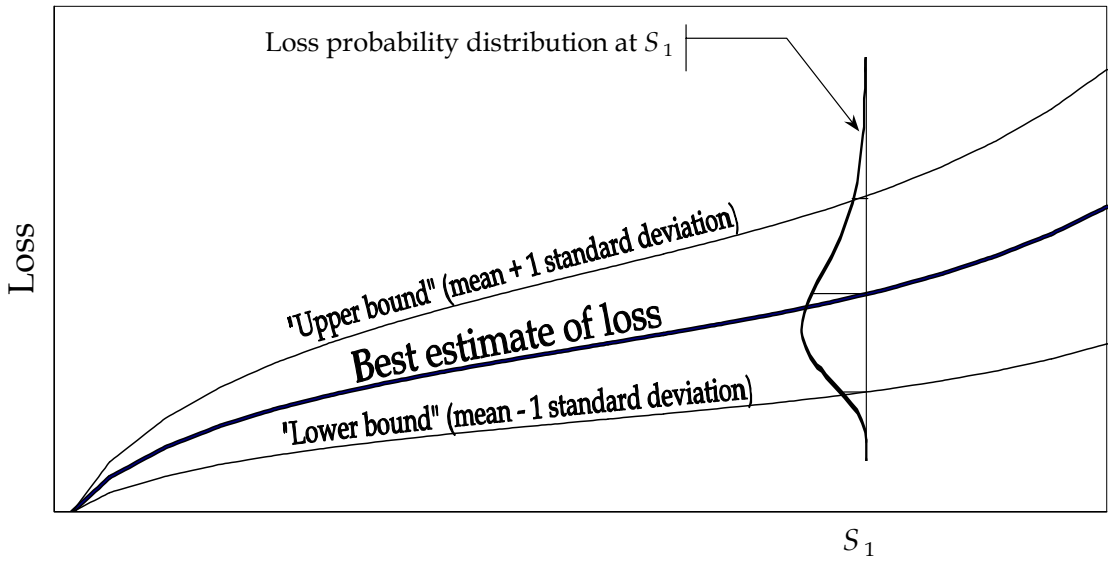

The horizontal axis of Figure 3-1 measures ground motion severity, *S*. There are many ways to measure severity: peak ground acceleration (PGA), Modified Mercalli intensity (MMI), spectral acceleration (S_a), spectral displacement (S_d), etc. (These last two spectral measures refer to the maximum acceleration or displacement experienced by an idealized, simple structure during the earthquake ground motion. They reflect the fact that a particular ground motion can affect two structures very differently, depending on the degree to which each structure resonates with the ground motion, and the amount of vibrational energy the buildings can dissipate.)

The vertical axis measures loss. As with shaking severity, loss can be measured in a variety of ways, in terms of deaths or injuries, dollar repair costs, loss-of-use costs, etc. In the present study, loss is measured in terms of the damage factor (*DF*), that is, the repair cost for structural and nonstructural building components, divided by the replacement cost of the entire building (Equation 3-1).

$$DF = \frac{Loss}{Replament\ Cost} \tag{3-1}$$

Since the vulnerability functions developed here are probabilistic, even if one knows exactly how strongly the ground shakes under a building, the resulting loss is uncertain, and can take on a range of values with varying probability, as shown in Figure 3-1. It is necessary to know the probability distribution on loss because many decision parameters depend on upper or lower values of loss, or the probability of loss exceeding a certain amount. For example, the amount of an insurance payment depends on the probability of loss exceeding the deductible. Even if the best estimate of loss is below the deductible, there can be a significant probability that the true loss is greater than the deductible and some insurance payment will be required.

The damage is uncertain because many of the steps between ground shaking and loss involve uncertainty. Most notable among these uncertainties are:

1. **Ground motion.** Variability in the moment-to-moment shaking of a ground motion that has a given overall severity level;
2. **Structural response.** Uncertainty in the mass, stiffness, and energy dissipation (i.e., damping) characteristics of the building that govern how much the building deforms during a given ground motion;
3. **Component capacity.** Uncertainty in the capacity of individual building components to resist damage when subjected to certain levels of force or deformation; and
4. **Construction costs.** Variability in contractor productivity, hourly labor costs, and costs of materials required for repair.

In the approach used for this project, these uncertainties are explicitly quantified and propagated using probability models. If one is attempting to create a seismic vulnerability function for an entire class of buildings, such as all woodframe structures of less than 5,000 square feet, then there is an additional, important source of uncertainty: the configuration, materials, design details, and quality of construction can vary substantially between two buildings of the same general type. This uncertainty is avoided in the present study because the vulnerability functions are developed for particular buildings with known configuration, materials, etc. By compiling a large number of building-specific seismic vulnerability functions, one can create a single category-based vulnerability function. In contrast, it is very difficult to go in the opposite direction, i.e., to create or infer a reliable seismic vulnerability function for a particular building from a category-based one. The difference between category-based vulnerability functions and building-specific ones is important for two reasons:

1. **Perceived weakness of expert opinion.** Category-based approaches have had to rely to varying degrees on expert opinion, which is sometimes seen as weakening the resulting conclusions.
2. **Blindness to details.** Category-based vulnerability functions cannot directly account for the unique design and construction features of an individual building. This is a problem when decisions are being made regarding risk from that building, such as whether the owner will find it worthwhile to construct the building to a performance standard greater than code-minimum, or how much of a reduction in premium an insurer should offer if the owner seismically retrofits the building.

Because the present study is intended to answer building-specific risk-management questions, a building-specific approach is applied to develop seismic vulnerability functions, and these two problems are avoided.

Summary of the Approach

Four individual structures (referred to as index buildings) were designed by researchers working on Element 3 of the CUREE-Caltech Woodframe Project to reflect some of diversity of woodframe construction. Nineteen variants of these four basic designs are examined here. The buildings and their variants are detailed in Chapter 4 of this report.

An analytical framework called assembly-based vulnerability (ABV) is used to create seismic vulnerability functions each building. The theoretical foundations and mathematical basis of ABV are detailed in Porter *et al.* (2001a, 2001b). The technical reader is referred to Appendix D for a copy of Porter *et al.* (2001a). For the nontechnical reader, ABV can be summarized as follows:

Simulation

ABV is implemented using a process called *simulation*. Because it may be unfamiliar to many readers, simulation will be summarized first. (Note that the ABV framework does not necessarily require a simulation approach, but it is by far the simplest way to implement an ABV analysis.) Simulation is often used with complicated systems to estimate the probability distribution of an output variable that can be calculated directly from one or more uncertain inputs. A simulation proceeds as follows: for each input variable, one draws random samples whose value is consistent with the probability distribution over its range of possible values. (That is, for a large number of samples, a chart of the sampled values—called a *histogram*—will reflect the true probability distribution.) One uses these samples to calculate the resulting output variable. By doing this repeatedly, one collects a large number of samples of the output variable, whose histogram approximates the probability distribution of the output variable. The more simulations one performs, the closer the histogram of the output samples comes to approximating the theoretical distribution of the output variable.

A simple example is the roll of two dice. It is straightforward to calculate the theoretical probability of the sum of any roll, but one can also find these probabilities by repeatedly rolling two dice. Each roll of the dice represents a single simulation: a simulation includes drawing one sample value of die 1, one sample value of die 2, and one sample value of the output variable (die 1) + (die 2). By simulating repeatedly and counting the fraction of total rolls that come up 2, 3, etc., up to 12, one can estimate the theoretical probability of rolling a 2, 3, etc. The more times one rolls the dice, the closer the estimated probability comes to approximating the theoretical probability distribution of the sum of two dice. Figure 3-2 illustrates this principle for 10 simulations (10 rolls of the dice), 100 simulations, 10,000 simulations, and the theoretical probability distribution of the sum of two dice. Note how 10,000 simulations provides probabilities almost equal to the theoretical values.

Figure 3-2:
Simulation to Find the Probability Distribution of the Roll of Two Dice

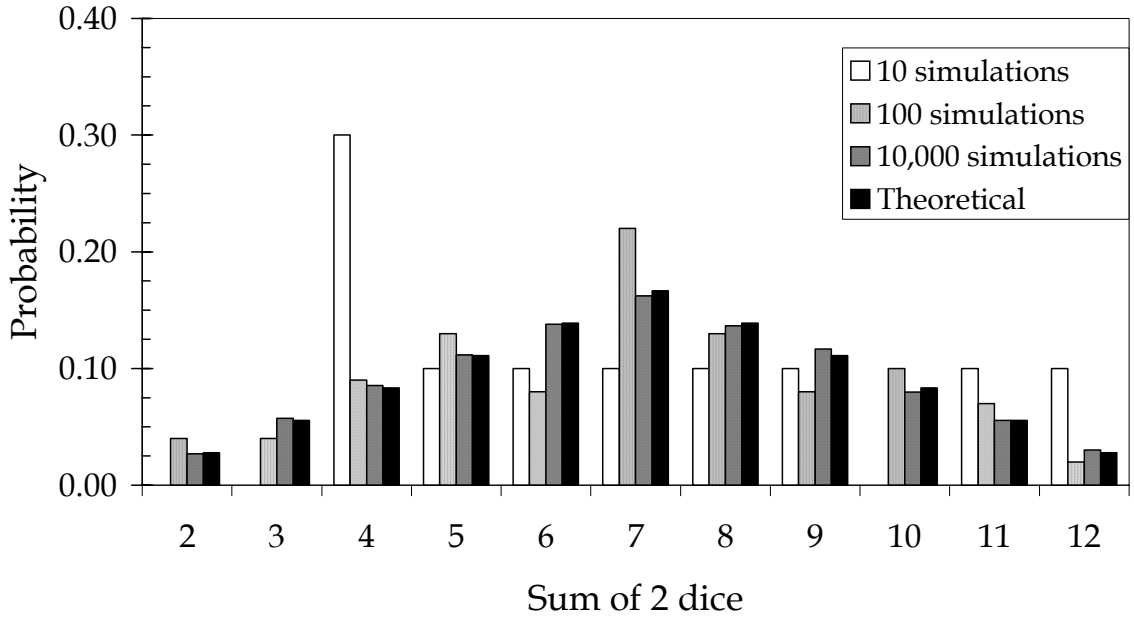

Applying Simulation to Evaluate Seismic Vulnerability

With this introduction in mind, consider how simulation is used to calculate the vulnerability function for a building. In the analysis, instead of the random input variables being the values on the faces of the dice, they include the ground motion at any point in time, the displacement of the various parts of the building, the damage to the components, and the costs to repair them. Figure 3-3 illustrates the ABV analysis procedure, which is now summarized.

Figure 3-3:
Overview of ABV Methodology

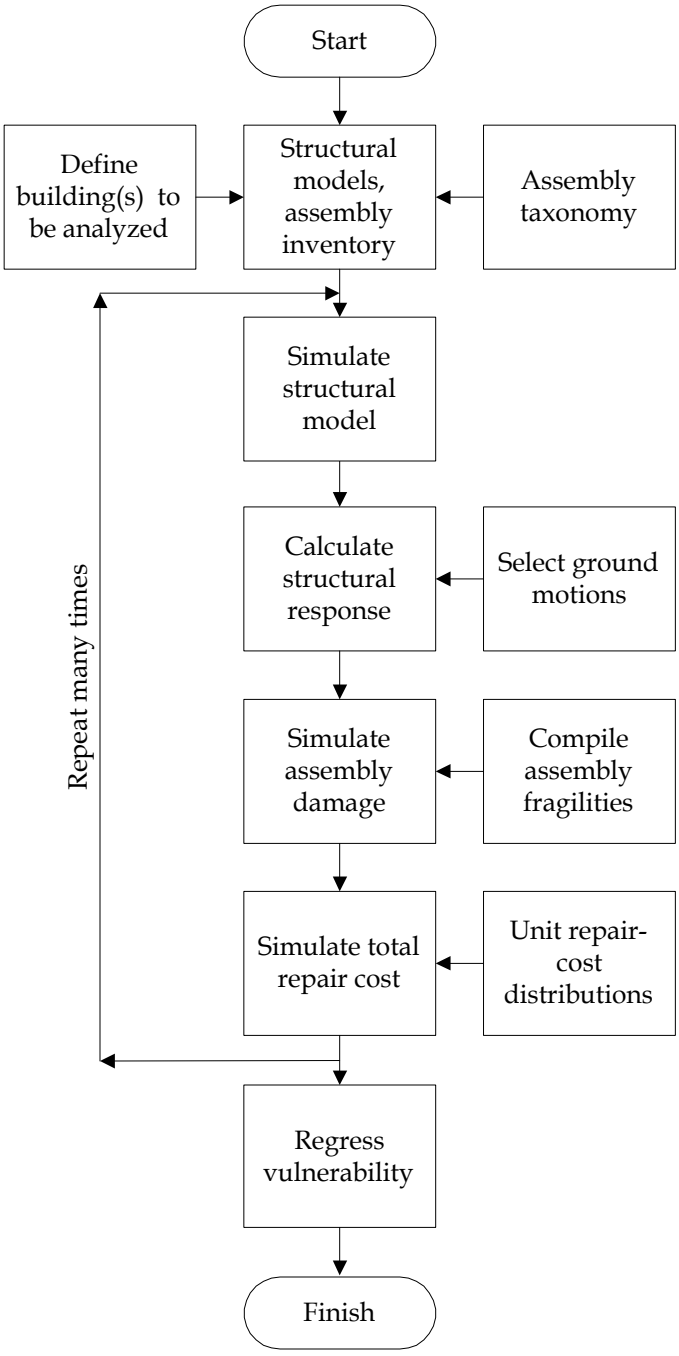

An ABV analysis starts by defining the building to be analyzed. The analyst determines the location, configuration, and material properties of all the building elements. The components are characterized and inventoried using a standard system of assembly classification, so that the assemblies in this building can be approximately equated with others that have been tested in a laboratory or have been observed in the field. That way, one can apply lessons learned about the past performance and repairs of similar assemblies with as little ambiguity as possible.

As part of the building definition, the analyst creates a structural model, that is, a mathematical idealization of the building, for use in a structural analysis. The model includes a characterization of the important uncertainties in building mass, stiffness, and damping, as well as the best estimates of these values. In the modeling, all the building's elements – walls, ceilings, etc. – are represented by springs and masses with uncertain properties.

Next, a set of ground motion records is collected that reflects the range of shaking intensities of interest. Several recordings are used for each level of ground shaking severity. These records can come from actual historic earthquakes, or one can simulate them using any of a variety of techniques. The recordings must reflect approximately the same soil conditions, earthquake magnitudes, fault distances, and fault types to which the building being studied is exposed.

A structural model is selected at random from a set of possibilities and subjected to a randomly selected ground-motion recording that has the desired shaking severity. Note that while the structural; model and gm are selected randomly, they nonetheless reflect the desired probability distributions of the uncertain parameters such as mass, damping, and so on. The analyst performs a time-history structural analysis, which calculates the peak structural responses of the building. "Structural response" means the movements and forces (as opposed to damage or cost) that the various parts of the building experience. These movements and forces can include the following:

1. Peak transient drift ratio (PTD). This is the maximum distance that the floor or ceiling above moves relative to the floor below, divided by the height of the story, at any time during the earthquake. The PTD values are captured for each wall line and each story in the building. The PTD strongly affects damage to building elements such as exterior walls, interior partitions, and windows.
2. Peak diaphragm acceleration (PDA). This is the maximum acceleration experienced by each floor, ceiling, or roof level during the earthquake. The PDA values tend to be strongly related to damage to floor- or ceiling-mounted components such as water heaters, fans, ductwork, etc.
3. Peak transient horizontal shear strain (PSS). This is the maximum in-plane deformation of ceilings and floors, that is, the degree to which one edge of a ceiling or floor level moves relative to the opposite edge. PSS is relevant to

horizontal elements such as drywall ceilings. PDA and PSS are captured for each diaphragm.

4. Peak member forces. These include the forces and bending moments that various structural elements experience during the earthquake, often relative to the expected strength of the member.
5. Residual drift ratio (RD). This is the distance that the floor or ceiling has displaced relative to the floor below, divided by the story height, after the earthquake motion stops. RD is relevant for determining whether doors will be jammed and whether a building will be perceived as a collapse hazard after an earthquake. The RD values are captured for each wall line and each story in the building.

At this stage in the ABV analysis, one knows for example that for ground motion *W* and structural model *X*, floor *Y* displaced at most *Z* inches relative to floor *Y*-1. Furthermore, one knows all the other important measures of load and deformation that the building experienced. These loads and deformations are then used to simulate damage to each of the building assemblies such as windows, walls, ceilings, etc. This damage simulation proceeds as follows.

For each damageable assembly in the building, the structural response that most strongly relates to the damage of that assembly is input to a relationship called a *fragility function*. The fragility function gives the probability that the assembly will be damaged in a particular way when it is subjected to a particular level of structural response. For example, a fragility function for a glass window could show the probability that the window will crack when subjected to a particular level of drift. One can use that probability and a random number between 0 and 1 to simulate whether the window cracks in this simulation.

For example, suppose the probability is 0.20 (1 in 5) that the window will crack when subjected to the calculated drift. One draws a random number between 0 and 1 (using a computer random-number generator, for example). If the random number is less than 0.20, then the window is said to have cracked, otherwise, it is not cracked in this simulation. In a similar manner, one simulates damage to every other assembly in the building, using the responses to which they are exposed (the drifts, accelerations, etc.), and the pre-established fragility functions.

The analysis thus produces a complete picture of the damage to the entire building in a particular simulation: these windows cracked, those unbroken; these segments of wall slightly damaged, those heavily damaged, etc. The analyst then counts the number and type of assemblies that must be repaired: a total number *M* broken windows, a number *N* cracked segments of drywall partition, etc. Next comes the simulation of the cost to repair these damages, which proceeds as follows.

The analyst compiles probability distributions for the cost to perform each repair task, i.e., the cost to repair one unit of each damageable assembly type (the *unit cost*), for example, the cost to repair one broken window. Published surveys of construction costs provide average values for many repair tasks, and other sources of unit costs are also available. Construction cost estimators can offer guidance on the uncertainty in the actual value of these unit costs in any particular case. However these distributions are compiled, the analyst draws a sample from each unit-cost distribution, and applies it to the number of assemblies that must be repaired. For example, suppose the cost to repair a single broken window is distributed according to a normal distribution (a probability distribution with the familiar bell shape) with average value $\$X$ and standard deviation $\$Y$. In a particular simulation the value $\$Z$ per broken window is drawn from the distribution. There were M broken windows in the simulation, so the cost to repair them all is $M*Z$ in this simulation. The same procedure is followed for all the other damages, and the total cost is summed from the individual costs. One then adds contractor overhead and profit (these too can be taken as randomly distributed), and thus produces one simulation of total repair cost.

The total cost represents the output variable. It can be plotted as a point on a scatter diagram (sometimes called an x-y chart), where the x-value gives the shaking severity of the ground motion with which the simulation began, and the y-value is the repair cost divided by the replacement cost of the building. The whole procedure is repeated many times for each level of shaking severity, producing a number of dots on the scatter diagram, all with the same x-value of shaking severity but with varying y-values of the damage factor. The procedure is then repeated many more times for the next level of shaking severity, and so on, until all the levels of shaking severity of interest have been examined. Curves can be fit to the data showing the best estimate of the damage factor and its associated uncertainty, as functions of shaking severity. See Figure 3-4 for a schematic illustration of the results of this procedure.

Figure 3-4:
Regression of Probabilistic Vulnerability Function from ABV Damage Samples

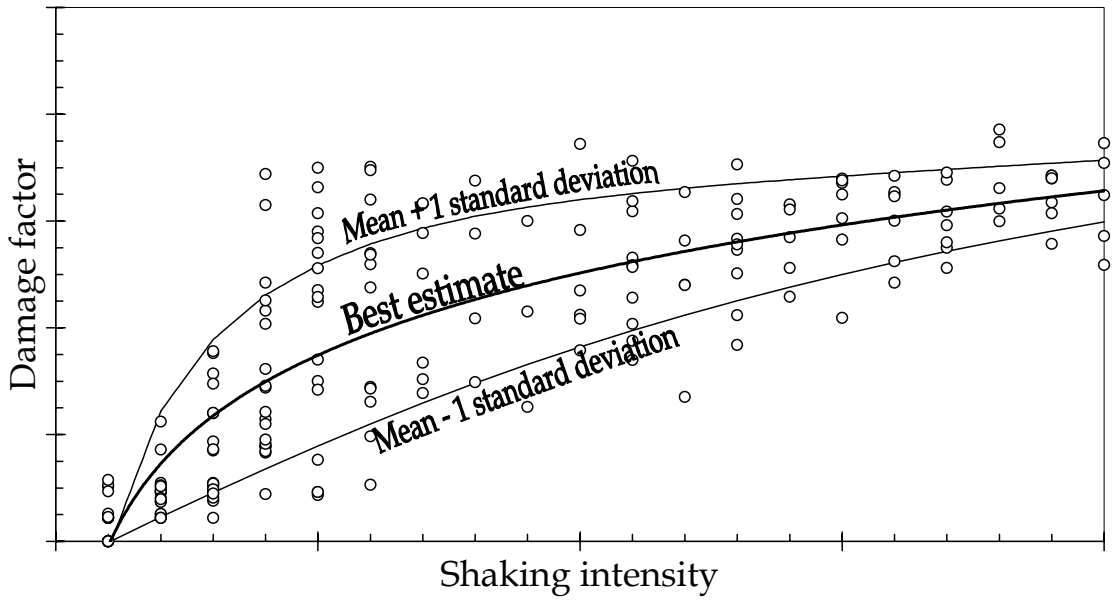

Creating HAZUS-Compatible Fragility Functions

The vulnerability data can be analyzed to estimate the probability that the damage factor will exceed a particular value at a given level of shaking severity. For example, suppose one is interested in the probability that damage factor will exceed some value y_{DS} at a particular level of shaking severity S. Each ABV analysis has an associated shaking severity S and a total repair cost C_T. By dividing C_T by the building's replacement cost new (RCN), one translates the simulated damage into damage factor, i.e., $Y = C_T/RCN$. If $Y > y_{DS}$, then the simulation has exceeded the damage factor of interest. The fraction of times that this occurs over all simulations for shaking severity S gives an estimate of the probability that $Y > y_{DS}$, given S. The objective is to fit a smooth curve to the probability that $Y > y_{DS}$, as a function of S. The smooth curve is the fragility function of interest.

In the present study, it is the HAZUS-compatible fragility functions that must be determined. HAZUS, developed by the National Institute of Building Sciences (NIBS) for the Federal Emergency Management Agency (1999) is a standardized, nationally applicable earthquake loss estimation methodology, implemented through PC-based geographic information system (GIS) software. It is intended as a tool for estimating future earthquake losses, for the purposes of risk mitigation, emergency preparedness, and disaster recovery.

To estimate economic losses to regional building stocks, HAZUS calculates building damage using a database that includes seismic hazard information, an estimated inventory of building stocks, and a set of fragility functions for various types and qualities of buildings and building components. The HAZUS fragility functions give the probability of structural and nonstructural components reaching or exceeding each of four damage states: slight, moderate, extensive and complete. In effect, there is a fifth damage state, collapse, which is a subset of complete. The damage states are defined both in terms of observable damage incurred by building components, and by a range of damage factors associated with each damage state, as shown in Table 3-1.

The HAZUS fragility functions are defined as functions of the damped elastic spectral displacement (S_d) at the intersection of a pushover curve and the earthquake response spectrum. The fragility functions are specified by a lognormal cumulative probability distribution, which has two parameters: the median, x_m, and logarithmic standard deviation, β.

The methodology for using ABV damage data to regress fragility parameters for pushover analysis is now summarized. Details of how each step is implemented for the index buildings is presented in Chapter 4.

1. Associate each index building and variant with a pushover curve.
2. Use ABV analysis (not pushover analysis) to determine the damage factor for each simulation. Determine the damage state based on the damage factor, using Table 3-1.
3. For each ABV simulation, find the spectral displacement (S_d) at the intersection of the selected pushover curve and the (S_d, S_a) response spectrum of the ground motion used in the ABV analysis.
4. Based on the results of steps 2 and 3, compile statistics of the probability of reaching or exceeding each damage state, versus S_d, and regress the parameters of the fragility curve.
5. Calculate statistics on the average fraction of assemblies damaged, by index building, by any meaningful group of assemblies, and by building damage state. These statistics represent a description of the damage state in terms of physical damage.

Table 3-1:
HAZUS Damage States

Damage state	Damage factor
Slight	0-5%*
Moderate	5-20%
Extensive	20-50%
Complete	50-100%

* Lower bound of slight damage is taken here as 0.1%

Other Fragility Functions

Although the present study is primarily concerned with repair costs, other variables relevant to risk-management decision-making can also be modeled with fragility functions. For example, one might wish to know the probability that a house will suffer particular types of damage that would render it unsafe to occupy, i.e., the chance that it would be red-tagged after an earthquake. A fragility function could be created to give that probability as a function of the shaking severity.

For the most part, red tagging occurs because of physical damage to the building, physical damage that is modeled in the present analyses. Thus, the results of the present study could be used to create such red-tagging fragility functions for each index building, variant, retrofit, and redesign measure, and use them to assess the benefit of retrofit on reducing the chance of red-tagging.

Other measures of performance that might be of interest include the FEMA 273 (Federal Emergency Management Agency, 1997) performance levels such as operational, immediately occupiable, etc. Because ABV is implemented using a database that saves all values of structural response, physical damage, and cost for each simulation, any decision variable that is a function of these can be modeled using the results of this study.

Chapter 4. Analysis of Index Buildings

Introduction

Four hypothetical but representative buildings, referred to as *index buildings*, were designed in detail by Element 3 of the CUREE-Caltech Woodframe Project, and are studied here. Each index building has several different versions, called *variants*, reflecting different quality of construction and maintenance, retrofit measures, and redesigns. These buildings and variants are exemplars for comparing baseline earthquake performance and examining the effects of varying construction quality, of applying certain retrofit measures, or of changing the initial design. The buildings and their attributes provide reference points for extrapolating cost and performance implications to other buildings.

The four buildings and their variants include features typical of residential buildings. Although these features are selected to represent construction practices related to the building codes once used in California, many features might be representative of buildings in other states. The buildings are used in this report to illustrate a general analytical methodology, to draw specific conclusions about these buildings, and to draw more general conclusions regarding broader building types. Index buildings can be used to evaluate the cost effectiveness of quality control practices, design detailing and retrofit measures including damage-limiting design approaches (i.e., above-code-minimum performance levels).

Each index building has been designed to the extent necessary for structural analysis and cost estimation purposes, but not for construction. (Note however that woodframe buildings have been constructed in the U.S., and are currently issued building permits, on the basis of drawings that show less information is provided for these hypothetical buildings.) Three variations of each building (poor, typical, and superior quality) are then defined to reflect different levels of construction quality and post-construction maintenance. The performance of the buildings constructed to the three quality levels is analyzed independently to narrow the uncertainty in total repair cost.

The drawings for each building are provided in Appendix B and in CAD format by CUREE through www.curee.org. Others are encouraged to use these buildings in engineering studies to analyze earthquake performance and cost of other features such as hillside homes on stepped cripple walls, dampening and isolation devices, and for evaluating the cost effectiveness of potential incentive programs.

Conclusions can be drawn by comparing the cost of earthquake-resisting options with the cost of repairs and other consequences estimated for each of the variations. For example, the difference between the estimated performance of poor quality construction and superior quality construction may imply the benefits of superior code enforcement. The performance differences illustrated between the small house on unbraced cripple walls

and on concrete stem walls can be used as a guide when considering the value of bracing and anchoring cripple walls. The cost of retrofit measures can be compared to avoided damage and the resulting consequences when considering the efficacy of incentives.

The methodology used for analysis of the index buildings and the resulting capacity-fragility-loss relationships are compatible with HAZUS 99. HAZUS currently represents all woodframe construction using a set of relationships relating ground motion with building losses for two building types, W1 (wood, light frame, less than 5,000 ft^2) and W2 (wood, commercial and industrial, at least 5,000 ft^2). The small house, large house, and townhouse modeled here would be categorized as W1, while the apartment building would be categorized as W2. The additional detail should enable more representative estimates of losses from woodframe buildings.

A Caution Regarding the Simplicity of Index Buildings

Note that the four buildings are meant to be representative of buildings typically found in California. Although they resemble actual buildings, the buildings analyzed here are exemplars only. Because of the variety of woodframe buildings in California—various sizes, configurations, architectural and structural features, site conditions and other features—the four buildings are not statistically representative of the building stock. Element-3 researchers intentionally kept building geometries simple, to correspond to the capabilities of the structural-analysis software employed here.

This software is used to calculate the structural response of a building to an input ground motion, a crucial intermediate step in the ABV analysis. Because of the software's limitations, it is impractical to model realistically many of the complex features of real homes, such as varying wall heights, re-entrant corners, split-level construction, hillside construction, multi-level roofs, and masonry fireplaces and chimneys. These features, if included, would likely tend to increase damage ratios, and *consequently the vulnerability functions produced here can be expected generally to underestimate the vulnerability of the actual housing stock*. Substantial improvements in analytical tools will be required before realistic modeling of these conditions can be achieved.

However, by drawing cost/performance conclusions from the features in the buildings or changes to the features, it may be possible to extrapolate the results to other buildings through informed judgment or additional response and loss modeling. The analyses performed here can however serve as a starting point for examination of more-complex structures in the future, as greater analytical resources become available. For discussion of the details and limitations of the structural analysis software employed here, the interested reader is referred to CUREE-Caltech Woodframe Project Element 3 (in progress).

Design of the Index Buildings

Four basic building designs are used here, but each basic design is modeled three ways, with versions representing poor-quality construction, typical quality, and superior quality, making 12 versions (called index building variants, or IBVs) in all. In addition to these twelve buildings, seven seismic retrofit measures were designed and applied to several of the IBVs making a grand total of 19 distinct buildings analyzed. The four basic index buildings are now described; details of the variants and retrofits follow. The index buildings are the following:

1. **Small House.** A small single-family dwelling, 1,200 ft^2 in floor area, one story in height, with two bedrooms and one bathroom built about 1950. Its exterior walls are of stucco. The small house has a framed floor with perimeter cripple walls and post-and-pier interior under floor supports and is on a level site. It has gypsum wallboard for the interior wall finish, as would have been typical of a tract home, even though a custom-built house of this vintage likely would have plastered button-board. The superior-quality variant of the small house includes a perimeter concrete foundation extending to the underside of the floor framing. All walls have let-in braces, and no structural sheathing (plywood or oriented strandboard) is used. The small house is representative of homes built as part of a housing development in either northern or southern California. The design is based on prescriptive (conventional) construction, meaning that the designer and builder followed prescriptive rules in the building code and common construction practice in California. The small-house index building is estimated to cost $137,000 to replace. That is, if the same building were built today, construction would cost $137,000. This cost estimate is provided in Appendix F.

2. **Large House.** This building is representative of large single-family dwellings constructed in the late 1980s or early 1990s as part of housing developments in either northern or southern California. It is a two-story dwelling with three bedrooms, 2-1/2 bathrooms, 2,420 ft^2 in floor area, and an attached 400-ft^2 two-car garage. The house is on a level site with a slab on grade and spread footings. Exterior walls have stucco finish; interior walls are finished with gypsum wallboard. Many but not all walls have structural sheathing of plywood or oriented strandboard (OSB). The design is engineered in accordance with the Uniform Building Code, 1988 Edition (International Conference of Building Officials, 1988), meaning that an engineer used formulas in the building code to calculate forces and specified materials and design features to resist the calculated forces. The large house is estimated to cost $221,000 to build, as summarized in Appendix F.

3. **Townhouse.** This building is representative of residential townhouses constructed in early- to mid-1990s as part of housing developments in either northern or southern California. Each of three units is a 2,000 ft^2, two-story townhouse, with

three bedrooms, two bathrooms, and a 420-ft^2 garage under part of the living area. A two-story atrium breaks the external wall into two segments. The townhouse is on a level site with a slab on grade and spread footings. Exterior walls have stucco finish; interior walls are finished with gypsum wallboard. Many but not all walls have structural sheathing of plywood or OSB. The design is based on the 1988 Uniform Building Code (International Conference of Building Officials, 1988), with some details of lateral resistance conforming to Los Angeles area post-Northridge Earthquake design practice. The townhouse (all three units) would cost approximately $498,000 to build. This study examines the seismic vulnerability of the end unit in the three-unit building.

4. **Apartment Building.** This building is representative of multi-family apartment buildings constructed during the 1960s in either northern or southern California. A three-story, 13,700-ft^2 apartment building with ten 850-ft^2 units. Two levels of residential space are located above the ground-level tuck-under parking. The building is on a level site. The ground floor has a slab on grade with spread footings. The second and third floors and roof are wood framed. The walls are wood-framed at all levels. Exterior walls have stucco finish; interior walls are finished with gypsum wallboard. Many but not all walls have plywood structural sheathing. The longitudinal front wall is open to provide access to parking spaces on the ground level. This open-front configuration produces a soft-story effect that has proven to be hazardous in several recent earthquakes. The design is partially engineered in accordance with the 1964 Uniform Building Code (International Conference of Building Officials, 1964). The in-plane shear capacity was designed in accordance with the code requirements, but overturning was not considered nor provided for in the detailing, as would be required with engineered construction in recent years. The apartment building would cost approximately $797,000 to build.

Architectural and structural drawings are presented in Appendix B, showing plan views, exterior elevations and cross sections, and construction details in sufficient detail to define the structural model, create an inventory of assemblies, determine the required fragility functions, and to estimate unit repair costs and the replacement cost of the building. Note that the definition of the index buildings sufficient to conduct a detailed structural analysis is a novel feature of the method presented here, as compared with approaches that use model building types that are described in general terms.

Building Variants and Retrofit Measures

Objectives in Defining Variants

Some features of a building design contribute strongly to the average total earthquake repair cost. Some or all of these features also contribute significantly to the overall

uncertainty in total repair cost because of the high variability in their quality of construction or post-earthquake degradation. Of this latter group, the more one knows about their condition prior to an earthquake, the less uncertain one will be about future repair cost. This idea is illustrated schematically in Figure 4-1, which shows an unknown-quality vulnerability function with wide dispersion, compared with the three known-quality curves.

Figure 4-1:
Variants Selected to Reduce Total Uncertainty in Vulnerability

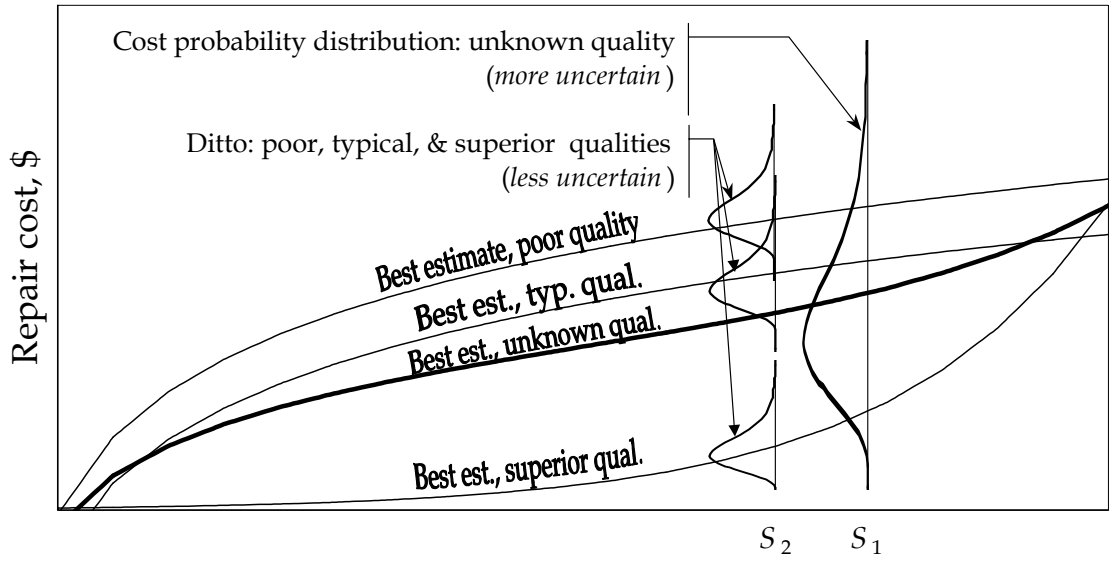

Objectives in Selecting Retrofit and Redesign Measures

The managers of the CUREE-Caltech Woodframe Project Element 3 (Building Codes and Standards) selected seven measures for benefit-to-cost evaluation in the present task. The measures include seismic retrofit of existing buildings, as well as redesigns appropriate for new construction, as opposed to application to existing buildings. Initial lists of items considered for evaluation came from:

- Element 1 (Testing and Analysis) research tasks;
- Current design issues, many of which are discussed in CUREE Publication W-01 (CUREE-Caltech Woodframe Project, 1999);
- Retrofit guidelines from the Uniform Code for Building Conservation (International Conference of Building Officials, 1997) and FEMA 273 (Federal Emergency Management Agency, 1997); and

- Common standard retrofit measures identified by ABS Consulting (formerly EQE International) and Caltech.

Many of the seven measures were included based on their potential, in the judgment of the Element-3 managers, to provide clear cost-to-benefit guidance for persons making policy decisions. Several measures were included in order to provide design methodology guidance.

The choice of measures was influenced by the programs used by Task 1.5.4 for analysis (Isoda *et al.*, 2001), which provide information on the system behavior, but are not appropriate for evaluation of small variations in detailing. Priority was given to measures seen as practical to include in construction today. Emerging technologies such as energy dissipation are not included, but could be considered in future studies. In addition to discussion provided in this report, results of these benefit-to-cost evaluations are discussed in the Element 3 report (CUREE-Caltech Woodframe Project, Element 3, in progress).

Description of Variants and of Retrofit and Redesign Measures

In the present study, engineers selected three to five key characteristics that contribute most strongly to repair cost, and defined these characteristics for a poor-quality, typical-quality, and superior-quality variant. Table 4-1 summarizes these features qualitatively, for all index buildings, variants, and retrofit measures. Features of the small-house variants and retrofit measure 1 are illustrated schematically in Figure 4-2. Detailed characteristics with numerical values of material strength, nail spacing and nailing quality, etc., follow.

Small house, poor quality. This variant has unbraced cripple walls with poor quality stucco (strength is 50 to 60% relative to laboratory test results for a high-quality specimen), poor quality stucco on the first floor walls (65 to 75% strength), poor nailing of interior gypsum wallboard (75% strength), and missing, cut, or split let-in braces (25% missing or inactive). The water heater is not strapped to the wall.

Small house, typical quality. The typical-quality variant has unbraced cripple walls with average quality stucco (80% strength), average quality stucco on the first floor walls (90% strength), good nailing of interior gypsum wallboard (80 to 90% strength), and good let-in braces (10% missing or inactive). The water heater is not strapped to the wall.

Table 4-1:
Selection of Variants and Retrofit Details

IB/V	Features
Small house	
Poor	Poor stucco cripple walls: low-strength, thin stucco; extensive degradation, poor furring and connection of mesh, poor anchorage
	Poor stucco finish on exterior walls, similar to cripple walls
	Poor nailing of interior walls: many missing, overdriven or common nails
	Extra mass: 3 layers of roofing material instead of 2
Typical	Average-quality stucco on cripple walls
	Exterior walls above floor level similar to cripple walls
	Good nailing of interior walls, few missing or over-driven nails.
Superior	Reinforced concrete stem wall instead of stucco cripple wall.
	Stucco: high strength, good thickness, good furring & connection of mesh, no deterioration
	Good nailing of interior walls
	Water heater strapped to wall
	Light mass: 1 layer of roofing instead of 2
Braced	Retrofit typical-quality variant with new partial-length plywood shearwalls at cripple walls
Large house	
Poor	Poor nailing of shearwalls and diaphragms
	Poor connections between structural elements
	Poor quality stucco
	Poor nailing of gypsum wallboard
Typical	Average nailing of shearwalls and diaphragms
	Average connections between structural elements
	Average-quality stucco
	Average nailing of gypsum wallboard
Superior	Good nailing of shearwalls and diaphragms
	Good connections between structural elements
	Good quality stucco
	Good nailing of gypsum wallboard
Waist walls	Redesign with structural sheathing added to exterior walls above & below openings
Immediate	Redesign to meet FEMA 273 (Federal Emergency Management Agency, 1997) IO performance
Occupancy	in BSE-1 event: thicker, high-grade sheathing, heavier, closer and heavier nailing
Rigid diaphragm	Redesign assuming rigid behavior of 2nd-floor diaphragm, flexible roof diaphragm
Townhouse	
Poor	Features similar to poor-quality large house
Typical	Features similar to typical-quality large house
Superior	Features similar to superior-quality large house
Limit drift	Redesign: thicker sheathing and foundation sills to produce more-uniform interstory drifts
Apartment	
Poor	Features similar to poor-quality large house
	Extra mass: 3 layers of roofing material
	Poor connection of pipe columns at parking
Typical	Features similar to typical-quality large house
	Good connection of pipe columns at parking
Superior	Features similar to superior-quality large house
	Light mass: 1 layer of roofing instead of 2
	Superior connection of pipe columns: bottom fixity, some moment resistance at top
Moment frames	Retrofit typical building with steel moment frames at garage openings
Shearwall	Redesign to add structural sheathing to wall at ground floor, wall line 2.5

Small house, superior quality. This variant includes a reinforced-concrete perimeter stem wall extending to the underside of the floor framing, where anchor bolts connect the concrete substructure to the wood superstructure. Stucco is of good quality (full strength, relative to laboratory tests of high-quality specimens), good nailing of interior gypsum wallboard (full strength), and good let-in braces (none missing or inactive). The water heater is strapped to the wall.

Small house, braced cripple walls. This retrofit of the typical-quality variant includes a partial length cripple wall retrofit to minimum standards set by 1997 UCBC (40% of wall length on each side), and replacement of damaged or misplaced existing sill anchor bolts. The water heater is strapped to the wall.

Figure 4-2:
Small-House Variants and Retrofit Measure

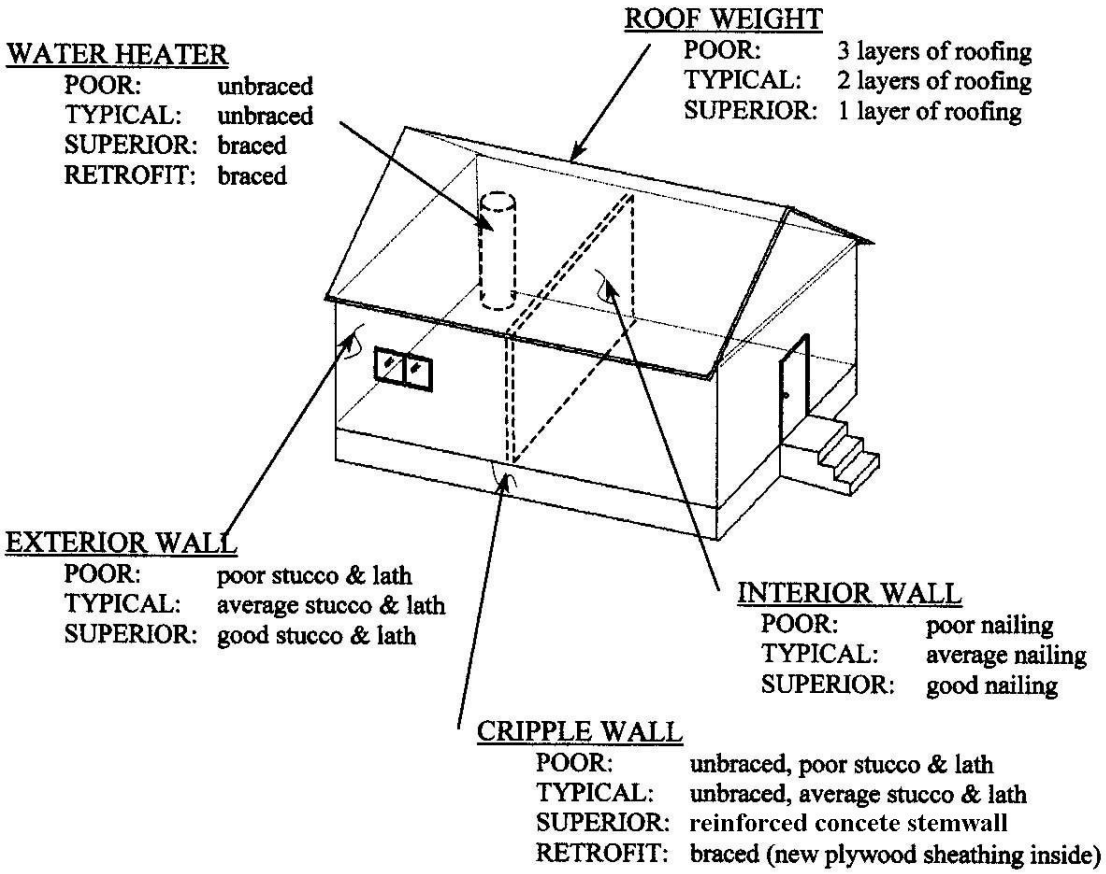

Large house, poor quality. This variant has poor nailing of shearwalls and diaphragms (20% stiffness reduction in diaphragms), poor connections between structural elements (15-20% reduction in shearwall stiffness), poor quality stucco (strength is 65 to 75%), and poor nailing of interior gypsum wallboard (strength is 85%).

Large house, typical quality. The typical-quality variant has average nailing of shearwalls and diaphragms (5% stiffness reduction in diaphragms), average connections between structural elements (5 to 10% reduction in shearwall stiffness), average quality stucco (strength is 90%), average nailing of interior gypsum wallboard (strength is 90%).

Large house, superior quality. This variant has good nailing of shearwalls and diaphragms, good connections between structural elements, good quality stucco and good nailing of gypsum wallboard. All components exhibit full strength, relative to high-quality laboratory test specimens.

Large house, waist-wall construction. This variant reflects typical-quality new construction using a perforated shearwall approach, wherein plywood or OSB structural sheathing above and below windows and doors is of the same material and nailing as the adjacent structural sheathing. This is in comparison to the poor, typical, and superior-quality variants in which scrap material is used above and below windows and doors, or stucco is simply tapered to mask the absence of sheathing.

Large house, immediate-occupancy redesign. This variant reflects new construction designed according to the requirements of FEMA 273 (Federal Emergency Management Agency, 1997) for immediate occupancy in the BSE-1 event (approximately 10% probability of exceedance in 50 years). The effect of this redesign is that structural sheathing is thicker, nails are more closely spaced, and other connections are significantly stronger than in the typical-quality variant.

Large house, rigid-diaphragm redesign. The rigid-diaphragm variant reflects new construction, designed according to the UBC, but assuming that floor diaphragms are rigid in their own plane. The effect of this assumption is that shearwalls are distributed differently than with a flexible-diaphragm design.

Townhouse, poor-quality. The poor-quality variant has poor nailing of shearwalls and diaphragms (20% stiffness reduction in diaphragms), poor connections between structural elements (15 to 20% reduction in shearwall stiffness), poor quality stucco (strength is 65 to 75%), poor nailing of interior gypsum wallboard (strength is 85%).

Townhouse, typical quality. This variant has average nailing of shearwalls and diaphragms (5% stiffness reduction in diaphragms), average connections between structural elements (5 to 10% reduction in shearwall stiffness), average quality stucco (strength is 90%), and average nailing of interior gypsum wallboard (strength is 90%).

Townhouse, superior quality. The superior-quality variant has good nailing of shearwalls and diaphragms, good connections between structural elements, good quality

stucco and good nailing of gypsum wallboard (all components exhibit strength and stiffness comparable with high-quality laboratory test specimens).

Townhouse, limited-drift redesign. This modification of the typical-quality variant is designed to limit drift. The effect of this redesign is thicker and more extensive use of structural sheathing and closer nailing.

Apartment building, poor quality. The poor quality variant has poor nailing of shearwalls and diaphragms (20% stiffness reduction in diaphragms), poor quality stucco (strength is 65 to 75%), poor nailing of interior gypsum wallboard (strength is 85%), and extra mass due to three layers of roofing.

Apartment building, typical quality. This variant has average nailing of shearwalls and diaphragms (5% stiffness reduction in diaphragms), average quality stucco (strength is 90%), average nailing of interior gypsum wallboard (strength is 90%). Roof mass is moderate, with two layers of roofing in place.

Apartment building, superior quality. The superior-quality variant has good nailing of shearwalls and diaphragms, good quality stucco and good nailing of gypsum wallboard, and light mass (one layer of roofing material).

Apartment building with steel frames. This retrofit of the typical-quality variant entails adding five moment-resisting steel moment frames at the ground floor open front.

Apartment building with shearwalls. In this redesign of the typical quality variant, column line 2.5 at the ground floor is designed as a longitudinal shearwall, with structural sheathing rather beneath the gypsum wallboard, based on Schmidt *et al.* (ND).

Note that several of these characteristics were selected based on the experience of a few structural engineers and researchers (Dave McCormick, John Shipp, Porter, and Scawthorn), who also judged numerical parameters such as strength of stucco relative to laboratory tests, for which little empirical data are available. In addition, as discussed by Isoda *et al.* (2001), judgment was employed to model the force-deformation behavior of some structural elements such as stucco. The interested reader is referred to Isoda *et al.* (2001, included in Appendix C of this report) for details of the structural-modeling effort.

Creation of Assembly Taxonomy and Inventory

The engineers involved in this task examined the structural drawings and those assemblies in each building that are damageable by the effects of ground shaking. Table 4-2 lists the distinct damageable components identified in the variants of the small house, next to a unique numerical identifier. Once the assembly types are defined, it is a matter of accounting to measure the quantity of each assembly type in each building, along with its location in terms of floor level and wall line.

These are not the only damageable components in the building, but it is believed that they are the ones that contribute the vast bulk of the potential earthquake-induced damage. Note also that the damageable components represent only a portion of the total replacement cost of the building. A cost estimator on the project team estimated the cost to replace the small house. The methodology used is described below, but it is worthwhile at this point to examine the fraction of building value comprising damageable components. Figure 4-3 shows how damageable components represent slightly less than half the value of the building. That is not to say that the more rugged components in the building are safe from loss: if the house were to collapse, the otherwise rugged components would have to be replaced as well.

As suggested above, the selection of damageable components depends on the nature of the hazards being considered. The present study considers shaking and excludes fire following earthquake, landsliding, liquefaction, lateral spreading, and tsunami. As ground failure is not considered in this analysis, foundations and floor slabs are excluded from the list of damageable components. As Osteraas points out (2001),

> **This approach is consistent with current and past practice of other loss-estimation methodologies. Damage to foundations or to concrete floor slabs of woodframe structures has historically been associated with earthquake-induced ground failure (fault rupture, landsliding, liquefaction, lateral spreading, densification). Foundation and concrete floor slab damage is generally addressed in loss-estimation models by use of a factor or factors associated with site-specific soil conditions. Northridge Earthquake claim history notwithstanding, actual earthquake-induced damage to foundations and concrete floor slabs of residential woodframe construction in the absence of earthquake-induced ground failure is extremely rare and not amenable to systematic analytical prediction. Estimation of losses associated with perceived, as opposed to actual, earthquake damage cannot be addressed with a methodology based on rigorous analysis.**

Table 4-2:
Principal Damageable Assemblies in the Index Buildings

Assembly Type	Description
4.5.110.2101.01	Exterior shearwall, 3/8 C-D ply, 2x4, 16" OC, 7/8" stucco ext, no interior finish
4.5.110.2101.02	Exterior shearwall, 15/32 C-D ply, 2x4, 16" OC, 7/8" stucco ext, no int. finish
4.5.110.2111.01	Exterior shearwall, 7/16 OSB, 2x4, 16" OC, 7/8" stucco ext, no interior finish
4.5.110.2501.01	Exterior wall, no structural sheathing, 2x4, 16" OC, 7/8" stucco ext, no int. fin.
4.6.152.1700.01	Doors, sliding, patio, aluminum, std., 6'-0"x6'-8", wood frame, insulated glass
4.7.100.3001.01	Windows, wood, double hung, standard glass, pane < 25 sf
4.7.110.6600.01	Window, Al frame, sliding, standard glass, pane < 25 sf
4.7.110.6609.01	Window, Al frame, fixed, standard glass, 80"x80" pane
6.1.510.1202.01	GWB partition, no structural sheathing, 1/2" GWB one side, 2x4, 16" OC
6.1.510.1203.01	GWB finish, 1/2", one side, on 2x4, 16"OC
6.1.520.1201.01	Interior shearwall, 3/8 C-D ply, 2x4, 16" OC, 1/2" GWB finish one side
6.1.520.1201.02	Interior shearwall, 15/32 C-D ply, 2x4, 16" OC, 1/2" GWB finish one side
6.1.520.1202.01	Interior sheathing, 3/8 C-D ply, 1/2" GWB finish one side, on 2x4 16" OC
6.1.520.1202.02	Interior sheathing, 15/32 C-D ply, 1/2" GWB finish one side, on 2x4, 16" OC
6.1.520.1211.01	Interior shearwall, 7/16 OSB, 2x4, 16" OC, 1/2" GWB finish one side
6.1.520.1212.01	Interior sheathing, 7/16 OSB, 1/2" GWB finish one side, on 2x4 16" OC
8.1.160.1820.01	Electric water heater, residential, 100F rise, 50 gal, 9 kW 37 GPH

Figure 4-3:
Breakout of Construction Costs for the Small House

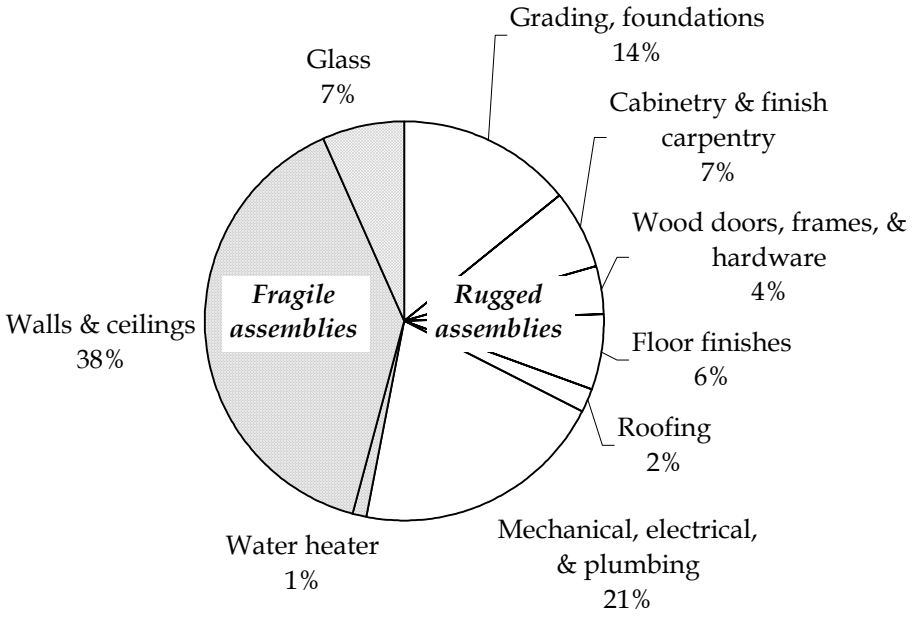

Structural Modeling

Appendix C contains a detailed report by Isoda *et al.* (2001) on the structural modeling performed by UCSD. In summary, the authors create a deterministic structural model for each index building, variant, and retrofit. The structural model involves idealizing the major building components as springs and masses, and assembling them in a mathematical idealization of the building. The concept is shown schematically in Figure 4-4, in which the walls, floors, and ceilings have been replaced by linear and rectangular spring elements, and by point masses (the black dots in the figure).

The masses represent all the building components with significant weight, such as the walls, ceiling, floor, windows, and roofing. The springs represent building elements (e.g., walls, ceilings, columns, beams, etc.) that resist deformation. For example, it requires a particular level of load (i.e., force) to cause the top of a wall to move relative to the bottom of the wall, just as it takes a certain amount of load to cause a spring to extend or contract by a certain amount. In both cases—the wall and the spring—the ratio of the load to the deformation is a measure of stiffness.

Figure 4-4:
Idealized Structural Model of a Building (Isoda *et al.*, 2001)

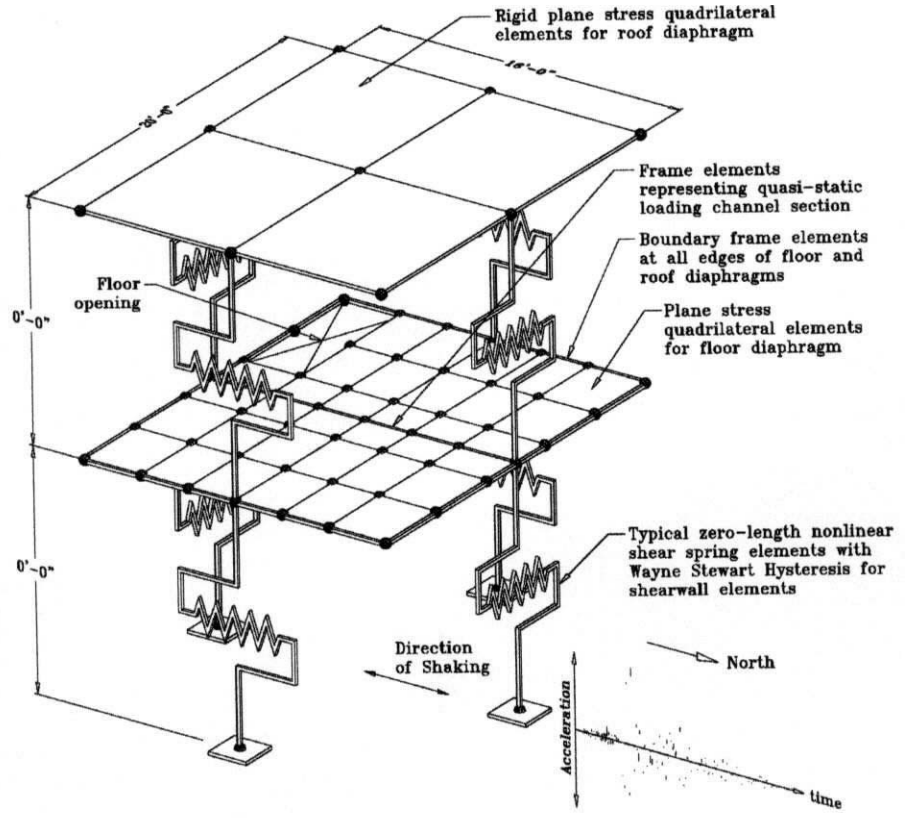

It is sometimes quite difficult to create these idealized springs. The relationship between load and deformation in structural elements can be complex and has been the subject of extensive engineering research. In the present study, the wall, ceiling, and floor elements are analyzed using a recently developed software program called CASHEW (an acronym standing for Cyclic Analysis of Shearwalls; see Folz *et al.*, 2001). CASHEW is used to create idealized springs that represent the complicated collection of nails, wood studs (typically the 2x4s inside the wall) and sheathing panels (e.g., sheets of plywood, oriented strandboard, or wallboard covering the studs) that comprise the typical shearwall. CASHEW is capable of showing how a shearwall degrades—grows weaker and more flexible—as it is subjected to repeated back-and-forth loading, based solely on knowledge of how the nails, studs, and sheathing panels behave individually, and how they are assembled. The extensive experimental knowledge base is described in Folz *et al.* (2001).

Calculating the masses is much simpler. The materials that comprise a building are very familiar, as is their weight per unit length, area, volume, etc. (i.e., their *unit weight*). It is a matter of simple bookkeeping to add up the length of wood studs in a particular wall, the square footage of plywood, etc., multiply these quantities by their unit weights, and sum the total. The total weight, divided by the acceleration due to gravity, gives the mass.

Next, the masses and spring parameters are input to a structural analysis program, which can calculate how each point in the building displaces when subjected to given forces or ground accelerations. (Recall that CASHEW calculates idealized spring values; it does not perform the actual structural analysis on the entire building.) In the present study, a software code called Ruaumoko and developed in New Zealand is used to perform the structural analysis (Carr, 1998). (Ruaumoko is the Maori god of earthquakes.) This software package offers a variety of advantages over more familiar programs, chief amongst them being that it allows one to account for strength and stiffness degradation of the building elements, along with other complications called nonlinearities. (The meaning of nonlinearity is probably of marginal interest to the non-technical reader. Suffice it to say that the use of a structural analysis package that accounts for various nonlinearities produces a more-accurate picture of likely building performance.)

Next, uncertainties in the structural model are accounted for. (Note that Isoda *et al.* [2001] do not address randomness in mass and damping. The present authors modified Isoda's results before performing the actual structural analyses, to account for these uncertainties.) Mass, damping, and stiffness are never known perfectly, and can be treated as random variables. In the present study, uncertainty in stiffness is addressed deterministically (i.e., not randomly) through the use of poor, typical, and superior-quality variants. Many of the variant features are defined in terms of how the strength (and indirectly, the stiffness) differs from the average value. Thus, uncertainty in stiffness is treated deterministically here. However, mass and damping were treated as

random variables. (Damping is a measure of how much energy the building disperses, in the same way that a car's shock absorbers disperse energy when the car hits a pothole.)

The findings of Ellingwood *et al.* (1980) help to account for uncertain mass. The authors report that masses measured in the field after various buildings were constructed were on average 5% greater than those calculated by the structural engineer who performed the design. Furthermore, the masses varied by ±10% (that is, the coefficient of variation, a measure of uncertainty, is 0.10) from the average measured value. All masses in a building model were allowed to vary in this way, and 20 simulations of each model were created for use in the structural analysis. Likewise, damping was randomly distributed in these 20 simulations. Camelo *et al.* (2001) find that in a number of woodframe buildings that experienced strong motion, damping ranges between 10% ± 3%.

Thus, for each index building variant and retrofit model, 20 randomized models were created to account for uncertainties in the mass, damping, and stiffness characteristics of the building.

Ground Motions and Structural Analysis

As discussed in Chapter 3, once the structural models are created, the analyst performs a series of structural analyses of random variations of the basic model, subjecting the models to various earthquakes. In the present study, earthquake recordings were taken from Phase 2 of the SAC Steel Project (Somerville *et al.*, 1997). These ground motions were developed for the Los Angeles region, and were therefore considered appropriate for use here.

For each level of shaking intensity, 20 recordings were selected at random from among the 100 provided by Somerville *et al.* (1997). Each recording was scaled (magnified up or down) to match the desired shaking intensity. As noted in Chapter 3, shaking intensity can be measured a variety of ways. In the present study, spectral acceleration (S_a) was used. Spectral acceleration is somewhat like peak ground acceleration, but it is much more strongly predictive of how much a particular structure will deform in an earthquake. The reason has to do with resonance between the earthquake and the building. If the earthquake resonates with the building, i.e., if it tends to push the building at the same frequency as the building's natural mode of vibration, then the building will respond much more strongly than if the earthquake does not resonate with the building. Spectral accelerations of the subject ground motions were calculated using BiSpec (Hachem, 2000).

A building has an inherent tendency to complete one to-and-fro cycle of motion in a particular amount of time, that is, its natural period, in the same way that a pendulum or tuning fork does. (Actually, buildings have many natural periods, each corresponding to a mode of vibration, but the important ones are the first few, that is, the longer ones. The longest one is called the fundamental period.) The period used to scale ground motions

was the small-amplitude fundamental period of the building according to the formula developed by Camelo *et al.* (2001), which estimates building period as a function of building height.

A building also has a tendency to cease vibrating after in the absence of ground motion or other excitation, just as a pendulum will. The rate at which this vibrational energy is removed is measured by the damping ratio; a higher damping ratio indicates a more-rapid removal of this energy. In the base of buildings, the damping ratio is typically on the order of 2% to 15%. Camelo *et al.* (2001) estimated that woodframe buildings have on average a damping ratio of 10%, based on system-identification analysis of several woodframe buildings that were subjected to strong motion or forced vibration. Based on the observations of Camelo *et al.* (2001), a 0.40 coefficient of variation on the damping ratio is reflected in the model simulations. The periods and damping ratios for the index buildings addressed here are shown in Table 4-3.

Table 4-3:
Fundamental Period and Damping Ratios Used to Scale Ground Motions.

Index building (all variants)	Height	Estimated period, sec.	Damping, % critical
Small house	12 ft.	0.13	10%
Large house	20 ft.	0.17	10%
Townhouse	22 ft.	0.18	10%
Apartment	30 ft.	0.21	10%

Ground motions for use in the analyses were selected at random from among those of Somerville *et al.* (1997), with certain constraints. First, these ground motions are provided in pairs, i.e., one recorded in the *x*-direction at a particular site in a particular earthquake, one in the *y*-direction for the same site and earthquake. These pairs were always used together. Furthermore, there are limits on how much one should scale a ground motion. The nature of these limits is discussed in Somerville *et al.* (1997). Suffice it to say that recordings were selected so that they need not be scaled by more than ±50%. Additional considerations led to the following set of rules for selecting ground motions:

1. Prefer records whose $0.5*(S_a(\text{record})) \leq \text{scaled}(S_a) \leq 1.5*(S_a(\text{record}))$, i.e., maximum ± 50% scaling. Since each record in Somerville *et al.* (1997) is one of an (*x, y*) pair, the S_a for the pair is taken as the maximum of the two directions, when measured at the period and mean damping ratio of the building of interest.
2. Prefer real records over simulated.
3. Prefer California records to non-California records.

4. If more than 20 meet these criteria, select 20 at random for a given level of S_a.
5. If fewer than 20 meet these criteria, ignore criterion 3 and select 20 at random for each level of S_a.
6. If still fewer than 20 meet these criteria, ignore criterion 2 and select 20 at random for each S_a.
7. If still fewer than 20 meet these criteria, relax criterion 1 (lower min scaling, higher max) until 20 are selected for each S_a. (This rule has had to be applied primarily for low values of S_a, of 0.3g and below).

The ground motions used for the analysis of the small house are shown in Table 4-4. Ground motions and scaling factors used for the large house, townhouse, and apartment buildings are shown in Table 4-5, Table 4-6, and Table 4-7, respectively. In the tables, each row corresponds to a ground motion record used as the *x*-direction excitation in one or more analyses. The *y*-direction ground motion is always the other in the pair provided by Somerville *et al.* (1997). The table columns correspond to a level of shaking intensity, measured in terms of S_a. The values in the table are the scaling factors used. Thus, the first row of Table 4-4 shows that record LA01 is scaled by 0.53 and applied as the *x*-direction ground motion to the small house to simulate an earthquake with S_a = 0.8 g. (Its complement, LA02, is applied to the *y*-direction, and is also scaled by 0.53.)

Thus, for each index building variant (IBV), 20 randomized models (random mass and damping) were prepared. Nonlinear time-history structural analyses were performed, 20 each for each ground shaking intensity from $S_a = 0.1g$, $0.2g$, … $2.0g$, for a total of 400 nonlinear time-history structural analyses per IBV. The maximum responses were captured from each analysis, including peak diaphragm accelerations, peak transient drift ratios at each story and wall line, and shear strains in floor and ceiling diaphragms. (Analysis of the small house index building indicated that ceiling and floor shear strains and consequent damage was negligible. Thereafter these assemblies were assumed to be rugged.)

Table 4-4:
Ground Motions and Scaling Factors Used with Small House.

X-direction record	Spectral acceleration, g																			
	0.1	0.2	0.3	0.4	0.5	0.6	0.7	0.8	0.9	1.0	1.1	1.2	1.3	1.4	1.5	1.6	1.7	1.8	1.9	2.0
LA01									0.85		1.03		1.22		1.41		1.60	1.69	1.78	1.88
LA02								0.75	0.85	0.94					1.41	1.50				
LA03								0.76			1.04		1.23	1.32	1.42			1.70	1.80	1.89
LA04										0.95		1.14				1.51	1.61		1.80	1.89
LA05	0.24	0.49	0.73	0.97	1.21	1.46	1.70	1.94												
LA06	0.24	0.49	0.73	0.97	1.21	1.46		1.94												
LA07	0.16	0.31	0.47	0.63	0.78		1.10			1.57	1.73									
LA08	0.16	0.31	0.47	0.63	0.78	0.94	1.10		1.41											
LA09	0.16	0.32	0.49	0.65	0.81	0.97	1.14	1.30	1.46											
LA10	0.16	0.32	0.49	0.65	0.81	0.97	1.14		1.46	1.62	1.78	1.95								
LA11																		0.73	0.77	
LA12																		0.73	0.77	
LA13									0.71									1.41		1.57
LA14									0.71		0.86	0.94					1.34		1.49	1.57
LA15						0.76	0.89	1.02	1.14	1.27		1.53	1.65	1.78	1.91					
LA16						0.76		1.02	1.14			1.53			1.91					
LA17										0.79	0.87	0.95	1.03	1.11		1.27	1.34			
LA18									0.71	0.79	0.87	0.95	1.03	1.11		1.27	1.34	1.42	1.50	
LA19																0.69	0.73	0.78	0.82	0.86
LA20																	0.73			
LA23	0.16	0.33	0.49	0.66	0.82	0.99	1.15			1.65										
LA24	0.16	0.33	0.49	0.66	0.82	0.99	1.15			1.65		1.98								
LA25									0.70						1.17		1.33	1.41		
LA26									0.70		0.86		1.02		1.17	1.25	1.33	1.41		1.56
LA27														0.68				0.87		
LA28																	0.83		0.92	
LA29																0.69	0.73			
LA30																			0.82	0.86
LA39	0.17	0.33	0.50	0.66																
LA40	0.17	0.33	0.50	0.66																
LA41										0.69	0.76				1.03	1.10			1.31	1.38
LA42										0.69	0.76	0.83		0.96	1.03	1.10	1.17	1.24		1.38
LA43	0.51	1.02	1.53																	
LA44	0.51	1.02	1.53																	
LA45	0.48	0.96	1.44	1.92																
LA46	0.48	0.96	1.44	1.92																
LA47	0.15	0.31	0.46	0.61	0.77	0.92		1.23				1.84	1.99							
LA48	0.15	0.31	0.46	0.61	0.77	0.92	1.07	1.23	1.38	1.53			1.99							
LA49						0.74	0.86	0.98												
LA50							0.86				1.35		1.59	1.72		1.96				

Table 4-4:
Ground Motions and Scaling Factors Used with Small House. (Cont.)

X-direction record	Spectral acceleration, g																			
	0.1	0.2	0.3	0.4	0.5	0.6	0.7	0.8	0.9	1.0	1.1	1.2	1.3	1.4	1.5	1.6	1.7	1.8	1.9	2.0
LA51												0.91	0.99		1.14	1.21	1.29			1.52
LA52									0.68		0.83		0.99					1.37	1.44	
LA53										0.68		0.82	0.89				1.16	1.23		1.37
LA54										0.68			0.89			1.09	1.16	1.23	1.30	
LA55									0.71		0.86	0.94		1.10	1.18	1.26			1.49	
LA56									0.71	0.79		0.94		1.10	1.18			1.41	1.49	1.57
LA57	0.17	0.34	0.51	0.68	0.85	1.02	1.19		1.54		1.88									
LA58	0.17	0.34	0.51	0.68	0.85	1.02														
LA59							0.68					1.17	1.27	1.36	1.46	1.56	1.66	1.75		1.95
LA60							0.68		0.88			1.17	1.27	1.36	1.46		1.66		1.85	1.95
NF01														0.70		0.80	0.85	0.90	0.95	1.00
NF02														0.70		0.80		0.90	0.95	1.00
NF03					0.66	0.80		1.06			1.46		1.72	1.86	1.99					
NF04					0.66	0.80	0.93	1.06			1.46	1.59			1.99					
NF05					0.68	0.81	0.95	1.08	1.22			1.63	1.76							
NF06					0.68	0.81	0.95	1.08		1.36	1.49	1.63		1.90						
NF07				0.57	0.71	0.85		1.14						1.99						
NF08				0.57	0.71	0.85	0.99	1.14	1.28	1.42	1.56									
NF09	0.17	0.35	0.52	0.70	0.87															
NF10	0.17	0.35	0.52	0.70	0.87															
NF11								0.73		0.92			1.19	1.28	1.37	1.46	1.56		1.74	1.83
NF12														1.28	1.37	1.46		1.65		

Table 4-5:
Ground Motions and Scaling Factors Used with Large House.

X-direction record	Spectral acceleration, g																			
	0.1	0.2	0.3	0.4	0.5	0.6	0.7	0.8	0.9	1.0	1.1	1.2	1.3	1.4	1.5	1.6	1.7	1.8	1.9	2.0
LA01	True	True								0.71	0.80	0.89					1.33		1.51	1.60
LA02	True	True								0.71		0.89	0.98		1.16					
LA03	True	True							0.67		0.87		1.06	1.16	1.25	1.35			1.64	1.73
LA04	True	True							0.67				1.06	1.16		1.35	1.44	1.54		1.73
LA05	True	True	0.24	0.48	0.71	0.95	1.19	1.43	1.66	1.90										
LA06	True	True	0.24	0.48	0.71	0.95	1.19	1.43												
LA07	True	True	0.17	0.34	0.51	0.68	0.85	1.03	1.20	1.37		1.71	1.88							
LA08	True	True	0.17	0.34	0.51	0.68	0.85	1.03	1.20	1.37			1.88							
LA09	True	True	0.14	0.29	0.43	0.58	0.72	0.87	1.01		1.30		1.59		1.88					
LA10	True	True	0.14	0.29	0.43	0.58	0.72	0.87	1.01						1.88					
LA11	True	True																		
LA12	True	True																		0.68
LA13	True	True										0.68	0.74	0.81	0.88	0.95		1.08	1.15	1.22
LA14	True	True										0.68	0.74							
LA15	True	True						0.69	0.80	0.91	1.03	1.14	1.26		1.48	1.60	1.71	1.83		
LA16	True	True						0.69		0.91	1.03			1.37				1.83		
LA17	True	True								0.68	0.77			1.02			1.28	1.36	1.45	
LA18	True	True									0.77		0.94	1.02	1.11	1.19	1.28	1.36	1.45	1.53
LA19	True	True																	0.69	0.73
LA20	True	True																		0.73
LA23	True	True	0.15	0.29	0.44	0.59	0.73	0.88	1.03				1.62							
LA24	True	True	0.15	0.29	0.44	0.59	0.73	0.88	1.03	1.17		1.47		1.76						
LA25	True	True										0.70		0.84		0.98	1.05	1.12		
LA26	True	True											0.77	0.84	0.91		1.05			1.26
LA27	True	True													0.68					0.94
LA28	True	True														0.73		0.84		
LA29	True	True																	0.68	0.72
LA30	True	True																	0.68	
LA41	True	True															0.83		0.94	0.99
LA42	True	True															0.83		0.94	
LA43	True	True	0.50		1.50	2.00														
LA44	True	True	0.50	1.00	1.50	2.00														
LA45	True	True	0.39	0.78	1.17	1.56	1.95													
LA46	True	True	0.39	0.78	1.17	1.56	1.95													
LA47	True	True					0.66	0.79	0.93	1.06	1.19		1.45		1.72	1.85				
LA48	True	True					0.66	0.79		1.06	1.19		1.45	1.59	1.72					
LA49	True	True							0.74	0.85		1.06		1.27	1.38			1.70		1.91
LA50	True	True							0.74		0.95	1.06	1.17			1.48	1.59	1.70		1.91
LA51	True	True									0.73		0.89	0.97		1.14			1.38	
LA52	True	True										0.81				1.14	1.22	1.30	1.38	
LA53	True	True														0.68		0.78	0.83	0.88
LA54	True	True														0.68	0.73		0.83	
LA55	True	True									0.98			1.31			1.63		1.85	1.96
LA56	True	True							0.76		0.98	1.09	1.20		1.41		1.63		1.85	
LA57	True	True	0.19	0.38	0.57	0.76	0.95	1.15	1.34	1.53	1.72									
LA58	True	True	0.19	0.38	0.57	0.76	0.95	1.15		1.53										

Table 4-5:
Ground Motions and Scaling Factors Used with Large House (Cont.)

X-direction record	Spectral acceleration, g																			
	0.1	0.2	0.3	0.4	0.5	0.6	0.7	0.8	0.9	1.0	1.1	1.2	1.3	1.4	1.5	1.6	1.7	1.8	1.9	2.0
LA59	True	True								0.76	0.86	0.95		1.14	1.24	1.33	1.43	1.52	1.62	1.71
LA60	True	True												1.14	1.24					
NF01	True	True																0.72		
NF02	True	True															0.68	0.72		
NF03	True	True						0.73	0.86	0.98	1.10	1.22		1.47	1.59	1.71				
NF04	True	True						0.73		0.98	1.10		1.35	1.47		1.71				
NF05	True	True	0.14	0.29	0.43	0.57	0.71	0.86	1.00	1.14		1.43	1.57							
NF06	True	True	0.14	0.29	0.43	0.57	0.71	0.86	1.00		1.28			1.71	1.85					
NF07	True	True	0.14	0.28	0.42	0.56	0.70	0.84	0.98		1.27	1.41	1.55		1.83					
NF08	True	True	0.14	0.28	0.42	0.56	0.70	0.84	0.98	1.13		1.41								
NF09	True	False	0.15	0.30	0.45	0.61	0.76													
NF10	True	False	0.15	0.30	0.45	0.61	0.76													
NF11	True	True									0.86	0.95		1.14		1.33		1.52	1.62	1.71
NF12	True	True														1.33	1.43	1.52		
NF13	True	True										0.83		1.00		1.17	1.25			
NF14	True	True													1.08		1.25	1.33	1.42	
NF15	True	True								0.73		0.91				1.27	1.36	1.45	1.54	1.63
NF16	True	True													1.18			1.45		1.63

Table 4-6:
Ground Motions and Scaling Factors Used with Townhouse

X-direction record	Spectral acceleration, g																			
	0.1	0.2	0.3	0.4	0.5	0.6	0.7	0.8	0.9	1.0	1.1	1.2	1.3	1.4	1.5	1.6	1.7	1.8	1.9	2.0
LA01									0.79	0.87		1.05		1.22	1.31	1.4	1.49			1.75
LA02									0.79					1.22		1.4	1.49	1.57		
LA03											1.15			1.47	1.57	1.68		1.89	1.99	
LA04							0.73	0.84	0.94				1.36	1.47	1.57			1.89	1.99	
LA05	0.24	0.48	0.72	0.96	1.2	1.44	1.68	1.92												
LA06	0.24	0.48	0.72	0.96	1.2	1.44	1.68													
LA07	0.16	0.33	0.49	0.66	0.82	0.99	1.15	1.32		1.64										
LA08	0.16	0.33	0.49	0.66	0.82	0.99	1.15			1.64		1.97								
LA09					0.66	0.79	0.93	1.06							1.98					
LA10				0.53	0.66	0.79	0.93						1.72		1.98					
LA11																				0.73
LA12																			0.7	0.73
LA13												0.81					1.15			
LA14											0.74	0.81	0.88		1.02	1.08		1.22	1.29	
LA15								0.89	1	1.11	1.22						1.89			
LA16							0.78				1.22					1.77		2		
LA17									0.79	0.88	0.97		1.14					1.58	1.67	1.75
LA18									0.79						1.32					
LA19																			0.83	0.87
LA20																0.7	0.74		0.83	
LA23	0.15	0.3	0.45	0.6	0.75	0.91		1.21		1.51		1.81	1.96							
LA24	0.15	0.3	0.45	0.6	0.75	0.91		1.21	1.36			1.81								
LA25										0.68	0.75		0.89	0.95	1.02		1.16	1.23		1.36
LA26												0.82	0.89		1.02	1.09	1.16			
LA27													0.7		0.81	0.86	0.92		1.02	1.08
LA28													0.7				0.92	0.97	1.02	1.08
LA29																		0.74		
LA30																	0.7	0.74		
LA39	0.14	0.28	0.41	0.55																
LA40	0.14	0.28	0.41	0.55																
LA41												0.69	0.75	0.81		0.92		1.04	1.1	1.15
LA42															0.86					1.15
LA43	0.5	1.01	1.51																	
LA44	0.5	1.01	1.51																	
LA45	0.35	0.71	1.06	1.42	1.77															
LA46	0.35	0.71	1.06	1.42	1.77															
LA47				0.52	0.65	0.78	0.91	1.05		1.31		1.57			1.96					
LA48					0.65	0.78			1.18		1.44		1.7	1.83						
LA49						0.69		0.92	1.03	1.15				1.61			1.95			
LA50						0.69	0.8			1.15	1.26	1.38		1.61						
LA51									0.68	0.76	0.84			1.06			1.29		1.45	1.52
LA52											0.84	0.91			1.14	1.22	1.29			1.52
LA53														0.68		0.78		0.87	0.92	
LA54														0.68	0.73				0.92	
LA55								0.88		1.11	1.22	1.33	1.44			1.77	1.88	1.99		
LA56							0.77	0.88	1	1.11	1.22	1.33	1.44		1.66	1.77	1.88	1.99		

Table 4-6:
Ground Motions and Scaling Factors Used with Townhouse (Cont.)

X-direction record	Spectral acceleration, g																			
	0.1	**0.2**	**0.3**	**0.4**	**0.5**	**0.6**	**0.7**	**0.8**	**0.9**	**1.0**	**1.1**	**1.2**	**1.3**	**1.4**	**1.5**	**1.6**	**1.7**	**1.8**	**1.9**	**2.0**
LA57	0.18	0.36	0.54	0.72	0.9	1.08	1.26	1.44												
LA58	0.18	0.36	0.54	0.72	0.9	1.08	1.26	1.44												
LA59									0.78			1.04	1.13		1.3		1.48	1.56	1.65	
LA60										0.87	0.95			1.22			1.48	1.56		1.74
NF01																0.67	0.71		0.79	0.83
NF02																0.67			0.79	0.83
NF03						0.73	0.85		1.09	1.21	1.33	1.45	1.58	1.7		1.94				
NF04						0.73		0.97	1.09	1.21	1.33	1.45	1.58	1.7		1.94				
NF05	0.14	0.29	0.43	0.58	0.72	0.87	1.01	1.16	1.3		1.59	1.74								
NF06	0.14	0.29	0.43	0.58	0.72	0.87	1.01			1.45			1.88							
NF07	0.14	0.28	0.42	0.56	0.7	0.84	0.98	1.12		1.4			1.82							
NF08	0.14	0.28	0.42	0.56	0.7	0.84	0.98	1.12	1.26		1.54	1.68		1.96						
NF09	0.14	0.27	0.41	0.54	0.68															
NF10	0.14	0.27	0.41	0.54	0.68															
NF11							0.68	0.78	0.87			1.16	1.26	1.36	1.46	1.55				1.94
NF12							0.68	0.78	0.87	0.97	1.07	1.16			1.46	1.55		1.75	1.84	
NF13										0.83	0.91		1.07	1.16			1.41	1.49	1.57	1.65
NF14									0.74					1.16	1.24		1.41	1.49	1.57	1.65
NF15											0.98			1.25	1.34	1.43			1.7	1.78
NF16								0.71	0.8									1.61		1.78

Table 4-7:
Ground Motions and Scaling Factors Used with Apartment Building

X-direction record	Spectral acceleration, g																			
	0.1	**0.2**	**0.3**	**0.4**	**0.5**	**0.6**	**0.7**	**0.8**	**0.9**	**1.0**	**1.1**	**1.2**	**1.3**	**1.4**	**1.5**	**1.6**	**1.7**	**1.8**	**1.9**	**2.0**
LA01									0.84			1.12	1.21	1.30		1.49	1.58	1.68		1.86
LA02								0.74	0.84	0.93	1.02							1.68	1.77	1.86
LA03							0.74							1.48	1.59	1.69	1.80	1.90		
LA04							0.74				1.16			1.48		1.69	1.80			
LA05	0.22	0.43	0.65	0.87	1.08	1.30	1.52	1.73	1.95											
LA06	0.22	0.43	0.65	0.87	1.08	1.30	1.52	1.73	1.95											
LA07	0.15	0.29	0.44	0.58	0.73	0.88	1.02	1.17	1.31				1.90							
LA08	0.15	0.29	0.44	0.58	0.73			1.17			1.60	1.75	1.90							
LA09						0.73	0.85	0.98				1.46	1.59		1.83	1.95				
LA10						0.73	0.85		1.10	1.22		1.46	1.59	1.71	1.83	1.95				
LA11																		0.67	0.71	0.74
LA12																				0.74
LA13										0.68				0.95		1.08	1.15			1.35
LA14														0.95	1.01	1.08		1.22		
LA15							0.73	0.83	0.94	1.04	1.14				1.56	1.66	1.77	1.87	1.98	
LA16								0.83	0.94					1.46	1.56			1.87	1.98	
LA17									0.79	0.88		1.05	1.14	1.23	1.32		1.49		1.67	1.76
LA18											0.97				1.32	1.41			1.67	
LA19																	0.67	0.71	0.75	0.79
LA20																	0.67	0.71	0.75	
LA23	0.16	0.32	0.48	0.64	0.80	0.97		1.29				1.93								
LA24	0.16	0.32	0.48	0.64	0.80	0.97	1.13					1.93								
LA25													0.83	0.89		1.02			1.21	
LA26																			1.21	
LA27																0.86	0.92	0.97	1.03	1.08
LA28															0.81	0.86		0.97		
LA29																		0.70		0.78
LA30																				0.78
LA39					0.63															
LA40					0.63															
LA41										0.71			0.92	0.99	1.06		1.20		1.34	1.41
LA42													0.92	0.99	1.06		1.20			
LA43	0.45	0.91	1.36	1.82																
LA44	0.45	0.91	1.36	1.82																
LA45	0.36	0.72	1.09	1.45	1.81															
LA46	0.36	0.72	1.09	1.45	1.81															
LA47	0.15	0.30	0.45	0.60	0.74	0.89	1.04	1.19		1.49	1.64	1.79								
LA48	0.15	0.30	0.45	0.60	0.74	0.89	1.04	1.19	1.34			1.79								
LA49						0.67			1.00	1.11		1.33				1.78				
LA50						0.67	0.78		1.00	1.11		1.33	1.44		1.67	1.78				
LA51										0.74	0.81	0.89	0.96		1.11		1.26	1.33		1.48
LA52													0.96	1.04				1.33	1.40	1.48
LA53														0.71			0.86	0.92	0.97	1.02
LA54														0.71			0.86		0.97	1.02
LA55	0.14	0.28	0.42	0.56	0.71	0.85	0.99		1.27	1.41	1.55	1.69								
LA56	0.14	0.28	0.42	0.56	0.71	0.85	0.99	1.13	1.27					1.98						

Table 4-7:
Ground Motions and Scaling Factors Used with Apartment Building (Cont.)

X-direction record	Spectral acceleration, g																			
	0.1	0.2	0.3	0.4	0.5	0.6	0.7	0.8	0.9	1.0	1.1	1.2	1.3	1.4	1.5	1.6	1.7	1.8	1.9	2.0
LA57	0.18	0.35	0.53	0.71	0.88			1.41			1.95									
LA58	0.18	0.35	0.53	0.71	0.88	1.06	1.24	1.41	1.59	1.77										
LA59										0.72	0.80	0.87	0.94		1.09	1.16			1.38	1.45
LA60														1.01	1.09		1.23	1.30		1.45
NF01																				0.79
NF02																	0.67		0.75	0.79
NF03						0.74	0.87	0.99			1.37		1.61		1.86	1.99				
NF04						0.74	0.87		1.12				1.61		1.86					
NF05	0.14	0.29	0.43	0.58	0.72	0.87	1.01	1.16			1.59	1.74								
NF06	0.14	0.29	0.43	0.58	0.72	0.87		1.16	1.30	1.45	1.59	1.74								
NF07	0.14	0.28	0.42	0.56	0.70	0.84	0.97			1.39				1.95						
NF08	0.14	0.28	0.42	0.56	0.70	0.84			1.25	1.39	1.53	1.67								
NF11							0.73	0.83		1.04	1.15		1.36	1.46	1.57	1.67	1.77	1.88		
NF12								0.83		1.04	1.15	1.25	1.36	1.46		1.67	1.77			
NF13									0.70	0.78	0.86		1.02		1.17			1.41	1.49	
NF14											0.86	0.94		1.10			1.33	1.41	1.49	1.57
NF15								0.70		0.88	0.96	1.05	1.14		1.32	1.40		1.58		
NF16									0.79		0.96		1.14			1.40	1.49		1.67	
LA57	0.18	0.35	0.53	0.71	0.88			1.41			1.95									
LA58	0.18	0.35	0.53	0.71	0.88	1.06	1.24	1.41	1.59	1.77										
LA59										0.72	0.80	0.87	0.94		1.09	1.16			1.38	1.45
LA60														1.01	1.09		1.23	1.30		1.45
NF01																				0.79

Structural Analysis Results

Some intermediate results are of interest here. Figure 4-5 illustrates the kinds of response data compiled during structural analysis. The left-hand figure shows samples of the peak transient interstory drift ratio in the large house, typical quality variant, on the first story, along column line 3. The right-hand figure shows similar statistics for the apartment building, poor-quality variant, at the second story, along column line G. In each case, each of the 400 dots represents one simulation: one combination of spectral acceleration, ground motion, mass, and damping. Such structural response values are gathered for each column line, each floor, and each simulation.

Figure 4-5:
Samples of Peak Interstory Drift Ratio

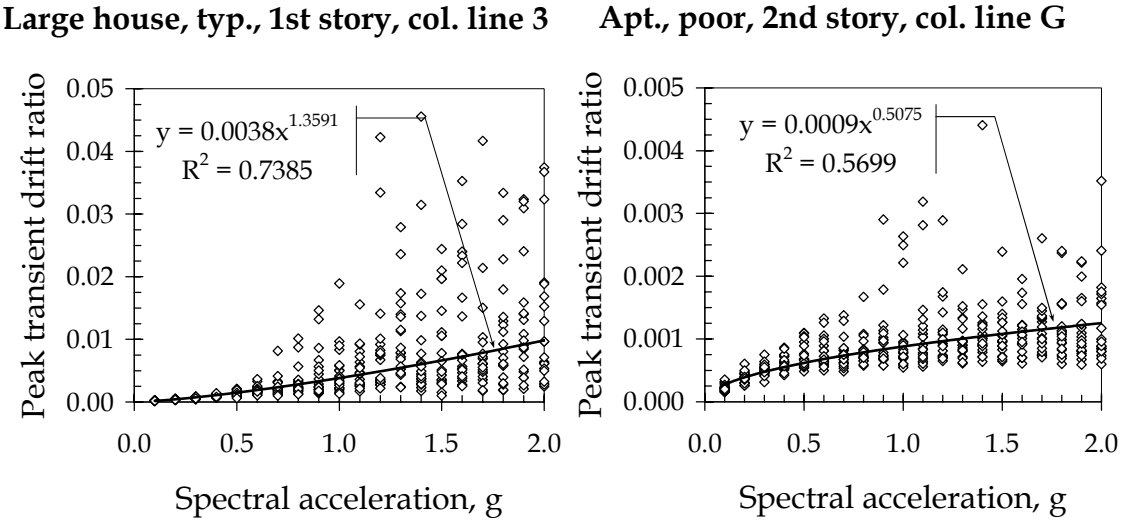

While charts such as Figure 4-5 illustrate the quantity of data involved, they are not very informative of overall behavior. More instructive are figures of average peak story drift ratio (averaged overall all column lines on a floor) and measures of uncertainty of those drifts. Figure 4-6 shows the mean values of peak transient drift calculated during the structural analyses of the typical-quality variants and retrofits, as a function of spectral acceleration. Drift values are averaged over all simulations at a given level of S_a, and over all column lines. (Two simple checks of the results presented in this figure are performed in the next section.)

The figure for the small house shows that bracing the cripple walls reduces mean drift by approximately 1/3, and that the deformation in the small house is concentrated at the cripple-wall level. The figure shows that building deformation is nonlinear with shaking intensity. This is not surprising, since the cripple-wall level is far more flexible than the first story, and most of the mass is attributed to the ground floor. The dominance of the lowest wall level in overall drift is common throughout the other index buildings and variants.

Figure 4-6 also shows a similar overview of the large-house first-story drift ratios by S_a. The figure shows that the immediate-occupancy redesign reduces first-story drifts by 1/3 at low S_a to 2/3 at high S_a. Similar reduction in deformation is produced by the limited-drift redesign of the townhouse, with drift reductions reaching 75% at high S_a. The shearwall and steel-frame measures for the apartment building reduce drifts only modestly. (This last may seem counterintuitive; it is a consequence of the fact that drift was not recorded in the ABV analysis for the open front, owing to the absence of a structural member along this column line for all but the steel-frame variant.)

Figure 4-6:
Average Peak Interstory Drift Ratio

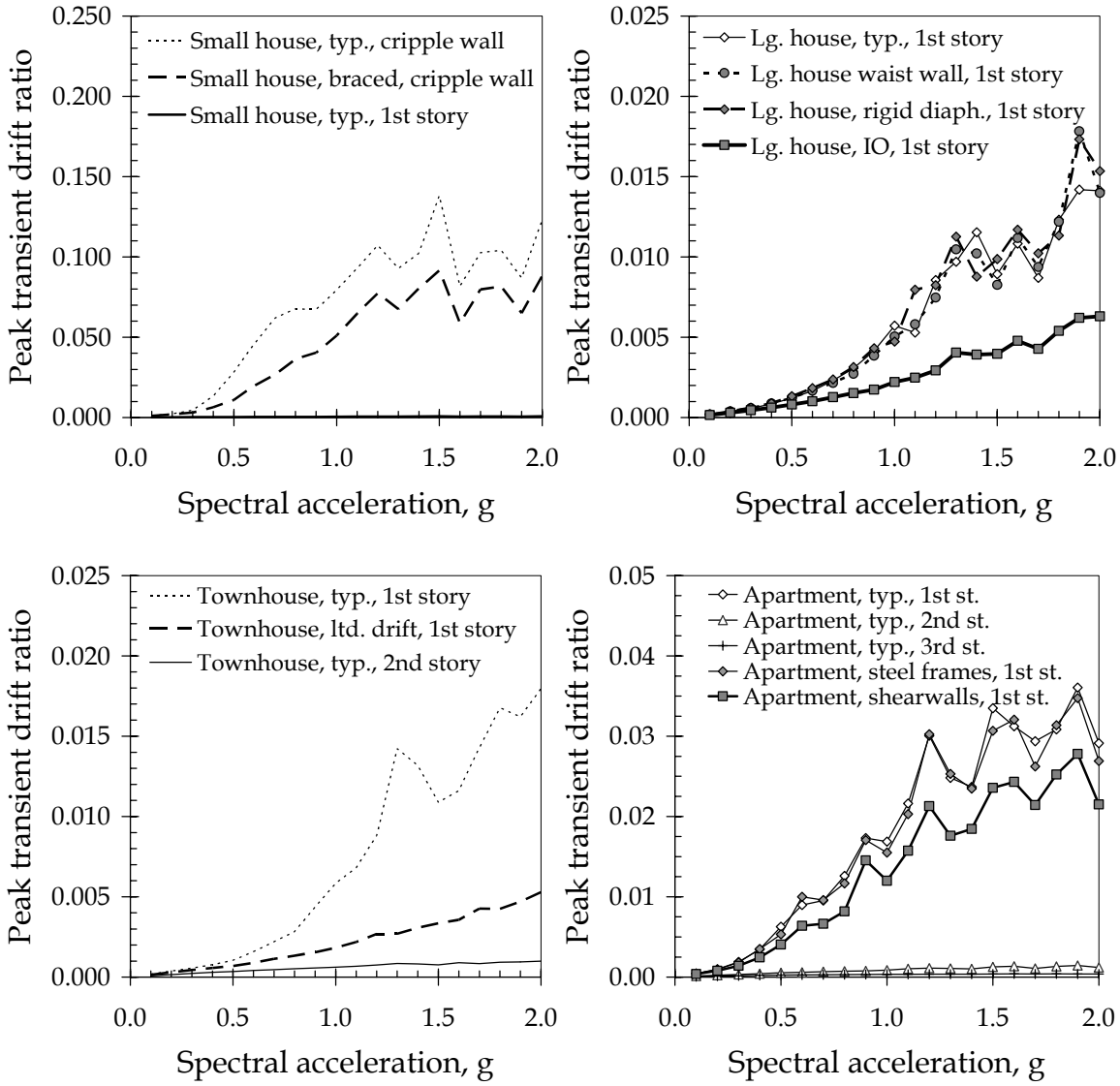

Figure 4-7 illustrates the variability in structural response. The coefficient of variation (COV) of peak transient drift in the small house and apartment building is substantial: 1.0 to 1.2 for strong shaking. For the technical reader unfamiliar with the notion of a COV, it is a measure of uncertainty (the standard deviation) normalized by the mean value (the average). A COV of 0.5 indicates that a sample of a random variable with a Gaussian (normal) distribution would probably lie within the mean value plus or minus 0.5 times the mean value, with approximately 2 in 3 odds.

Variability is less marked in the large house and townhouse, which exhibit coefficients of variation of the first-story drift ratio of between 0.5 and 1.0. These values mean that

the uncertainty on drift for any given column line and given S_a is about as large as the drift itself.

Are the differences between average drift ratios meaningful, considering coefficients of variation reaching 1.0? Bearing in mind that 20 observations are made per S_a level, and that drifts are averaged over 8 to 10 (correlated) observations from different column lines, the standard error would be on the order of σ times $20^{-0.5}$ to $200^{-0.5}$, or 7% to 22% of the standard deviation. Hence, a difference of 25% between the average drifts of two different buildings should be seen as meaningful, and a consistent trend over many S_a levels even more so.

Figure 4-7:
Variability of Peak Interstory Drift Ratio

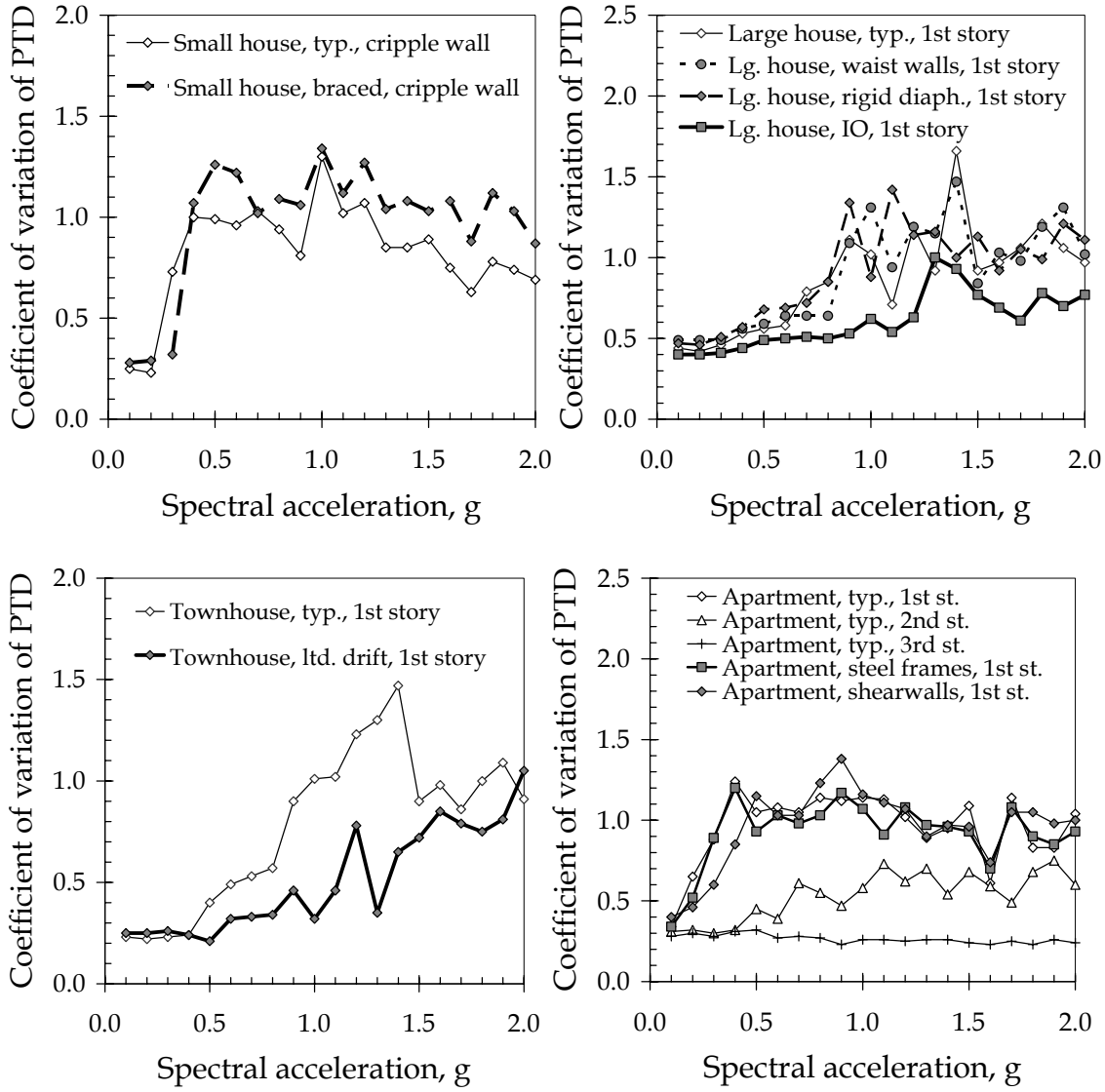

Checking Structural Response Estimates

Are the drift levels reasonable? Two simple checks can be performed. Assuming linear elastic behavior, the roof displacement can be approximated as $D \approx 1.3S_d \approx 1.3S_a/\omega^2$, where S_d is damped elastic spectral displacement and ω is the natural frequency, equal to $2\pi/T$, where T is the small-amplitude, fundamental period of the building. The 1.3 factor accounts for modal participation.

Next, recognize that the spectral accelerations shown in Figure 4-6 are for the maximum direction, $S_{a,\max}$. Let us assume that the S_a in the normal direction is approximately 0.3 times the maximum direction. Consequently, the average spectral acceleration, $S_{a,avg}$, is approximately equal to $0.65S_{a,\max}$. For linear elastic response, roof displacements should therefore be on the order of $1.3*0.65*(T/2\pi)^2*S_{a,\max} = 0.02T^2S_{a,\max}$. For $S_{a,\max}$ = 1.0g and using T = 0.13 sec, D evaluates as 0.13 in. For nonlinear response, where the structure softens significant and hysteretic damping is modest (as suggested by Camelo *et al.*, 2001), the roof displacement calculated by nonlinear time-history structural analysis should be greater than the amount estimated for linear elastic behavior.

Figure 4-6 shows that the structural analysis of the small house produces an estimate of the peak transient drift ratios under S_a = 1.0g excitation to be on the order of 8% for the cripple wall and 0.04% for the first-story walls. This equates with 0.08*24 in + 0.0004*96 in = 2.0 in, or approximately 15 times the drift expected under linear elastic behavior, which is perhaps reasonable if the cripple walls experience significantly nonlinear behavior. (As shown later, the cripple walls are estimated to experience substantial damage, indicating significant nonlinear behavior.)

It is possible to look more closely. The figure of 8% drift (2.0 in) for the cripple wall seems reasonable; it is the very small drift (0.04% or 0.04 in) in the first story that appears to be questionable. The drift in the first story should be on the order of $D = F/K$, where D refers to shear displacement, F refers to shear force, and K is the shear stiffness of the wall elements. F can be approximated as $F \approx 0.65S_aW$, where W is the weight of the building above the floor of interest, S_a is measured in units of gravity, and the 0.65 factor reflects the fact that ground motion is operating in two directions, with one on the order of 30% of the other. The shear stiffness K can be estimated as $(L_SK_S + L_GK_G)$, where L_S is the average length of stucco walls in one direction, K_S is the shear stiffness of 8-ft. high stucco walls per unit length of wall, L_G is the average length of the gypsum wallboard in one direction, and K_G is the shear stiffness of an 8-ft. high gypsum wall per unit length of wall. Thus, average peak transient drift should be on the order of:

$$D = \frac{0.65WS_a}{L_SK_S + L_GK_G} \tag{4-1}$$

The weight of the roof, ceiling, and the upper half of the first-story walls is approximately 29.1 kip, or 24 psf of floor area (see Appendix B). The average length of stucco in each direction, L_S, is 70 ft. The average length of wallboard in each direction, L_G, is approximately 160 ft. The shear stiffness of the stucco, K_S, is approximately 1.50 kip/in per ft of wall length (see Isoda *et al.*, 2001, in Appendix C). The shear stiffness of the gypsum wallboard, K_G, is approximately 0.94 kip/in per ft of wall length (Isoda *et al.*, 2001). Evaluating Equation 4-1 for S_a = 1.0g, D = 0.07 in, which is of the same order of magnitude as the 0.04 in of drift estimated by structural analysis, suggesting

approximately linear elastic behavior of the first-story walls, which tends to agree with the observation (presented later) of minimal damage to walls above the first floor.

Simulation of Assembly Damage

The structural responses calculated in the previous step are used as input to fragility functions, for use in simulating physical damage to each assembly in the building. As noted in Chapter 3, each damageable assembly must be associated with one or more fragility functions, that is, relationships that give the probability that the assembly will reach or exceed some well-defined level of damage when subjected to a certain amount of structural response. The mathematical framework for simulating damage is presented in Appendix D, and the development of the assembly fragilities used in the present study is presented in Appendix E. These details are not repeated here. However, two analytical issues not discussed in the appendices are worthy of mention here: line-of-sight costs and collapse.

Line of Sight

Damage to some assemblies can require repair that affects other assemblies. A notable example of this is damage to walls. To repair the damage, it is often necessary to repaint the entire room (or *line of sight* in the terminology of insurance claims adjustment), including segments of wall that were not damaged. Furthermore, if two wall segments in a given line of sight are damaged, the amount of painting work does not change: the same room must still be repainted just once. To account for this phenomenon, each painted assembly is associated with a room or line of sight. In each simulation, damage to the assemblies in the line of sight are examined, and if any require repainting, then the entire line of sight is noted as requiring repainting. Different assemblies can require different paints, so one must keep track of the total area requiring each type of paint. In the present application, these total areas are represented as if they were simply another damaged assembly requiring repair.

Collapse

Note that some damage states in some assemblies lead to damage in others. In the present study, the collapse of any cripple wall on the small house, or the collapse of the longitudinal ground-floor shearwall on line 2.5 on the apartment building, is taken to indicate collapse of the building. In both cases, collapse of the shearwall is assumed to occur when the peak transient drift exceeds 2 to 3 inches, slightly more than the width of a stud, and enough to ensure that the finish material—stucco on the case of the small house, wallboard or structural sheathing in the case of the apartment—has disconnected from the framing. (The drift associated with collapse is taken as a random variable, with a median value of 2 inches in the case of the small house, 3 inches in the case of the apartment building, with a logarithmic standard deviation of 0.1. These are assumptions

necessitated by the structural analysis software employed here. The modeling of collapse in the index buildings needs further investigation.)

At this stage, the analysis has produced the simulated damage state of each assembly in the building: which windows are cracked and which are not, etc. The number of assemblies of each assembly type in each damage state can then be added up.

Repair Costs

The cost to repair a damaged assembly includes labor costs, material requirements, and when applicable, debris removal and equipment rental. The cost estimator on the project team (Boyd) considered a description of the damage associated with each assembly and each damage state, identified the tasks required to repair the damage, estimated the labor, materials, and other costs involved, and prepared an estimate of the cost to repair a single instance of the assembly, e.g., a single pane of glass, a single 8-ft segment of wall, etc. He estimated these costs for a particular location (Santa Monica, California) and a particular time (2001), and provided a best estimate, lower bound, and upper bound unit cost for each assembly type and damage state. Appendix F details the methodology used to estimate the construction costs employed here, as well as a summary of the unit costs and details of their estimation.

Note that the initial estimates in Appendix F include painting costs. To account for line of sight, it was necessary to separate the painting costs from the other labor and materials. This was done by Caltech, as noted on the bottom of each unit cost estimate in the Appendix. Note also that the estimator in general assumes a fairly modest degree of uncertainty in unit cost, with lower and upper bound costs differing from the best estimate by as little as 5%. Considering that total construction costs for well-defined projects have significantly greater uncertainty (a 15% difference between projected and actual total cost is not uncommon), uncertainty in unit cost was adjusted upward to a logarithmic standard deviation of 20%. A few tasks were estimated by Caltech, based on RS Means Co., Inc. (2001). Uncertainty in unit costs for these tasks was set to 30%. (These tasks contribute a very small portion of the total loss.)

Contractor overhead and profit is taken as a fraction of the total direct costs. In the present application, the cost estimator recommended a fraction of 0.15 to 0.20. Consequently, overhead and profit was taken as a random variable uniformly distributed between 0.15 and 0.20.

Results of the damage simulations are presented in Chapter 5, along with an examination of the sources of repair costs and an assessment of the resulting HAZUS-compatible fragility functions.

HAZUS-Compatible Fragilities

The general methodology for developing HAZUS-compatible fragilities was presented in Chapter 3. Details are now presented of how this calculation is performed for the index buildings.

Step 1: Associate Index Buildings with HAZUS Building Types

The construct of poor-, typical- and superior-quality variants of the index buildings facilitates the adoption of the resulting models within the HAZUS framework. The basic structural classes, called "model building types" within HAZUS, are differentiated by height (low-, mid-, and high-rise) and structural system (e.g., steel moment frame, concrete shearwall, etc.). Existing models for woodframe structures are limited to W1 (wood, light frame, less than 5,000 square feet) and W2 (wood, commercial and industrial, greater than 5,000 square feet). However, the models also consider the building's seismic design level (low-, moderate- and high-seismic design) and building seismic performance level or quality (code/ordinary, pre-code/inferior, and special/superior), allowing for as many as nine variations on a single model building type.

Within the HAZUS documentation, these seismic performance levels are minimally defined using qualitative and relative descriptions of strength and ductility (see Table 5.19, Federal Emergency Management Agency, 1999). For example, maximum strength versus high strength distinguishes the superior seismic performance level from the ordinary one, for a building in the high seismic design level category.

Nevertheless, mapping of the typical-quality index buildings to HAZUS classes is based on the age and code-related guidelines provided in the HAZUS Technical Manual (Table 5.20, Federal Emergency Management Agency, 1999). For UBC Seismic Zone 4 (NEHRP Map Area 7), the small house and apartment are considered typical of structures built between 1941 and 1975, and therefore fit within the HAZUS category of moderate seismic design level, code quality. The large house and townhouse can be considered typical of post-1975 construction, and therefore fit within HAZUS' high-seismic-design-level, code-quality category.

Poor quality variants are mapped to HAZUS categories with reduced strength relative to the category assigned for the typical structure. That is, when the typical structure is classified as a moderate strength structure (W1, moderate, code), the poor variant is modeled as a low strength structure (W1, moderate, poor, which has the same pushover curve parameters as W1, low, code). When the typical structure is modeled as a high strength structure (W1, high, code), the poor variant is modeled as a moderate strength structure (W1, moderate, code). Similarly, superior quality variants are mapped to HAZUS categories to reflect an increase in strength. This mapping is summarized for the

index buildings and their variants in Table 4-8, and for the proposed retrofit and redesign measures in Table 4-9.

Table 4-8:
HAZUS Model Building Types for the Index Buildings and Variants

Index Building	Poor Variant	Typical Variant	Superior Variant
Small House	W1, moderate, poor	W1, moderate, code	W1, high, code
Large House	W1, moderate, code	W1, high, code	W1, high, superior
Townhouse	W1, moderate, code	W1, high, code	W1, high, superior
Apartment	W2, moderate, poor	W2, moderate, code	W2, high, code

Table 4-9:
HAZUS Model Building Types for the Index Building Retrofits

Retrofit Measure	HAZUS Model Building Type
Small house, braced	W1, high, code
Large house, waist wall	W1, high, code
Large house, immediate occupancy	W1, high, superior
Large house, rigid diaphragm	W1, high, superior
Townhouse, limited drift	W1, high, superior
Apartment, steel frames	W2, high, code
Apartment, shearwall.	W2, high, code

An Important Distinction between HAZUS Categories and CUREE Index Buildings

It should be noted that the damage functions in HAZUS represent categories of buildings, and are not building-specific. As noted in Chapter 2 of this report, HAZUS is a category-based approach to damage estimation. In fact, the HAZUS Technical Manual (Federal Emergency Management Agency, 1999) states:

> **While the fragility and capacity curves are applicable, in theory, to a single building as well as to all buildings of a given type, they are more reliable as predictors of damage for large, rather than small, population groups. They should not be considered reliable for prediction of damage to a specific facility without confirmation by a seismic/structural engineering expert.**

In contrast with HAZUS' category approach, the current project approach and the resulting fragility curves represent individual buildings within a category (i.e., are building-specific). While the intent of this project is to develop HAZUS-compatible functions, caution should be used when utilizing the results within HAZUS. That is, damage functions for various woodframe structures will be developed for incorporation into HAZUS, but should only be used when specific information is known about the structures, and the structures can be reasonably associated with an index building or variant. Accordingly, the resulting woodframe fragility curves would not be directly applicable for a HAZUS Level 1 analysis (baseline run utilizing default building inventory data provided with the program that is developed from census and other economic data), but might be applicable for a Level 2 analysis, wherein the user is expected to import more detailed building inventory data. With that caution, the resulting fragility curves could be incorporated as replacement or supplemental woodframe fragility functions, with variants mapping into the HAZUS categories as delineated in the tables.

Also note that within HAZUS, separate fragility curves are used for structural and nonstructural components, whereas the final result from the ABV assessment aggregates damage to the building level, i.e., the sum of structural and nonstructural damage. The ABV methodology can in theory be employed to separate structural and nonstructural damage. However, in this study, our construct employs one fragility function for each building as a whole. For use within HAZUS, the user must assign the entire building value to the structural portion by editing the repair costs by damage state, rather than segregating the building into structural and nonstructural components, as is normally done within HAZUS.

Default W1 and W2 nonstructural acceleration-sensitive fragility parameters should be stored in addition to the data provided here for use in estimating contents and inventory losses. (HAZUS uses acceleration sensitive nonstructural damage state probabilities to estimate these losses, not explicitly addressed in the current project.)

As of this writing in late 2001, FEMA is releasing its Advanced Engineering Building Module (AEBM) for HAZUS. The AEBM is intended to facilitate site-specific building analysis. This module will allow the user to input building-specific data and override the default vulnerability functions for individual structures. This should simplify the process of inputting the new CUREE functions for a building-specific analysis.

Step 2: Determine Damage Factor and Damage State

ABV analysis is performed as described before. The damage factor is calculated as the repair cost divided by the replacement cost new ($Y = C_T/RCN$), and the damage state DS is determined based on the damage factor and the HAZUS damage-state ranges provided in 3-1. Because of the vast quantity of Y data produced here, the data are not reproduced in this report.

As a sample calculation however, consider an ABV simulation of the apartment building, poor quality, subjected to ground motions LA45 (x-direction) and LA46 (y-direction), scaled so that the maximum of the two has S_a = 0.1 g (T = 0.20 sec., 10% damping). The scaling factor is 0.41, as noted in Table 4-7. The simulation produced repair cost C_T = \$2,280, Y = 0.00286, and DS = slight.

Step 3: Determine S_d

For each simulation, the spectral displacement at the intersection of the response spectrum and the pushover curve is determined as follows. The response spectrum is calculated for the ground motion used in each simulation, rather than being based on assumptions of constant-acceleration, constant-velocity, and constant-displacement regions.

The technical reader is reminded that the ABV vulnerability functions expressed are functions of S_a at the small-amplitude fundamental period, whereas HAZUS-compatible fragilities are functions of a different period, one that is implied by the point at the intersection of the pushover curve and the response spectrum. Because of this difference in period, our S_a and HAZUS' S_d are not simply related, hence the necessity for an involved procedure to calculate the S_d.

In the present study, BiSpec (Hachem, 2000) was used to calculate the (S_a, S_d) spectrum of each ground motion at 0.05-second period increments between 0.05 and 4.0 sec, at the damping ratios shown in Table 4-3. For a given simulation, the ground-motion scaling factor (tabulated by ground motion and spectral acceleration in Table 4-4 through Table 4-7) is applied to both coordinates, and the intersection of the HAZUS pushover curve and the scaled (S_a, S_d) spectrum is found.

The HAZUS pushover curves for woodframe buildings are represented in Figure 4-8. Although HAZUS provides for 20 different woodframe types, some of the types have identical yield and ultimate points, resulting in the 11 distinct pushover curves shown in the figure. The HAZUS documentation does not specify the form of the pushover curve between the yield and ultimate points. The curves shown here assume a power spline between yield and ultimate. (Note that HAZUS employs an elliptical spline, but there is no obvious reason to prefer one over another.) Thus, the equation of the pushover curve is taken as:

$$A = \begin{cases} D\dfrac{A_y}{D_y} & D < D_y \\ A_u - \left(A_u - A_y\right)\left(\dfrac{D_u - D}{D_u - D_y}\right)^{K_e/K_y} & D_y \le D < D_u \\ A_u & D \ge D_u \end{cases} \quad (1)$$

where

$$K_e = \frac{A_y}{D_y}$$

$$K_y = \frac{A_u - A_y}{D_u - D_y}$$

Figure 4-9 illustrates the methodology for finding the intersection of the pushover curve and the response spectrum. The illustration is drawn from an ABV simulation for the small house, typical quality, at S_a = 0.5g. The *x*-direction ground motion record is LA05; the *y*-direction record is LA06, and the scaling factor is 1.21. The pushover curve is that of HAZUS' W1, moderate, code category, as noted in Table 4-8. Dots show the S_d values at which the pushover curve is evaluated. The shaded dot at (S_d, S_a) = (0.70 in., 0.53g) is the first point where the pushover curve lies outside of the response spectrum. Thus, the S_d for this simulation is taken as 0.70 in. The damage state from this simulation was "slight."

A zero kappa value is used for simplicity. (In the HAZUS approach, kappa increases the damping ratio to account for hysteretic damping, as a function of ground-motion duration.) Note well: the use of a zero kappa value here does not mean that hysteretic damping is ignored, nor does it indicate that duration effects are neglected. The structural analysis model accounts for hysteresis, and the selection of ground-motion time histories from the SAC records ensures that various durations are considered. The use of zero kappa merely simplifies the calculation of the response spectrum.

Figure 4-8:
HAZUS Pushover Curves for Woodframe Buildings

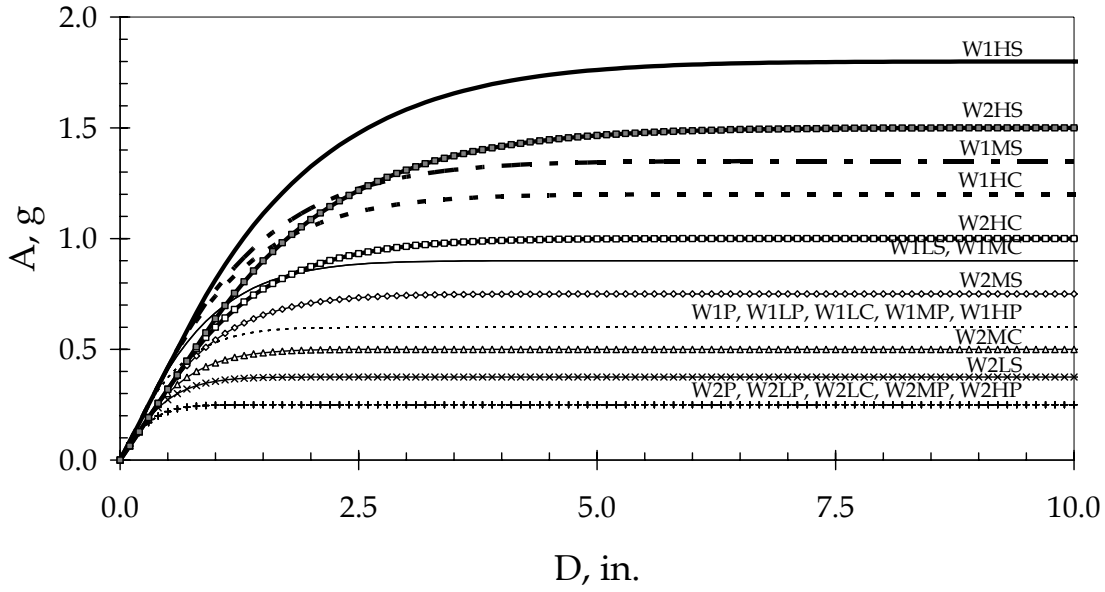

Figure 4-9:
Determination of Pushover S_d

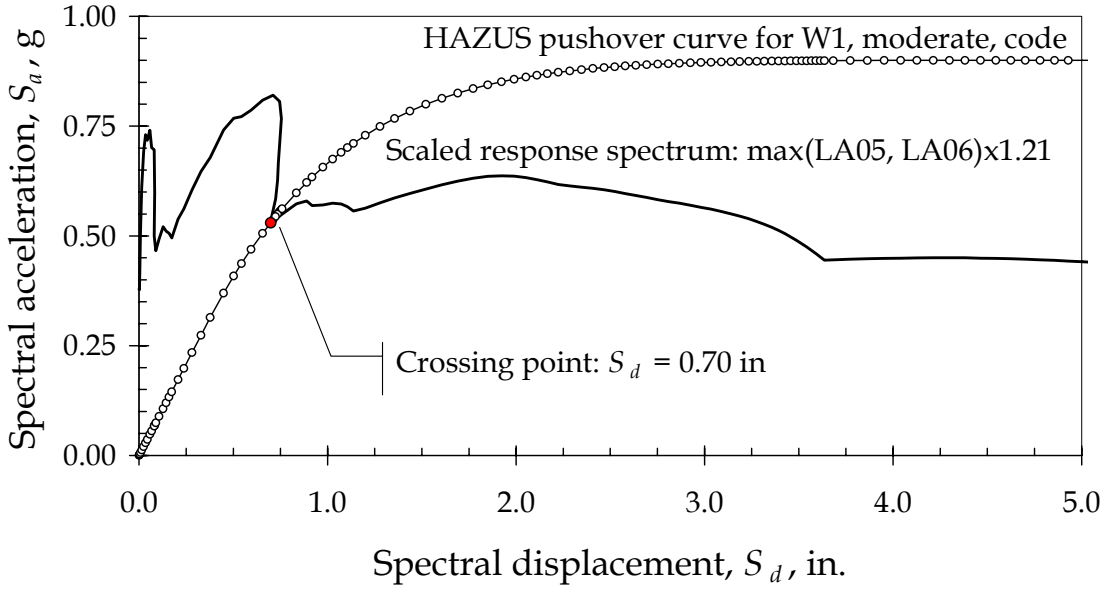

Step 4: Calculate Fragility Parameters

Considering all the ABV simulations for a particular building, one compiles the set of pairs (S_d, DS). There are 400 such pairs for each building in the present application. For each damage state, these pairs are mapped to data pairs (S_d, I($Y \geq y_{DS} \mid S_d$)), where I is the indicator function: 1 if the condition in parentheses is true, 0 otherwise; Y is the damage factor for a given simulation; and y_{DS} is the lower-bound damage factor for damage state DS. The parameters of the HAZUS-compatible fragility function are found by least-squares fit of the lognormal cumulative distribution to the (S_d, I($Y \geq y_{DS} \mid S_d$)) data. The resulting fragility parameters for all the index buildings and damage states are presented with results in Chapter 5.

Step 5: Describe Damage States

The HAZUS Technical Manual qualitatively describes the physical damage associated with damage states in terms of degree of damage to various parts of the building. In the present study, it is possible to quantify fractions of assemblies damaged by index building and damage state, according to any meaningful grouping of assembly types. Groupings used here are as follows:

1. Glazing
2. Exterior shearwalls
3. Exterior nonstructural walls
4. Interior shearwalls
5. Gypsum wallboard, including wallboard partitions
6. Water heater

Chapter 5 presents resulting statistics of fraction of assembly groups damaged, by index building and damage state.

Computational Effort

In the present study, for each index building variant (IBV), 20 simulations are performed at each level of shaking intensity (S_a = 0.1g, 0.2g, … 2.0g), for a total of 400 simulations of damage per IBV. The small house has 4 IBVs (poor, typical, superior, and one retrofit), for a total of 1,600 simulations for the group. The algorithm presented here is implemented in computer code, through a combination of batch-processed Ruaumoko analyses and a database application. The structural analyses were performed on a Pentium III 900 MHz computer with 256 MB of RAM. The database application was employed on a Pentium II 333 MHz computer with 128 MB of RAM.

Each simulation involves one time-history structural analysis with earthquake excitation in both horizontal directions. The structural analyses account for material nonlinearities and neglect geometric nonlinearities. (In a time-history structural analysis, one calculates

the forces and displacements in the building on a moment-to-moment basis during the earthquake. Material nonlinearities indicate that the building components are modeled as potentially degrading in strength and stiffness. Geometric nonlinearities reflect that fact that forces in the building can change when the building components are displaced substantially from their initial configuration.) The 1,600 structural analyses took approximately 27 hours of computer time, i.e., approximately 7 hours per IBV.

In the database portion of the analysis, all simulations for an index building are compiled together. The database calculations for all four variants of the small house took less than an hour. Thus the entire analysis was quite manageable in terms of computer time, despite the large number of simulations and nonlinear time-history structural analyses.

The larger buildings took longer to analyze, requiring up to 50 hours of computer time for structural analysis per IBV, and 6 hours for database computation for all variants of an index building, which is considered to be still a manageable effort.

Chapter 5. Results

Description of Results

This chapter presents a variety of study results based on the foregoing methodology, including an examination of the associated uncertainty. The contribution to overall loss by type of assembly (i.e., walls, windows, etc) is examined, and this study's results are compared against findings by a number of previous investigators based on actual loss data in earthquakes ranging from the 1971 San Fernando to the 1994 Northridge events. Lastly, the HAZUS-compatibly fragility functions are presented. These appear last in the chapter because they depend on the vulnerability functions for their development.

Vulnerability Functions

Figure 5-1 illustrates the statistical repair-cost data produced by the ABV analysis. Each dot represents one simulation of the damage factor for the large house, typical quality at a given level of S_a. (Again, damage factor is defined as the repair cost divided by the replacement cost.) That is, each dot represents one randomly selected ground motion, one structural analysis with simulation of mass and of damping, one simulation of damage for each assembly in the building, one simulation of unit repair cost per assembly type and damage state, and one simulation of aggregate contractor overhead and profit.

Note that, although Chapter 4 presents intermediate statistical data about average story drifts, these statistics are presented for information purposes only. In any given simulation of damage to a particular assembly, the structural response that is input to the assembly fragility function is calculated for that assembly's location, from a particular ground motion and a particular simulation of the structural model. No intermediate assumption is made about the shape of the distribution of response, nor is a single column line used as indicative of the structural response for the entire floor. Nor are aggregate damage statistics subsequently simulated from assumed distributions, when simulating repair costs. This approach to generating seismic vulnerability functions propagates all identified sources of uncertainty though the analysis, preserving all consequent correlations.

As useful as Figure 5-1 is in illustrating the source of the vulnerability functions, it is less informative than a chart of the mean vulnerability function and a chart of uncertainty in the damage factor. As used here, "mean vulnerability function" refers to the mean damage factor as a function of seismic intensity.

Figure 5-2 shows the mean vulnerability function of the small house. The left-hand figure expresses the vulnerability function in terms of the mean damage factor as a function of damped elastic spectral acceleration, S_a, at the small-amplitude fundamental period of the small house. The right-hand figure gives the mean vulnerability function as

a function of peak horizontal acceleration (PHA), where the damage-factor data are averaged in bins of PHA ± 0.05g, in 0.1-g increments. (The data reflected in the vulnerability functions are tabulated in Appendix G.)

It is clear from the figures that significant damage occurs when the building is subjected to strong motion, $S_a > 0.3$g, and levels off at very high levels of shaking, $S_a > 1.0$g. This leveling off is the result of collapse, that is, above this level of shaking, the cripple wall is modeled as having collapsed, and the model neglects further damage. Damage is largely concentrated at the cripple-wall level, which acts as a sort of structural fuse, limiting damage above the cripple wall. (This is not to imply that no damage would occur above the cripple wall in the case of collapse. Appendix F contains a very approximate estimate of the cost to repair such damage.) It is clear from the figures that the superior-quality variant, which is designed with a reinforced concrete stemwall to the first floor, rather than a woodframe cripple wall, is substantially less vulnerable to damage.

Similar results for the large house are presented in Figure 5-3; Figure 5-4 for the townhouse; and Figure 5-5 for the apartment building. Figure 5-6 and shows the ratio of the mean damage factor of each variant to that of the typical-quality variant of each index building. Figure 5-7 through Figure 5-10 show the difference between the retrofit or redesign vulnerability and the typical-quality vulnerability, as opposed to the ratio.

These figures show that some trends are common through all the index buildings.

1. **A damage threshold exists.** There is a threshold of ground motion below which minimal damage occurs, typically on the order of 0.2 to 0.4 g of spectral acceleration. That is not to say that no damage is possible below these levels of ground shaking, but rather that in the 20 simulations per 0.1-g increment, little if any damage was modeled as having occurred, implying that the probability of damage is approximately 5% or less. One would expect in a large geographic region of moderate ground shaking ($S_a < 0.3$g, or approximately PHA < 0.2g), wherein thousands of homes are shaken, some would experience damage, possibly significant damage, but the overall fraction of significantly damaged homes would be small. *This is an important distinction*: the damage ratio (fraction of buildings damaged) would be small, although among damaged buildings, the damage factor (repair cost divided by replacement cost) could be significant. By providing only 20 simulations per 0.1-g increment, this implementation of ABV is insensitive to the damage at levels of shaking producing small damage ratios. More simulations would capture this statistically small level of damage.
2. **Quality of construction makes a difference.** Figure 5-6 shows that poor quality of construction or maintenance is estimated to increase repair costs by a factor of two or more at moderate to strong levels of shaking, relative to typical quality, while superior quality is modeled as reducing vulnerability by 30% or more, compared with typical. One not-very-surprising implication is that increased

inspection during construction could be highly beneficial in reducing future earthquake losses, if the inspection is targeted to the right quality parameters. We have identified some important parameters that seem to matter, but methodologies need to be developed for systematically examining likely all major issues of construction quality and deterioration, and determining their effects on performance.

3. **Most of the redesign and retrofit measures make a difference.** Figure 5-6 shows that, with the exception of the waist-wall and rigid-diaphragms measures, the retrofits and redesigns are effective in significantly reducing vulnerability, in some cases more so than ensuring superior quality construction and maintenance. Especially beneficial are the FEMA 273 immediate-occupancy redesign of the large house, and the limited-drift redesign of the townhouse. The steel-frame and shearwall measures for the apartment building are both quite effective. The small-house retrofit is an exception. The retrofitted small house is more vulnerable than the superior-quality variant, but the comparison is unfair: the small-house superior-quality variant has a reinforced concrete stemwall rather than a braced cripple wall. Nonetheless, bracing the cripple wall reduces mean vulnerability up to half.

Figure 5-1:
Sample Damage-Factor Data, Large House, Typical Quality

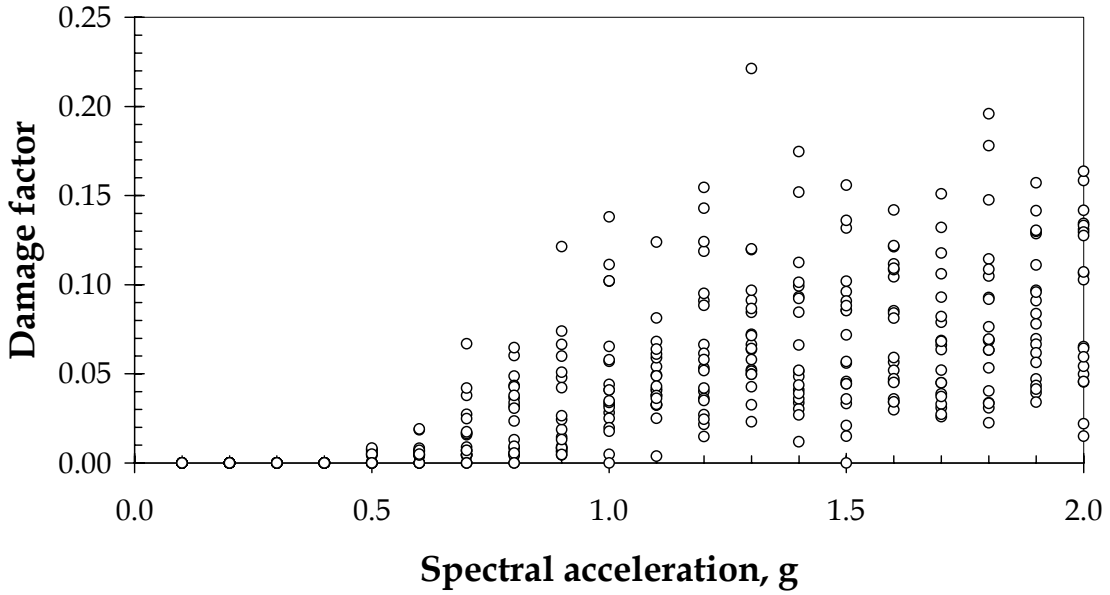

Figure 5-2:
Mean Vulnerability, Small House

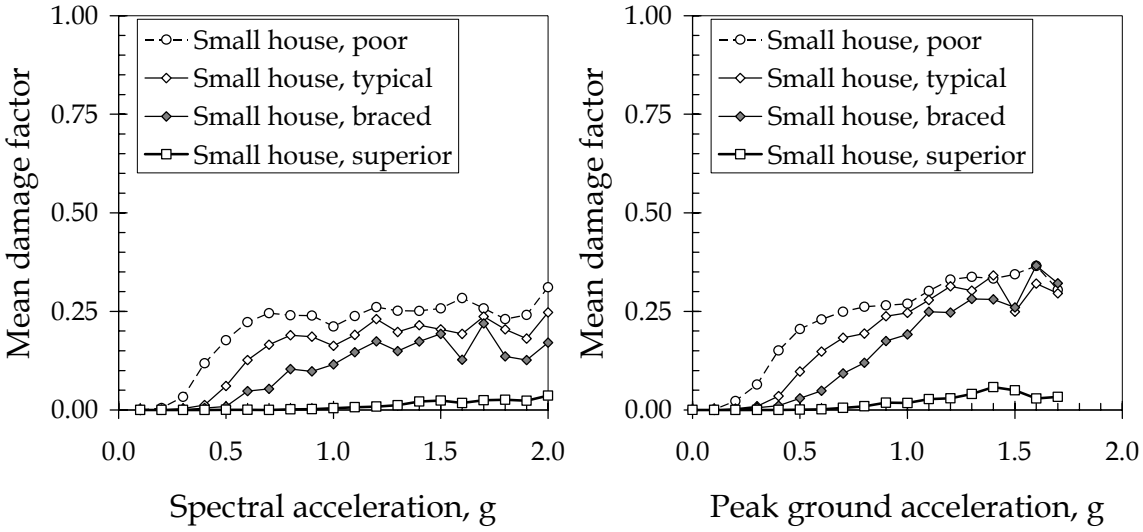

Figure 5-3:
Mean Vulnerability, Large House

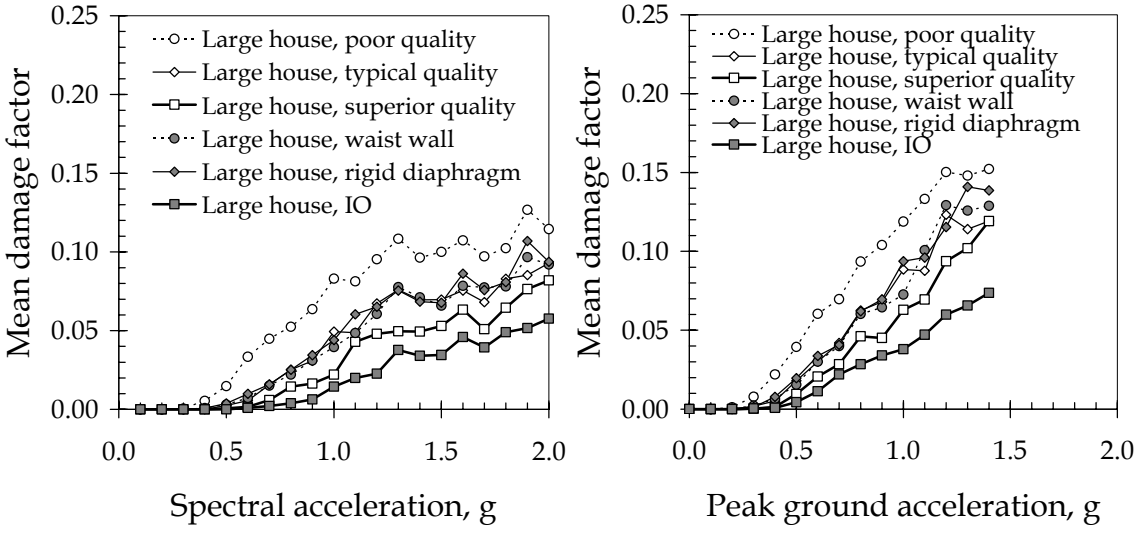

Figure 5-4:
Mean Vulnerability, Townhouse

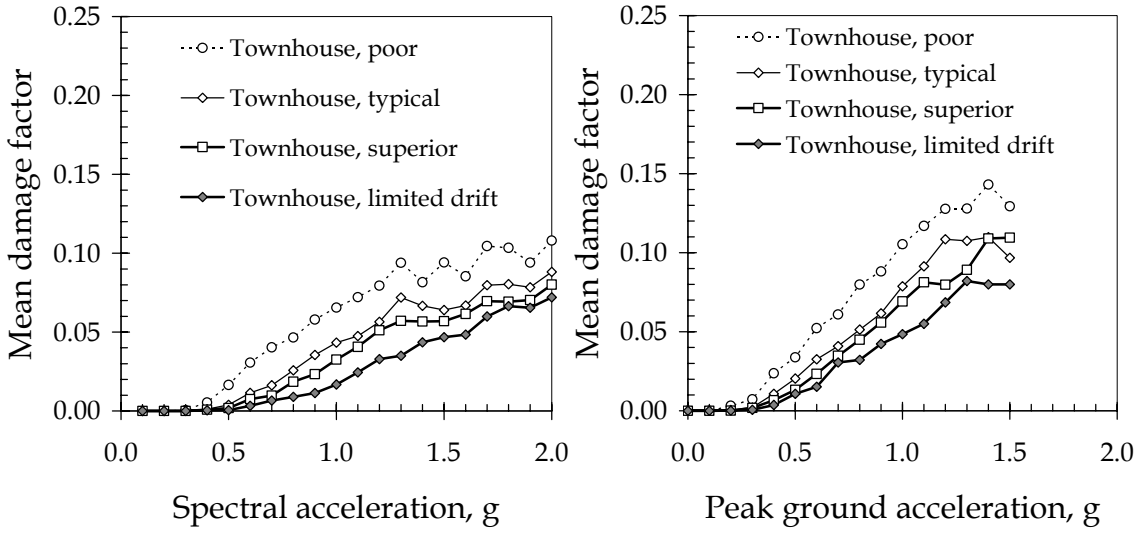

Figure 5-5:
Mean Vulnerability, Apartment Building

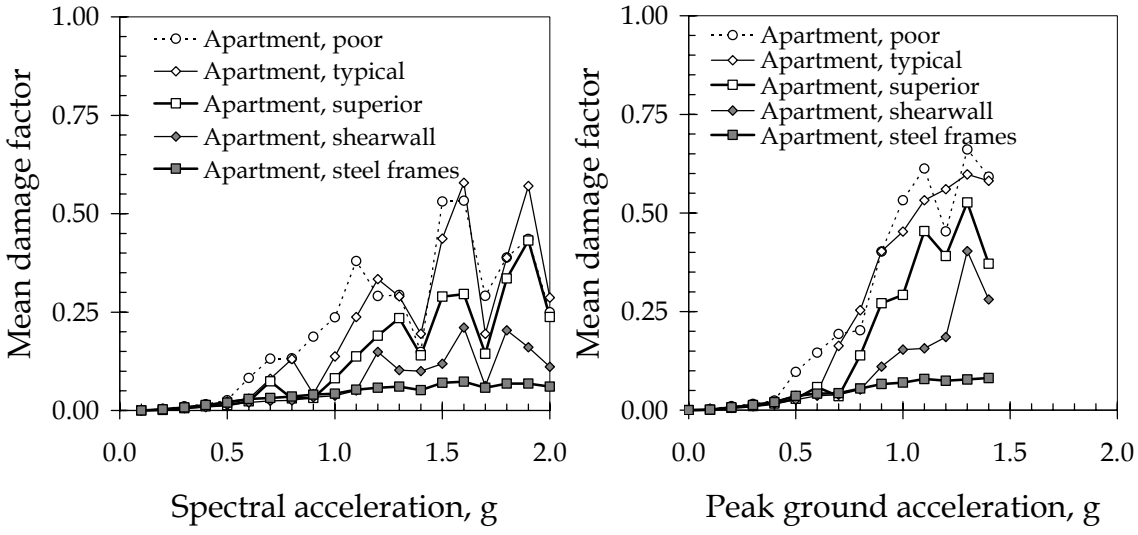

Figure 5-6:
Effect of Quality and Retrofit on Mean Vulnerability

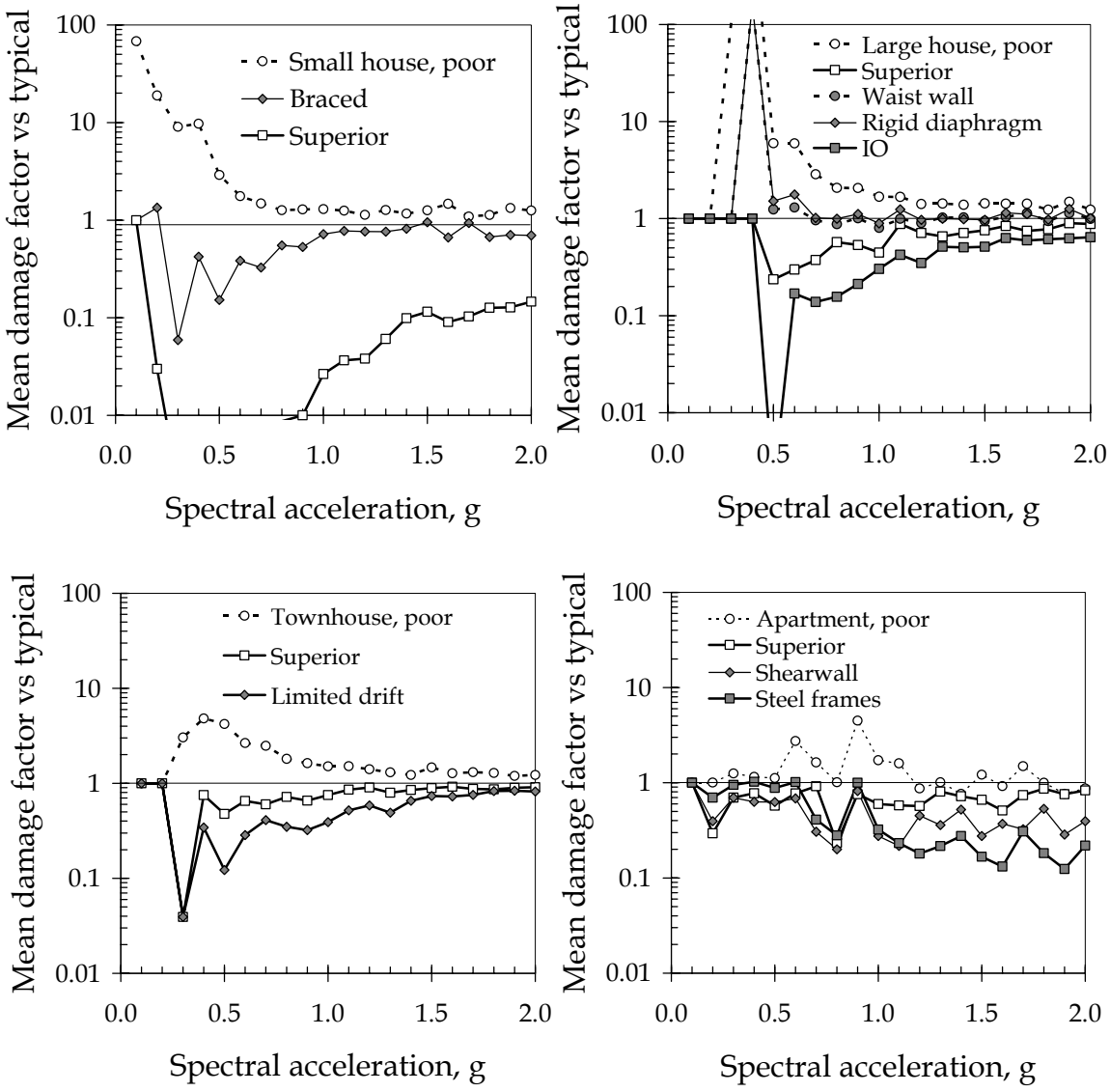

Figure 5-7:
Benefit of Small-House Retrofit in Terms of Repair-Cost Reduction

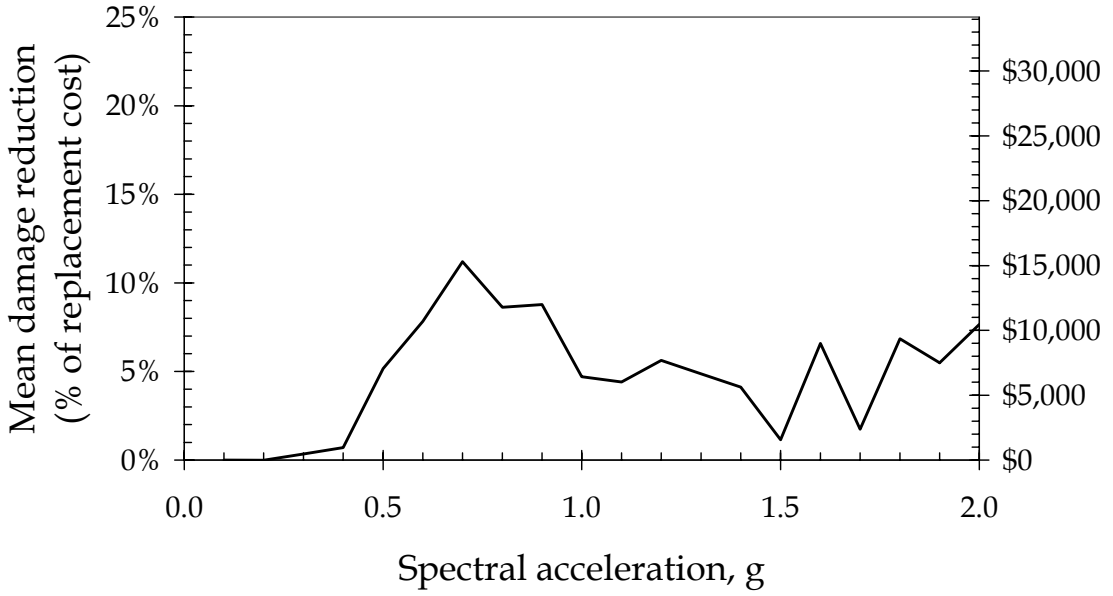

Figure 5-8:
Benefit of Large-House Redesign in Terms of Repair-Cost Reduction

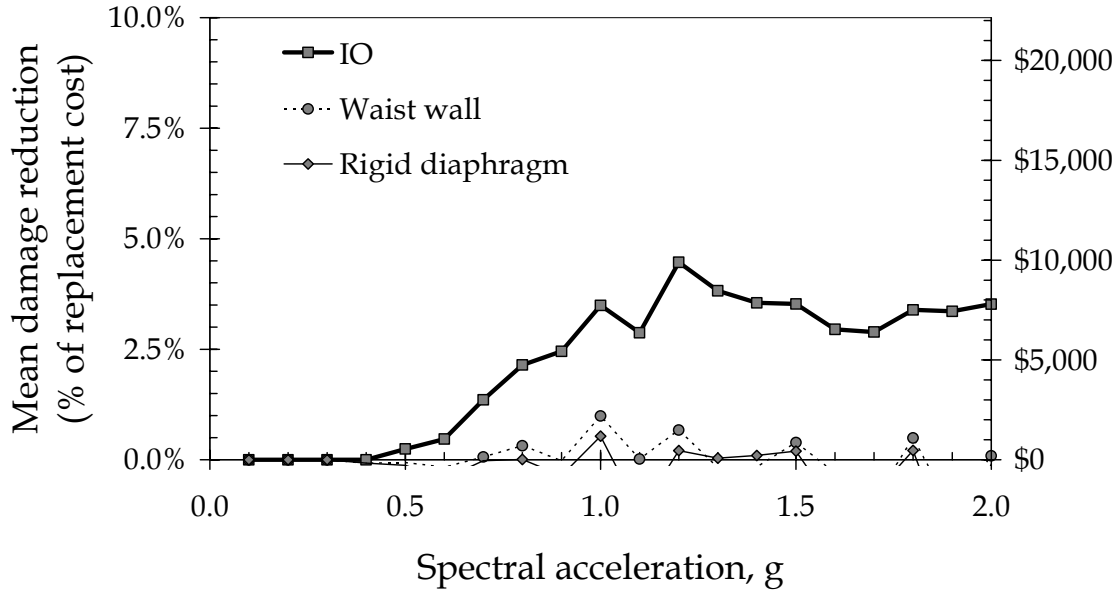

Figure 5-9:
Benefit of Townhouse Limited-Drift Design for Repair-Cost Reduction (per Unit)

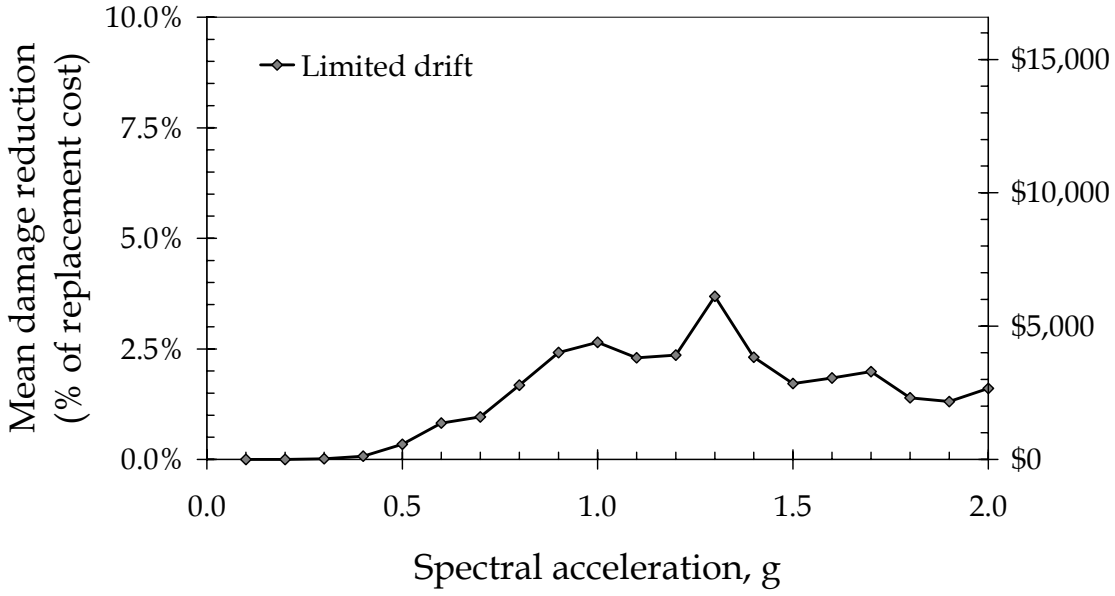

Figure 5-10:
Benefit of Apartment Retrofit in Terms of Repair-Cost Reduction

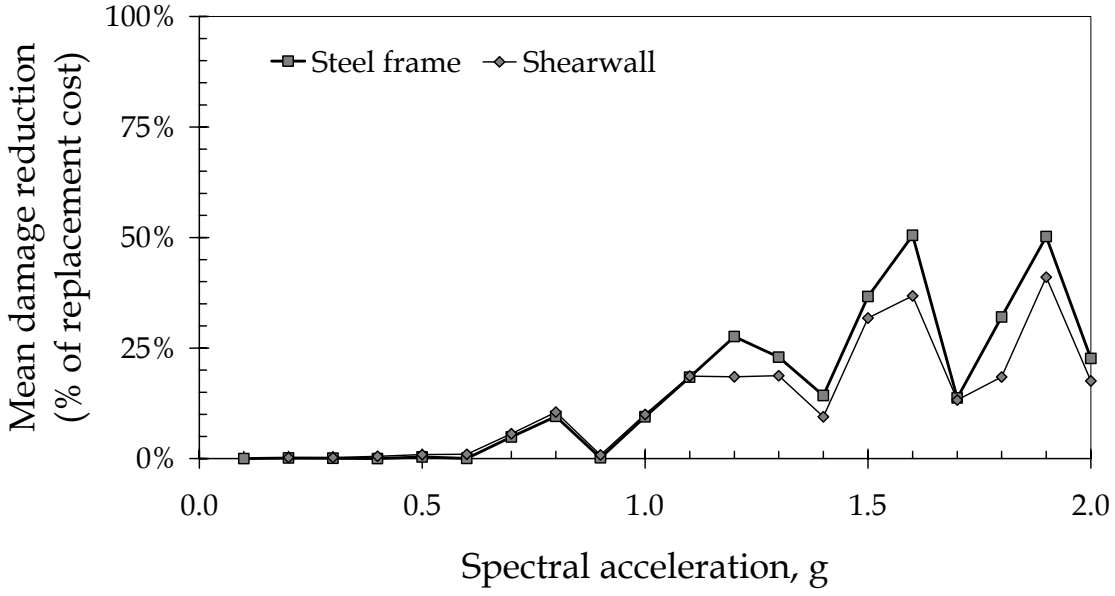

Residual Uncertainty in Vulnerability

The mean vulnerability functions give a best estimate of damage factor at a given level of S_a, but what about residual uncertainty? For each level of S_a, one can examine the distribution of the samples Y about the mean damage factor $\mu_{Y|Sa}$, normalized by the standard deviation of the distribution $\sigma_{Y|Sa}$, to create a standardized variate. That is, let us consider four new parameters:

- The standardized damage factor, denoted by Ψ_Y
- The standardized damage factor in the log domain, denoted by $\Psi_{\ln Y}$
- The residual coefficient of variation of the damage factor, $\delta_{Y|Sa}$, and
- The residual coefficient of variation of the damage factor in the log domain.

These are defined by:

$$\Psi_Y = (Y - \mu_{Y|Sa})/\sigma_{Y|Sa} \quad (5\text{-}1)$$

$$\Psi_{\ln Y} = (\ln Y - \mu_{\ln Y|Sa})/\sigma_{\ln Y|Sa} \quad (5\text{-}2)$$

$$\delta_{Y|Sa} = \sigma_{Y|Sa}/\mu_{Y|Sa} \quad (5\text{-}3)$$

$$\delta_{\ln Y|Sa} = \sigma_{\ln Y|Sa}/\mu_{\ln Y|Sa} \quad (5\text{-}4)$$

where $\sigma_{Y|Sa}$ and $\sigma_{\ln Y|Sa}$ represent the standard deviation in the damage factor Y and $\ln Y$ at a given level of S_a. For each simulation and ABV analysis of a building, one can calculate the values of Ψ_Y and $\Psi_{\ln Y}$. Because Ψ_Y and $\Psi_{\ln Y}$ are standardized using the mean damage factor at its given level of S_a, Ψ_Y and $\Psi_{\ln Y}$ should be relatively insensitive to S_a, and one can examine the marginal distributions of Ψ_Y and $\Psi_{\ln Y}$ to determine the general form of the distribution of Y.

The observed cumulative marginal distributions of Ψ_Y and $\Psi_{\ln Y}$ can be compared with the Gaussian distribution to see if the residual error in the damage factor can be approximated by a normal or lognormal distribution, respectively. Doing this for each of the typical-quality index buildings, it is found that the lognormal distribution is unacceptable for any of the index buildings. Figure 5-11 shows the comparison of the damage-factor distribution with the Gaussian; Figure 5-12 compares is with the lognormal. In each case, the fit fails the Kolmogorov-Smirnov goodness-of-fit test at the 5% significance level.

If one limits the data to $S_a \leq 1.0$g, the lognormal adequately fits the typical-quality variants of the small house, townhouse and apartment building at the 1% significance level, implying that at all intensity levels of shaking except rare, strong events, one can often but not always approximate the damage-factor as a lognormally distributed random variable whose mean value (in the linear domain) is approximated by a regression curve

fit to $\mu_{Y|Sa}$, and whose coefficient of variation (COV) in the linear domain is discussed next.

Figure 5-11:
Comparison of Damage-Factor Distribution with Gaussian

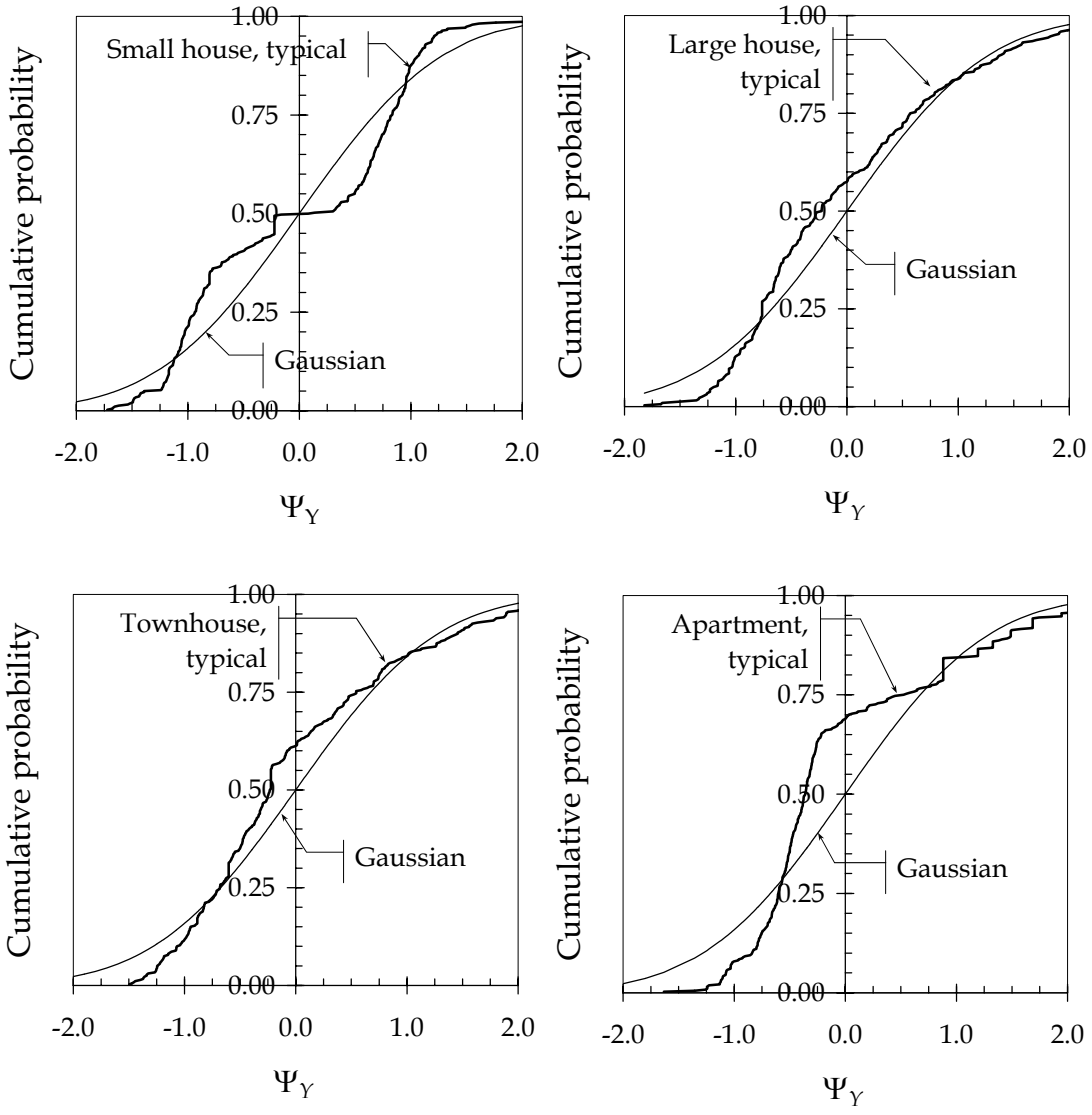

Figure 5-12:
Comparison of Damage-Factor Distribution with Lognormal

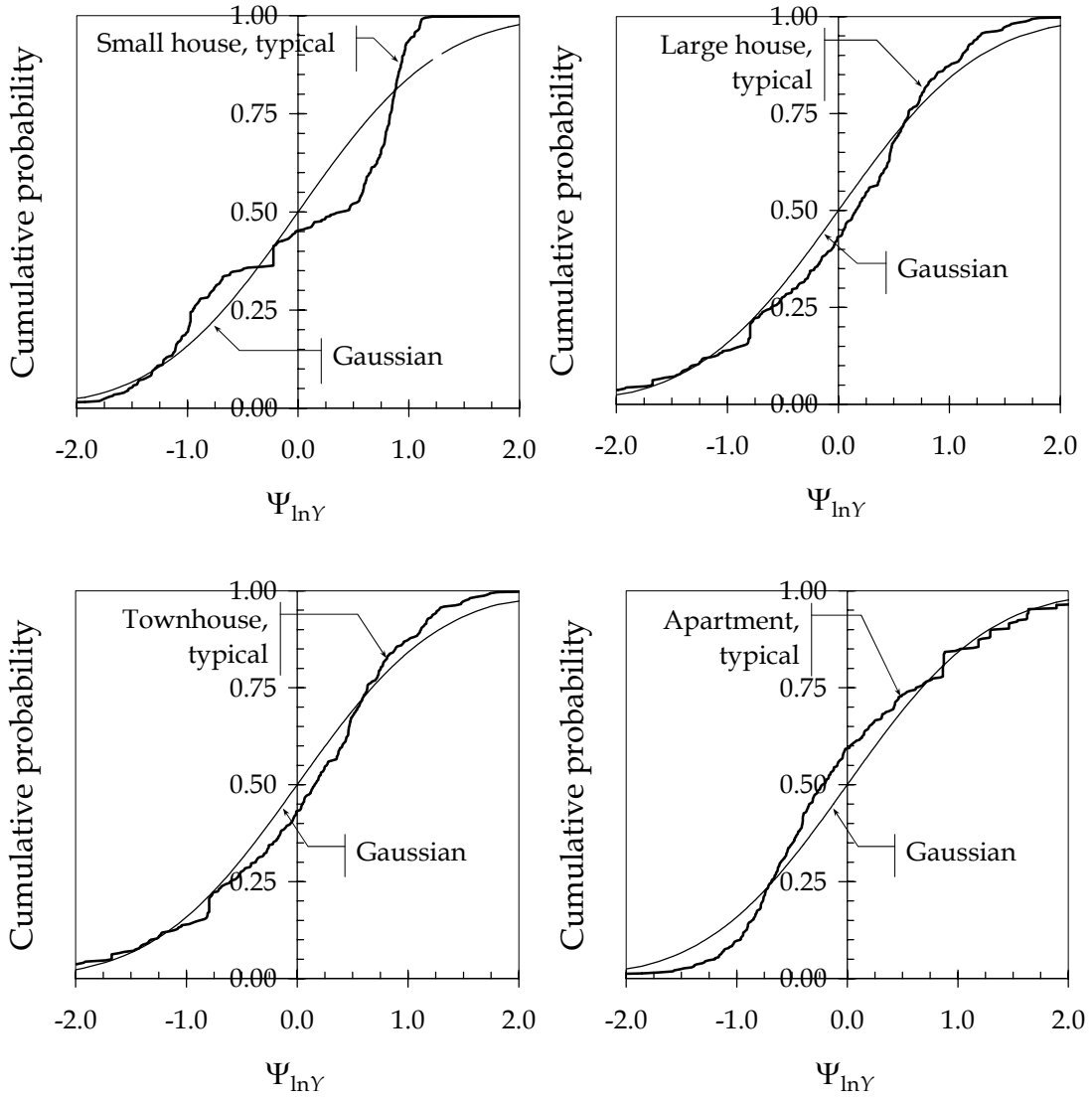

The COV of the damage factor appears generally to decrease with increasing intensity and damage. The trend is apparent when COV is compared with S_a (Figure 5-13), and is stronger when compared with mean damage factor (Figure 5-14). Figure 5-14 shows a discontinuity in this trend for the small house and apartment building, which both are modeled as having significant collapse potential. The discontinuity is associated with the bimodal behavior of the building: one mode of the distribution of repair cost for samples without collapse, another for samples with collapse.

Table 5-1 shows the average value of the residual COV, weighting all samples equally. The residual error of a loss estimate is observed to vary between 0.6 and 0.8 for buildings

where the collapse potential is small. The COV is much greater for the buildings with significant collapse potential, and varies between 0.9 and 1.4, again because of the bimodal behavior.

The COV values shown in Table 5-1 and Figure 5-14 probably underestimate total uncertainty on the cost to repair earthquake-induced damage, because the underlying loss estimates rely on observational data of ground motion, component damageability, and other factors. Particularly in the case of laboratory tests of building components, these observations do not represent all possible locations, configurations, and other variables that would otherwise increase uncertainty. For the present then, the COVs presented here should be viewed as lower-bound estimates.

Table 5-1:
Residual Coefficient of Variation of Damage Factor

Index building, variant	$\delta_{Y\|Sa}$	Index building, variant	$\delta_{Y\|Sa}$
Small house, poor	0.87	Townhouse, poor	0.61
Small house, typical	1.00	Townhouse, typical	0.74
Small house, superior	1.14	Townhouse, superior	0.65
Small house, braced	1.40	Townhouse, limited drift	0.73
Large house, poor quality	0.79	Apartment, poor	1.39
Large house, typical quality	0.57	Apartment, typical	1.21
Large house, superior quality	0.77	Apartment, superior	1.34
Large house, waist wall	0.71	Apartment, steel frames	0.47
Large house, IO	0.62	Apartment, shearwall	1.22
Large house, rigid diaphragm	0.75	Townhouse, poor	0.61

Figure 5-13:
COV of Damage Factor vs. S_a

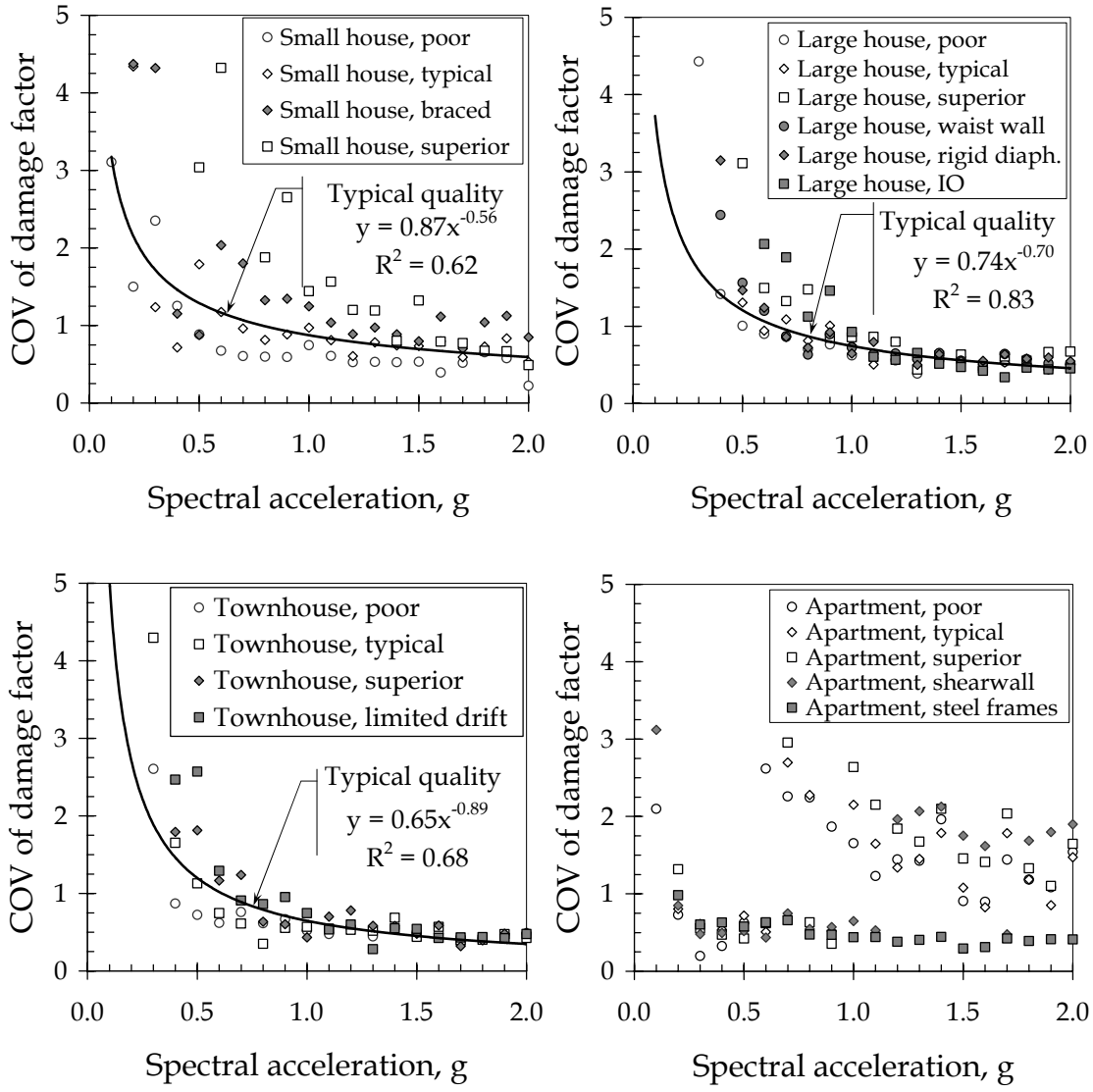

Figure 5-14:
COV of Damage Factor vs. Mean Damage Factor

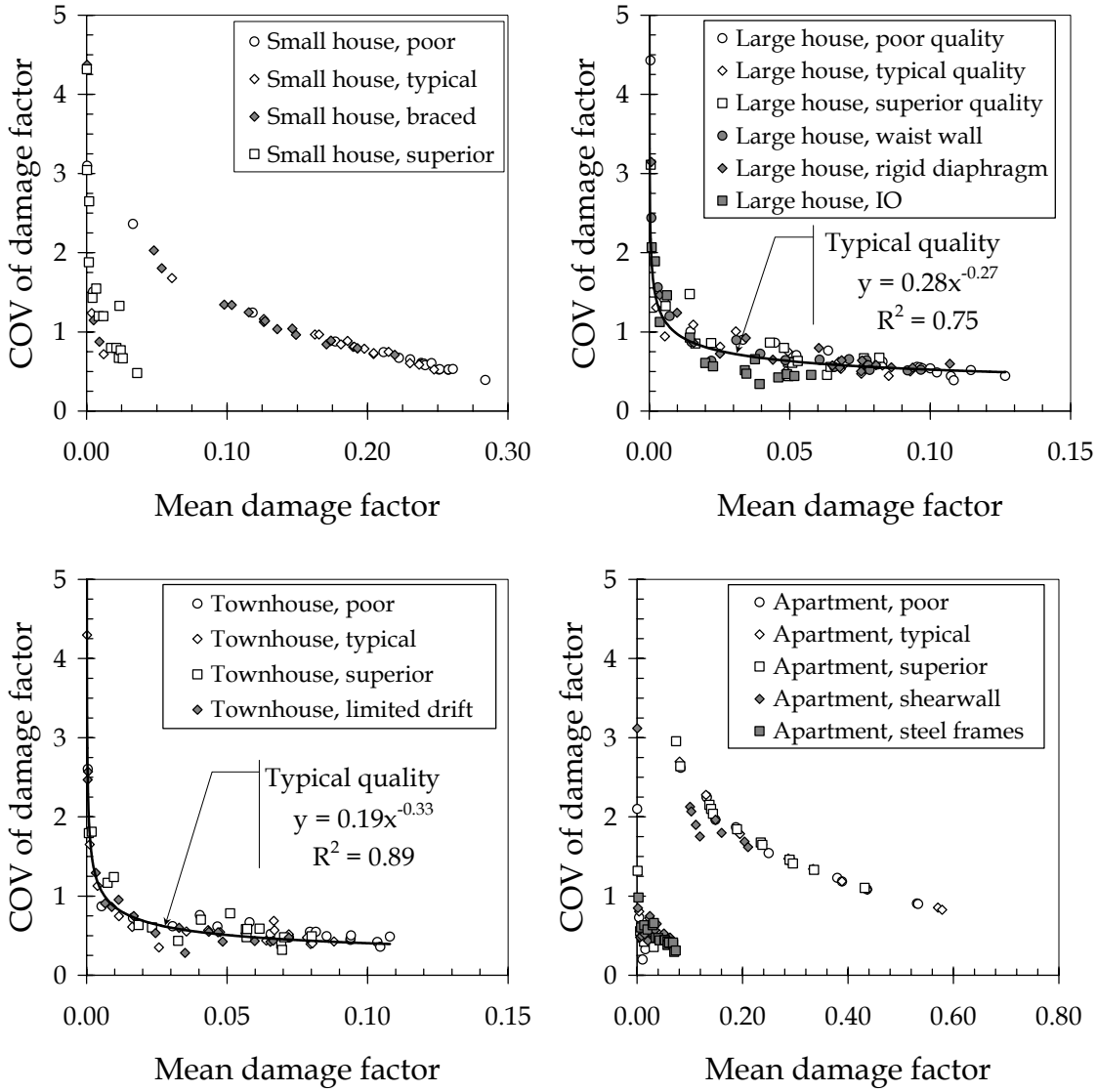

Assembly Contribution to Loss

It is interesting to examine the loss data to determine which assemblies contribute most to repair cost. Figure 5-15 through Figure 5-18 show the average fraction of total repair cost represented by each of five categories of assembly type: paint, water heater, glazing, gypsum wallboard, exterior nonstructural walls (i.e., stucco walls without structural sheathing), exterior shearwalls (stucco with structural sheathing), and interior shearwalls. Note that the figures' *x*-axis begins at the S_a value where nonzero losses are first observed. The figures show a few interesting trends.

1. **Line-of-sight costs are substantial.** Painting contributes about half the total repair cost. The reason is that even minor damage to the walls of a room, hallway, or exterior wall is modeled as requiring the entire portion of the wall within the line of sight to be painted.
2. **Drywall and exterior shearwall costs are about equal.** These assemblies contribute the bulk of the costs not attributable to painting. The small house is an exception, which can be explained by observing that most of the damage in the small house occurs at the cripple-wall level, where there is no gypsum wallboard. The other index buildings lack cripple walls. In them, the first-floor shearwalls and drywall experience about equal repair costs.
3. **Glazing costs are minor.** Repair of broken glass contributes less than 5% of the total repair costs; at moderate shaking intensity, glass contributes less than 1% of the total cost. In some of the plots, glazing costs are too minor to discern at this scale.

Figure 5-15:
Assembly Contribution to Total Repair Cost, Small House, Typical

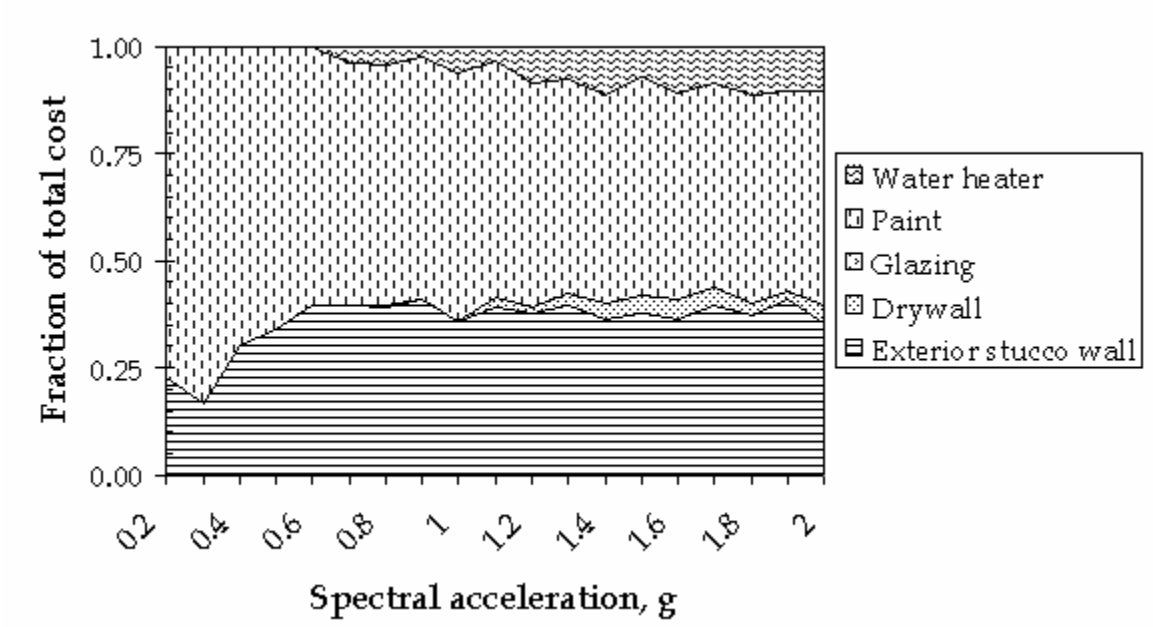

Figure 5-16:
Assembly Contribution to Total Repair Cost, Large House, Typical

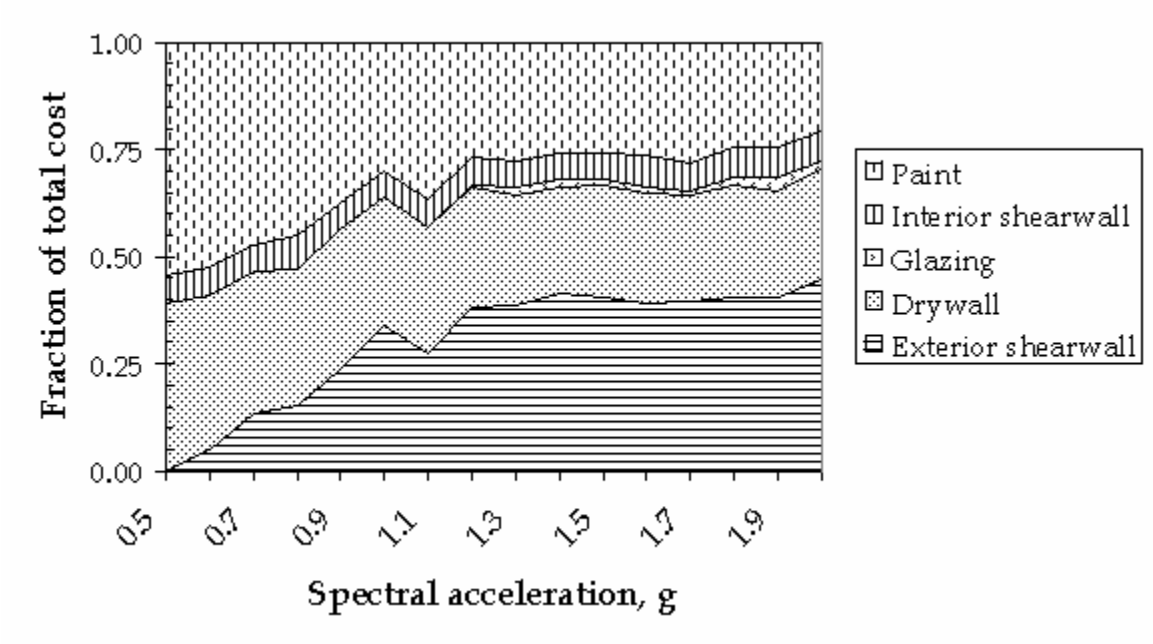

Figure 5-17:
Assembly Contribution to Total Repair Cost, Townhouse, Typical

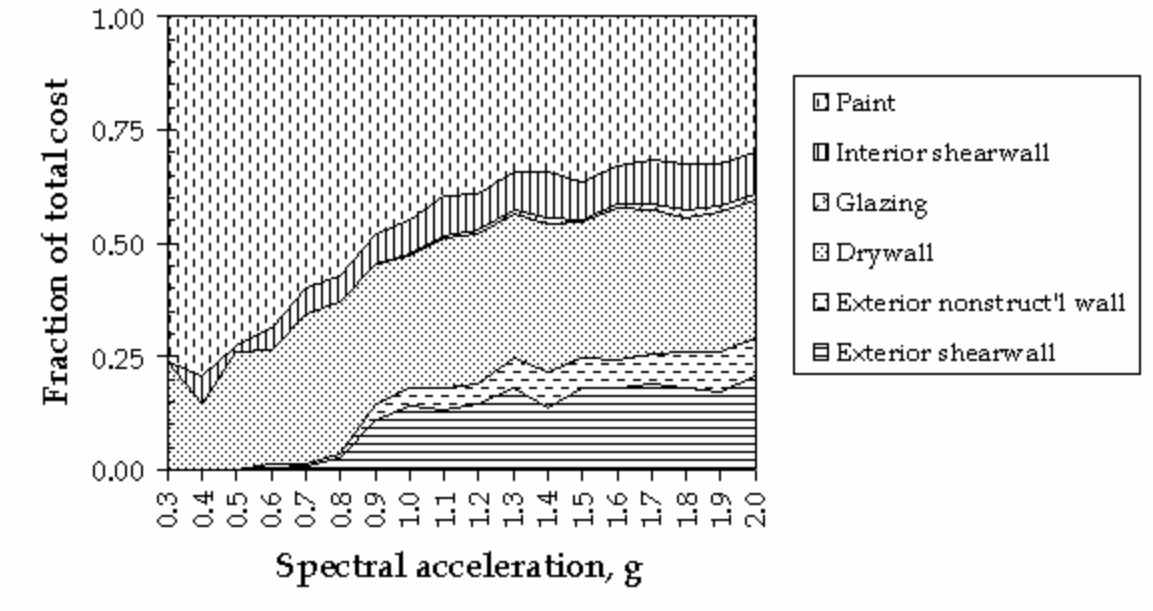

Figure 5-18:
Assembly Contribution to Total Repair Cost, Apartment Building, Typical

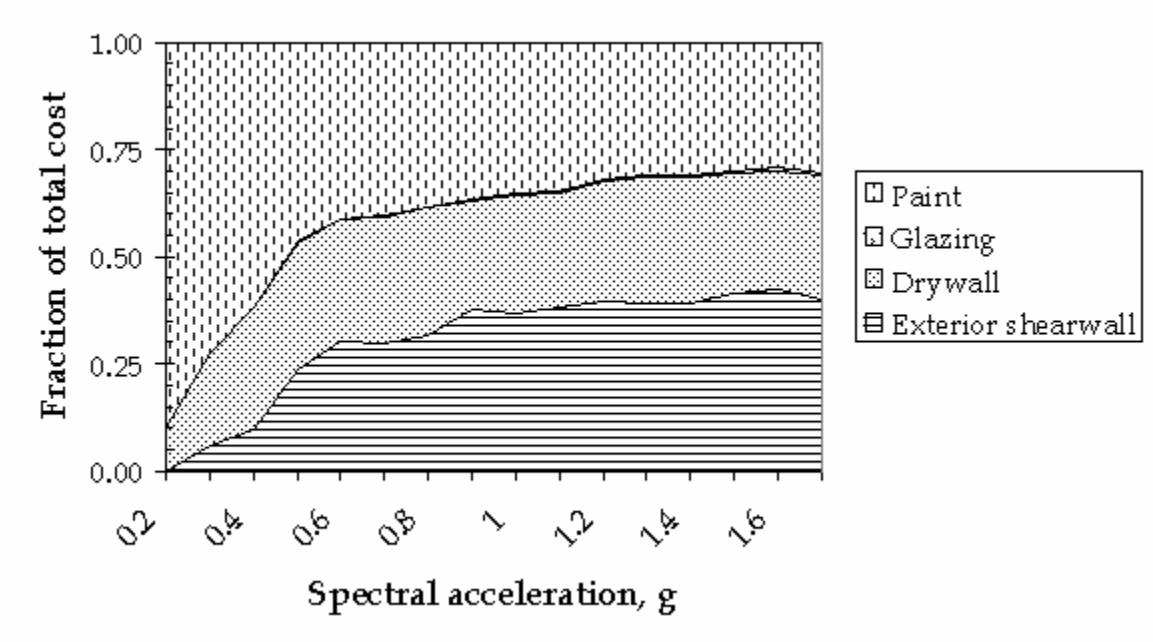

Comparison of Vulnerability Functions to Experience Data

To check the reasonableness of the vulnerability functions, a comparison to historic earthquake experience data and published models was performed. Published data from several earthquakes, including the 1994 Northridge, 1983 Coalinga and 1971 San Fernando Earthquakes, were utilized. It should be noted that much of the historic earthquake loss data has traditionally been tabulated in terms of Modified Mercalli Intensity (MMI), and that only since the Northridge Earthquake has systematic comparison to instrumental ground-motion severity measures such as PGA been widespread. To translate CUREE's vulnerability functions to MMI for comparison with Coalinga and San Fernando data, we evaluated the vulnerability function in terms of the PGA for each scaled ground motion, and then converted PGA (cm/sec^2) to MMI using the relationship proposed by Wald *et al.* (1999), valid for MMI values of V to VIII:

$$MMI = 3.66\log_{10}(PGA) - 1.66 \quad (\sigma = 1.08) \tag{5-5}$$

Experience Data Sources

Earthquake experience data reviewed for comparison purposes were derived from a number of sources, as described below. Information on the 1971 San Fernando and 1983 Coalinga Earthquakes are given by Steinbrugge and Algermissen (1990), based on insurance and other inspections. The 1994 Northridge Earthquake was the most well-

documented earthquake in recent history. Digital databases were developed and made available by numerous researchers and jurisdictions (such as the City of Los Angeles), with a significant number compiled and analyzed by members of the project team and the California Governor's Office of Emergency Services (OES). Data on the 1994 Northridge Earthquake is available from ATC-38 (Applied Technology Council, 2000), Schierle (2000), and EQE International *et al.* (1995). Some discussion of each resource is necessary to make meaningful comparisons.

Steinbrugge and Algermissen (1990), prepared in conjunction with the State of California Department of Insurance, focus on quantifying monetary damage in a manner relevant to the insurance industry. The San Fernando data give total repair costs as a fraction of property market value excluding land value, i.e., not as a fraction of replacement cost. Loss ratios must be reduced to compare with vulnerability functions based on replacement cost, and possibly further reduced to account for claims adjustment practice. The degree of either reduction is unknown.

Steinbrugge and Algermissen (1990) present loss data for several categories of buildings: one-story and two-story woodframe single-family dwellings; pre-1940, 1940-1949, and post-1949 construction; and houses with cripple walls or slab-on-grade construction. These data are therefore meaningful to compare with the small house and large house, but not the townhouse or apartment building.

Steinbrugge and Algermissen's (1990) Coalinga data are presented in two groups: field inspections unrelated to insurance, and insurance-related inspections. The data exclude dwellings that had shifted off their foundations or were posted as hazardous or had been demolished before the time of inspection. They therefore underestimate the vulnerability of housing affected by the Coalinga Earthquake.

The regions surveyed in the San Fernando Earthquake experienced ground shaking between 0.5 and 1.0g, and between MMI VIII and IX. (Compare Steinbrugge and Algermissen, 1990, Figure 14, with McClure, 1973, Figure 3.1, or with U.S. Geological Survey, 2001a and b.) Coalinga experienced ground shaking of MMI VIII. Table 5-2 summarizes the relevant loss data taken from the report, with categories directly comparable to the small house and large house highlighted in bold. The table shows the number of buildings surveyed and the associated damage factor (DF), as a percent of market value. Coalinga insurance-related data are expressed as percent of replacement cost.

Table 5-2:
Woodframe Dwelling Losses (Steinbrugge *et al.*, 1990)

		1971 San Fernando (MMI VIII-IX)				1983 Coalinga (MMI VIII)			
		All heights		1 story		Non-insurance		Insurance	
Construction	Built	No.	DF (%)	No.	DF (%)	No.	DF (%)	No.	DF (%)
Wood floor	Pre-1940	468	11.40	465	11.41	167	8.35	138	26.40
	1940–1949	2,391	8.29	2,379	**8.26**	130	**8.46**	72	**8.24**
	Post-1949	1,184	9.13	1,148	**8.72**	226	**10.51**	63	**5.25**
	All ages	4,123	8.87	4,072	8.73	532	9.28	279	16.49
Concrete floor	Pre-1940	106	6.40	106	6.40	9	5.78	3	5.33
	1940–1949	1,675	7.49	1,668	7.50	23	8.57	14	16.86
	Post-1949	4,343	**7.69**	4,142	7.56	300	**7.52**	84	**5.04**
	All ages	6,185	7.61	5,965	7.52	335	7.53	103	7.33

The objective of the ATC-38 study (Applied Technology Council, 2000) was to collect building exposure and damage data for buildings in close proximity to strong motion recording instruments, in an effort to correlate building performance and the severity of ground shaking. The study surveyed 530 buildings near 31 instruments that recorded ground motions ranging from 0.15g to 1.78g. The resulting database includes data on 235 light woodframe (W1) and 35 commercial or long-span woodframe (W2) structures, most of which (74% of W1 and 89% of W2) suffered insignificant damage.

A subset of the woodframe structures, 183 W1 and W2 buildings built after 1939, were evaluated for repair cost as well as damage, for purposes of comparison with the damage functions of ATC-13 (Applied Technology Council, 1985). For each building, the inspectors estimated the ATC-13 damage state of the structure and of the contents (i.e., separate damage states for structure and contents), by judging the damage factor on the basis of the observed physical damage. Of the 183 buildings, 57 were inspected inside and out and 62 were inspected outside only. The database does not indicate whether the remaining 64 buildings were inspected inside, although the content damage state is estimated for 48 of these. It therefore appears that the majority of the 183 buildings were inspected inside and out. The surveys were performed by teams of two licensed civil or structural engineers, with each survey taking approximately two person-hours per building.

Using the ATC-13 damage states, the ATC-38 authors created a damage probability matrix (DPM), which depicts the probability that a building will be in a given damage state, for each level of ground shaking in terms of Modified Mercalli Intensity. (For a more complete discussion of damage probability matrices, see ATC-13 or Whitman, 1974). It should be noted that comparisons at MMI VI and IX were not recommended due to a scarcity of data. The DPM can, in turn, be used to develop mean damage estimates (the mean damage factor) at each level of ground shaking by summing the

product of each damage state's central damage factor and the probability that the building will be in that damage state. Table 5-3 provides the ATC-38 post-1939 woodframe damage probability matrix, as well as the resulting mean damage estimates.

Table 5-3:
ATC-38 Post-1939 Woodframe Building Damage Probability Matrix

Damage State	Percent Damage (Central Damage Factor)	VI	**VII**	**VIII**	IX
None	0% (0%)	0	**26.5**	**13.0**	0
Slight	0 – 1% (0.5%)	100	**61.3**	**49.3**	96.3
Light	1 – 10% (5%)	0	**10.9**	**17.5**	0
Moderate	10 – 30% (20%)	0	**1.3**	**13.7**	3.7
Heavy	30 – 60% (45%)	0	**0**	**5.1**	0
Major	60 – 100% (80%)	0	**0**	**1.4**	0
Destroyed	100% (100%)	0	**0**	**0**	0
Overall mean damage estimate		*	***1.1***	***7.3***	*

* Mean damage not estimated at MMI VI and IX because of noted lack of data.

The Field Investigations element of the CUREE-Caltech Woodframe Research Project (Schierle, 2001) addresses performance of residential woodframe buildings through statistical analysis of damage data, and in-depth case studies of selected woodframe structures. Included in the report are a general study examining the performance of red- and yellow-tagged structures, a sample study examining 1230 randomly selected structures in more detail, and focused studies on apartments with tuck-under parking, buildings with expensive repairs, and demolished structures. Digital data utilized by the CUREE researchers includes electronic data on existing and damaged buildings from the City of Los Angeles. The draft report examines PGA-based data for single- and multi-family structures of three eras of construction: pre-1940, 1941-1976, and post-1976. Because the general study excluded green-tagged structures in its focused database, the resulting tabulations do not include structures with minor damage and would not be directly comparable to the vulnerability functions developed here. The sample study represents further analysis and supplemental data collection for a sample of structures selected from the database used in the general study. Accordingly, because of the exclusion of green-tagged structures, the data provided in Schierle (2001) are not comparable to the vulnerability functions developed in the current study.

EQE International *et al.* (1995) presents the results from an ambitious joint effort between the California Governor's Office of Emergency Services and EQE International to quantify and analyze information on economic and social losses caused by the Northridge Earthquake. The publication summarizes the data and analysis related to general building damage, and the public and private financial resources mobilized for

recovery. Extensive tabular data are provided regarding the inventory of buildings exposed to strong motion and damage surveys made by more than 150 jurisdictions.

The inventory data in EQE International *et al.* (1995) are based on data provided by the Los Angeles County Tax Assessor's Office. The data categorize buildings by construction type, occupancy, era of construction, and size. Address data are mapped to a geographic location, which is used to determine site conditions and shaking intensity in terms of MMI and PGA. The most useful damage data for present purposes are records of 71,234 woodframe buildings that were inspected by building-department officials, matched to a record in the tax-assessor file, and found to stand on soil sites (as opposed to rock).

The inspectors estimated building damage in terms of dollar repair cost based on a brief exterior examination. Building replacement cost for these buildings was estimated considering construction type and square footage, using RS Means Co., Inc. (1994). Damage and inventory data were binned by category and shaking intensity. The ratio of the total estimated repair cost in the damage database to the total estimated replacement cost in the inventory provides the damage factor for that bin of building category and shaking intensity.

Plotting these damage factors versus shaking intensity yields a vulnerability function that can be compared with those developed here. Note that later construction-permit data indicate that a substantial number of dwellings (35,000 in Los Angeles County) experienced damage but were not inspected, and are therefore not reflected in the damage database. Consequently, the EQE International *et al.* (1995) vulnerability functions tend to underestimate actual damage. The fact that the building inspectors' damage estimates were made primarily during rapid surveys would also tend to produce low estimates of loss and therefore of vulnerability.

The data discussed here are plotted along with the CUREE vulnerability functions from this project in several figures. Figure 5-19 compares the vulnerability function for the small house, typical quality, with the San Fernando, Coalinga, and Northridge data. The CUREE data are translated to an MMI basis using Wald *et al.* (1999), as discussed above. The figure suggests agreement between the CUREE vulnerability function and the San Fernando and Coalinga data and with Northridge data at MMI 7 to 8. However, it shows that CUREE's vulnerability function is substantially higher than indicated by the MMI 9 Northridge survey data discussed in EQE International *et al.* (1995), possibly for the reasons discussed above. The error bars in the figure provide ± 0.5 MMI units for the historic data. The figure overstates the ability to compare the CUREE vulnerability functions with the historic data, since the CUREE vulnerability function is mapped to MMI via Wald *et al.* (1999), whose uncertainty is ± 1 MMI unit. If ±1 MMI unit error bars were added to the CUREE curve, the curve would be a broad diagonal half the width of the chart.

Figure 5-20 addresses the large house. It shows that the CUREE vulnerability function for the large house is bracketed by the San Fernando, Coalinga, and ATC-38 data above it, and the EQE International *et al.* (1995) data below (perhaps because the EQE data underestimate damage, as discussed above). Figure 5-21 and Figure 5-22 deal with the typical-quality townhouse and apartment building vulnerability functions, respectively. The figures compare these with the EQE International *et al.* (1995) data on a PGA basis, for which no comparable data exist from the San Fernando or Coalinga studies. The figures show that the CUREE vulnerability function for the townhouse agrees well with the pre-1976 EQE/OES data, but is substantially greater than the post-1976 data, with which it should be more comparable. This again is consistent with the observation that the Northridge survey data probably underestimates actual losses, although the degree of the difference is unsettling, especially considering that the CUREE vulnerability functions, as they reflect simple, regular structures, probably also underestimate the vulnerability of actual structures.

Figure 5-19:
Vulnerability Model Comparison, Small House, Typical

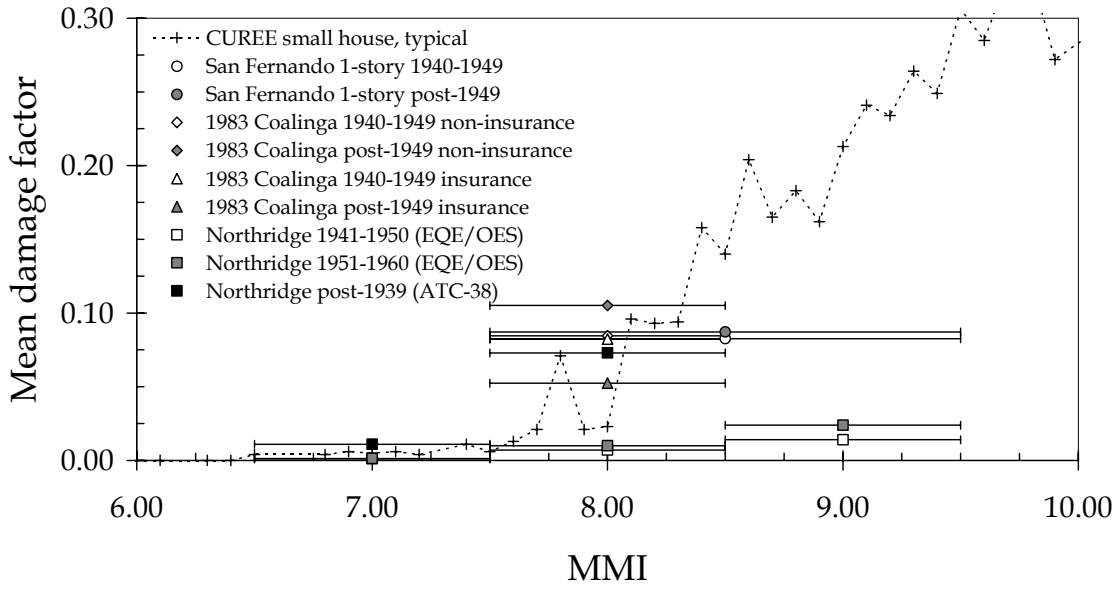

Figure 5-20:
Vulnerability Model Comparison, Large House

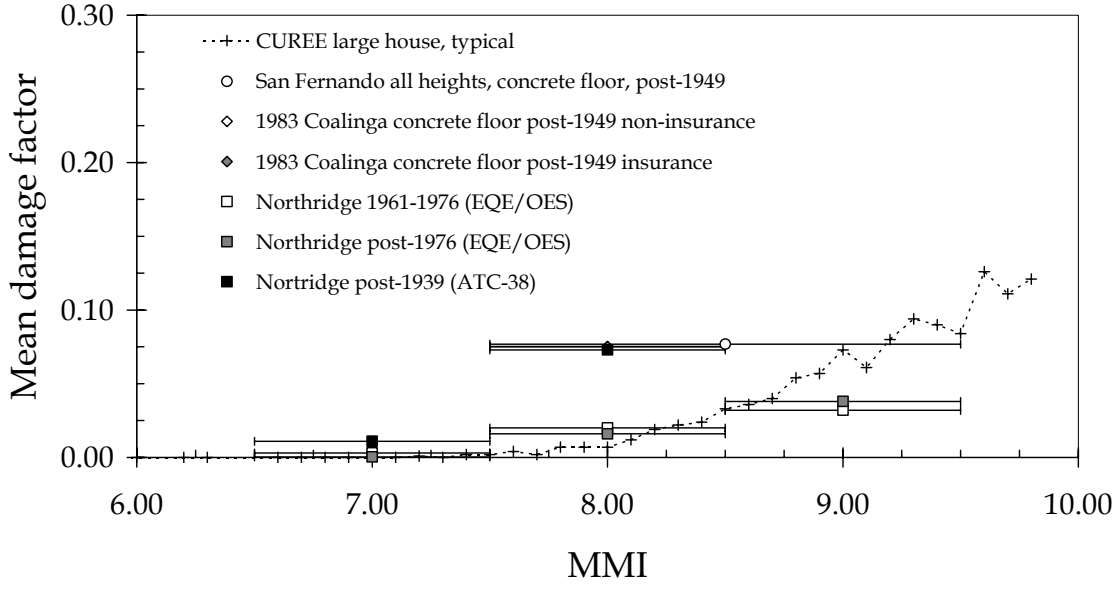

Figure 5-21:
Vulnerability Model Comparison, Townhouse, Typical Quality

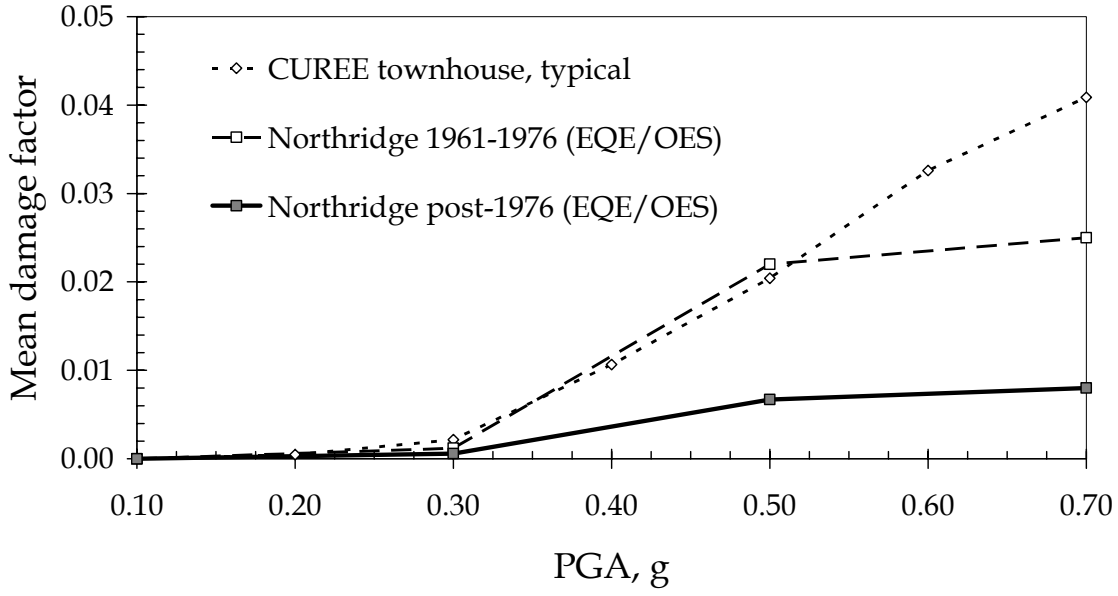

Figure 5-22:
Vulnerability Model Comparison, Apartment Building, Typical Quality

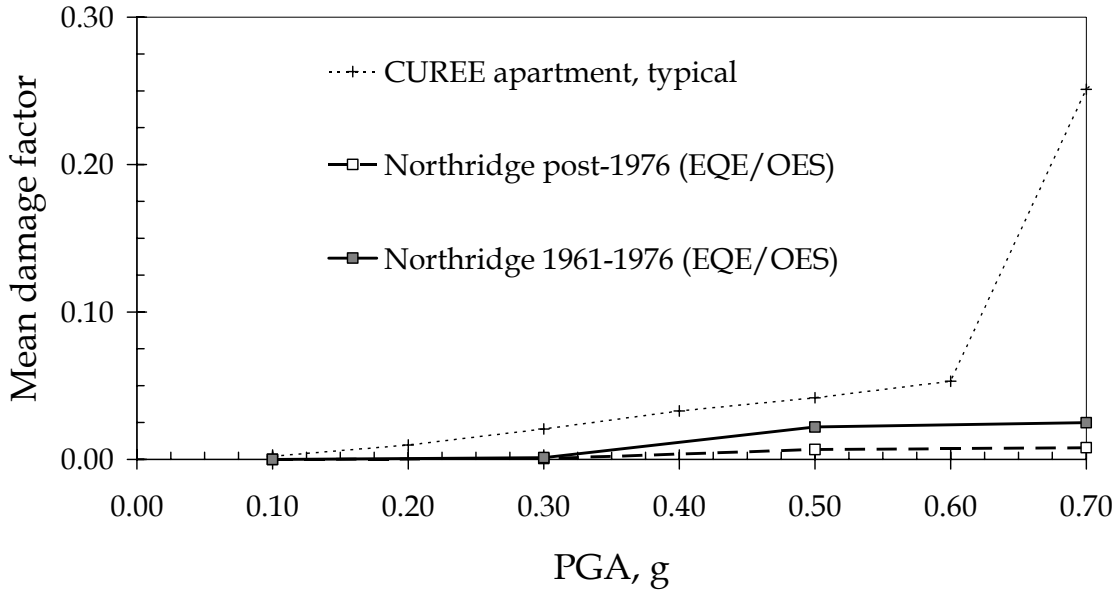

HAZUS-Compatible Fragility Functions

Using the foregoing results, it is possible to develop HAZUS-compatible fragility functions. That is, the vulnerability data are evaluated in terms that can be used directly in HAZUS. Six items, listed in Table 5-4, are required to express results of the present study in terms compatible with HAZUS.

Table 5-4:
Summary of Data Required for Implementation within HAZUS of CUREE Woodframe Loss-Estimation Results

Required Data
1. Building capacity (pushover) curve parameters: (S_d, S_a) at yield and at ultimate
2. Response parameters: elastic damping, degradation (kappa) factors, and nonstructural fraction
3. Fragility-curve parameters: damage-state medians (x_m) and logarithmic standard deviation (β) for each index building and each damage state
4. Description of damage states in terms of physical damage
5. Collapse rates for each index building in the complete damage state. This is used for the casualty-estimation module
6. Typical or mean repair costs per square foot for each index building in each damage state. This is used for estimating dollar losses

HAZUS Data Item 1: Pushover Curve Parameters

As discussed in Chapter 4, the shape of the pushover curves for the CUREE index buildings is taken from existing HAZUS types, by matching index buildings to HAZUS types by size, age, and quality. The HAZUS type for each index building and variant is given in Tables 4-8 and 4-9. The corresponding pushover curve parameters from the HAZUS documentation are presented in Table 5-5. The table provides the spectral displacement and spectral acceleration assumed by HAZUS to correspond to yield (denoted by D_y and A_y, respectively, as in the HAZUS manual) and ultimate (D_u and A_u, respectively).

Table 5-5:
HAZUS-Compatible Pushover Curve Parameters

Index Building, Variant	Yield		Ultimate	
	D_y (in.)	A_y (g)	D_u (in.)	A_u (g)
Small house, poor	0.24	0.2	4.32	0.6
Small house, typical	0.36	0.3	6.48	0.9
Small house, superior	0.48	0.4	11.51	1.2
Small house, braced	0.48	0.4	11.51	1.2
Large house, poor	0.36	0.3	6.48	0.9
Large house, typical	0.48	0.4	11.51	1.2
Large house, superior	0.72	0.6	17.26	1.8
Large house, waist wall	0.48	0.4	11.51	1.2
Large house, immediate occupancy	0.72	0.6	17.26	1.8
Large house, rigid diaphragm	0.72	0.6	17.26	1.8
Townhouse, poor	0.36	0.3	6.48	0.9
Townhouse, typical	0.48	0.4	11.51	1.2
Townhouse, superior	0.72	0.6	17.26	1.8
Townhouse, limited drift	0.72	0.6	17.26	1.8
Apartment, poor	0.16	0.1	2.35	0.25
Apartment, typical	0.31	0.2	4.70	0.5
Apartment, superior	0.63	0.4	12.53	1
Apartment, steel frames	0.63	0.4	12.53	1
Apartment, shearwall	0.63	0.4	12.53	1

HAZUS Data Item 2: Response Parameters

Elastic damping, denoted by B_E, is defined as the elastic pre-yield damping expressed as a percentage of critical damping, used to estimate effective damping. According to Kircher (1999), B_E for wood structures with nailed joints is about 15% of critical damping. The current HAZUS default for W1 is 15% regardless of code level, and 10% for W2. In the present study, however, 10% damping is used for all woodframe structures. This is based on system-identification work by Camelo *et al.* (2001), who examined a variety of woodframe buildings that were subjected to strong motion or forced vibration. Table 5-6 summarizes the HAZUS response parameters discussed here.

Kappa factors, denoted by K_S, K_M, K_L, are defined as the degradation of post-yield hysteretic response, expressed as a fraction of non-degraded hysteretic behavior for short, medium and long shaking duration, respectively. As discussed in Chapter 4, kappa factors are all taken as zero. The reader should not infer that duration effects and nonstructural component are ignored. Duration effects are accounted for by the use in the ABV analysis of historic ground-motion time histories of various durations.

Nonstructural fraction, denoted by FNS, is the fraction of acceleration-sensitive components and contents at lower floors, currently assumed by HAZUS to be 0.5 for lowrise construction. That default is suggested for use with the CUREE index buildings.

Table 5-6:
HAZUS Response Parameters

Index Building, Variant	B_E	K_S, K_M, and K_L	FNS
Small house, poor	10%	0	0.5
Small house, typical	10%	0	0.5
Small house, superior	10%	0	0.5
Small house, braced	10%	0	0.5
Large house, poor	10%	0	0.5
Large house, typical	10%	0	0.5
Large house, superior	10%	0	0.5
Large house, waist wall	10%	0	0.5
Large house, immediate occupancy	10%	0	0.5
Large house, rigid diaphragm	10%	0	0.5
Townhouse, poor	10%	0	0.5
Townhouse, typical	10%	0	0.5
Townhouse, superior	10%	0	0.5
Townhouse, limited drift	10%	0	0.5
Apartment, poor	10%	0	0.5
Apartment, typical	10%	0	0.5
Apartment, superior	10%	0	0.5
Apartment, steel frames	10%	0	0.5
Apartment, shearwall	10%	0	0.5

HAZUS Data Item 3: HAZUS-Compatible Fragility Curve Parameters

HAZUS' fragility functions are defined in terms of the probability of exceeding certain damage states, given a level of displacement defined as the x-coordinate of the intersection of a pushover curve and the (S_d, S_a) response spectrum. The probability is estimated as the cumulative lognormal distribution evaluated at that x-coordinate. The cumulative lognormal distribution has two parameters: x_m and β. The x_m term represents the x-coordinate at which there is an estimated 50% probability of exceeding the damage state. The β term is a measure of dispersion of the lognormal distribution. Viewed another way, x_m represents the median capacity of a building to resist the damage state, and β represents the logarithmic standard deviation of capacity.

Table 5-7 presents the HAZUS-compatible fragility curve parameters x_m and β for each index building, variant, and HAZUS damage state, determined from the ABV simulations as described in Chapter 4. In several cases, none of the simulations reached the damage state of interest. That is, for several of the buildings, the ground motions employed did not result in any simulation reaching for example the complete damage state. These cases are indicated with blank entries. It is recommended that in these cases, the user set the median capacity, x_m, to some high value such as 100 in., and the logarithmic standard deviation to some low value, such as 0.01.

The table contains very high median values for several of the extensive and collapse states of the apartment building. These are not intended to imply meaningful information about building performance at these high displacements, but rather to produce good approximations of low probability levels at realistic displacements.

Table 5-7:
HAZUS-Compatible Fragility Parameters for Index Buildings

Index Building, Variant	Damage State	x_m, in.	β
Small house, poor	Slight	0.30	0.08
	Moderate	3.15	0.77
	Extensive	3.15	0.77
	Complete		
Small house, typical	Slight	0.45	0.30
	Moderate	4.06	0.70
	Extensive	4.06	0.70
	Complete		
Small house, superior	Slight	2.38	1.46
	Moderate		
	Extensive		
	Complete		
Small house, braced	Slight	0.56	0.27
	Moderate	4.32	0.89
	Extensive	6.19	0.90
	Complete		
Large house, poor	Slight	0.56	0.25
	Moderate	1.80	0.49
	Extensive		
	Complete		
Large house, typical	Slight	0.68	0.23
	Moderate	3.37	0.99
	Extensive		
	Complete		
Large house, superior	Slight	0.83	0.29
	Moderate	3.96	0.77
	Extensive		
	Complete		
Large house, waist wall	Slight	0.69	0.32
	Moderate	4.42	1.09
	Extensive		
	Complete		
Large house, IO	Slight	0.94	0.36
	Moderate	11.09	1.23
	Extensive		
	Complete		
Large house, rigid diaphragm	Slight	0.69	0.20
	Moderate	2.24	0.48
	Extensive		
	Complete		

Blank entries: no simulations reached this damage state

Table 5-7:
HAZUS-Compatible Fragility Parameters for Index Buildings (Cont.)

Variant	Damage State	x_m, in.	β
Townhouse, poor	Slight	0.47	0.21
	Moderate	1.97	0.74
	Extensive		
	Complete		
Townhouse, typical	Slight	0.55	0.23
	Moderate	3.87	1.02
	Extensive		
	Complete		
Townhouse, superior	Slight	0.64	0.34
	Moderate	3.25	0.75
	Extensive		
	Complete		
Townhouse, limited drift	Slight	0.69	0.32
	Moderate	4.42	1.09
	Extensive		
	Complete		
Apartment, poor	Slight	0.24	0.55
	Moderate	11.49	0.95
	Extensive[(1)]	36.54	0.01
	Complete[(1)]	36.54	0.01
Apartment, typical	Slight	0.26	0.33
	Moderate	10.62	1.10
	Extensive[(1)]	40.66	1.44
	Complete[(1)]	40.66	1.44
Apartment, superior	Slight	0.32	0.37
	Moderate	6.78	1.14
	Extensive[(1)]	44.63	1.69
	Complete[(1)]	44.63	1.69
Apartment, steel frames	Slight	0.25	0.34
	Moderate	4.06	0.79
	Extensive		
	Complete		
Apartment, shearwall	Slight	0.29	0.35
	Moderate	5.06	1.15
	Extensive[(1)]	74.01	0.89
	Complete[(1)]	74.01	0.89

Blank entries: no simulations reached this damage state
[(1)] See text.

HAZUS Data Item 4: Description of HAZUS Damage States

Figure 5-23 depicts the average fraction of assemblies damaged, by index building (typical quality variants) and damage state. They are used to describe the damage states in terms of physical damage, which is summarized in Table 5-8. Note that physical damage descriptions neglect any effects of ground failure (e.g., faulting, liquefaction, landslide), as ground failure is not modeled in the present study. The numbers in Figure 5-23 and in Table 5-8 are the result of the ABV analyses, which enable one to quantify physical damage at a more detailed level than possible under the other methodologies discussed in Chapter 2.

Figure 5-23:
Damage-State Descriptions

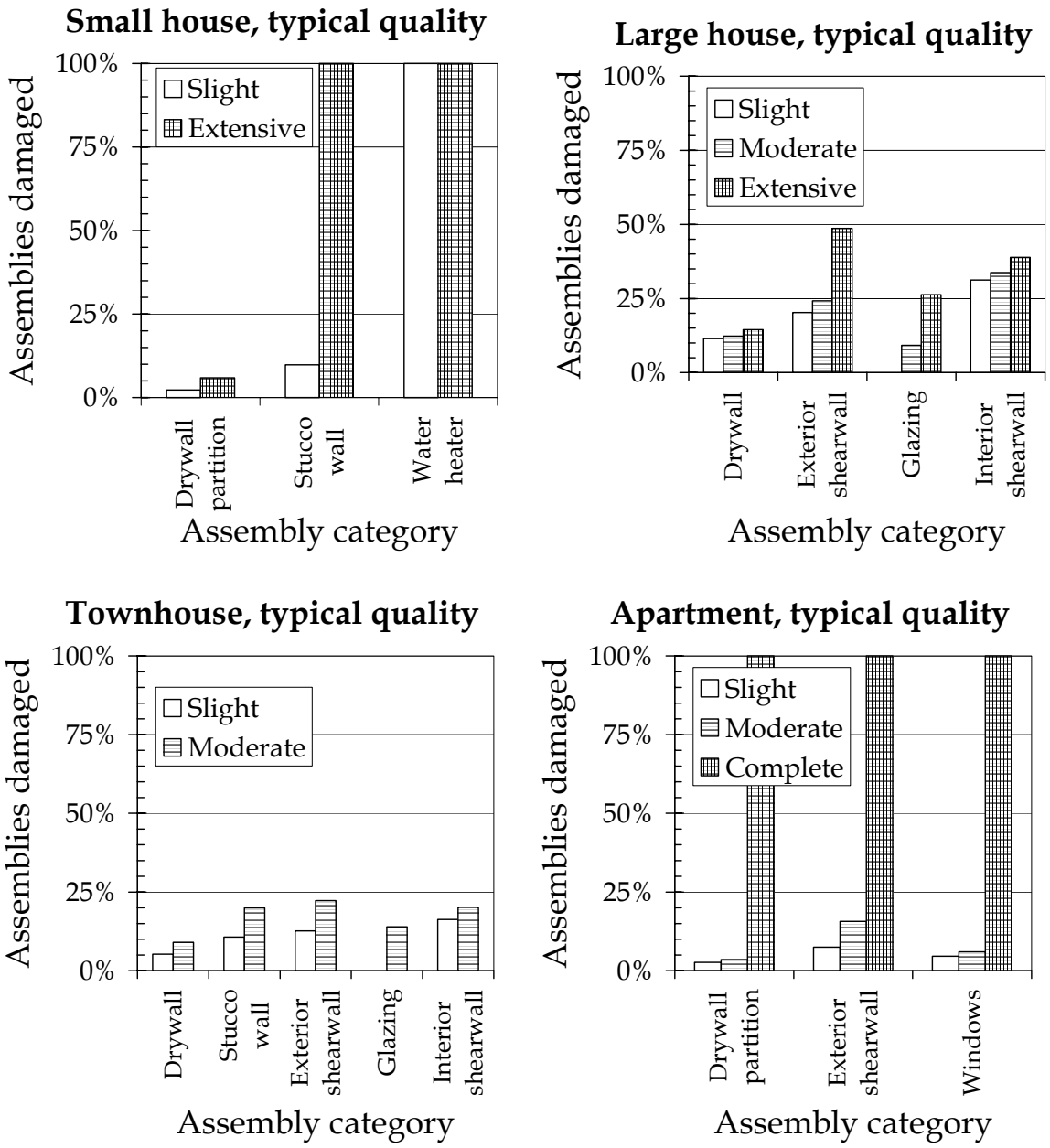

Table 5-8:
Description of Physical Damage by HAZUS Damage State

Index building	Slight	Moderate	Extensive	Complete
Small house, typical	<5% of drywall damaged; 10% of exterior nonstructural wall damaged, overturning of unbraced water heater is highly likely; <5% of windows damaged	No data available	Building has reached this damage state because unbraced cripple wall has collapsed.	No data available.
Large house, typical	10% of drywall, 20% of exterior shearwall, and 30% of interior shearwall damaged, <5% of windows damaged	10% of drywall, 25% of exterior shearwall, and 35% of interior shearwall damaged, 10% of windows damaged	15% of drywall, 50% of exterior shearwall, and 40% of interior shearwall damaged, 25% of windows damaged	No data available.
Townhouse, typical	5% of drywall, 10% of exterior stucco wall, 15% of exterior shearwall, and 15% of interior shearwall damaged, <5% of windows damaged	10% of drywall, 20% of exterior stucco wall, 20% of exterior shearwall, and 20% of interior shearwall damaged, 15% of windows damaged	No data available.	No data available.
Apartment building, typical	5% of drywall, 5-10% of exterior shearwall, 5% of windows damaged	5% of drywall, 15% of exterior stucco wall, 5% of windows damaged	Building has exceeded this damage state because garage level has collapsed.	Building has reached this damage state because garage level has collapsed.

HAZUS Data Item 5: Collapse Rates

All simulations of the apartment building that reached the complete damage state did so because they were modeled as having collapsed. All simulations of the small house that reached the extensive damage state did so because they were modeled as having collapsed. Note that none of the simulations of the small house reached the complete damage state, because the cost estimator estimates that the cost to restore the collapsed building is substantially less than 50% of the replacement cost. Collapse of the small house therefore qualifies as extensive damage.

This is not merely a semantic issue. Although the HAZUS authors describe the physical damage associated with each damage state, the states are *defined* in terms of repair cost. Because the cost to repair the collapsed small house is less than that associated with the lower bound of complete damage, the collapse does not qualify as complete damage. If the collapsed small house were misassigned to the complete damage state, future analyses using the resulting fragility functions would overestimate the repair cost.

No simulations of the large house or townhouse are modeled as having collapsed. This is a limitation of the modeling used in the present analysis. California buildings much like the small house and the apartment have collapsed in strong shaking, but except in cases of ground failure (which is not modeled here) there is little if any evidence that buildings like the large house or townhouse are significantly likely to collapse. Future ABV analysis using three-dimensional structural modeling of these structures could check this simplification.

Based on these observations, we recommend the following collapse probabilities. Again, these probabilities neglect the effects of ground failure (e.g., faulting, liquefaction or landslide), as ground failure is not modeled in the present study.

Small house:

P[collapse | extensive] = 100%
P[collapse | complete] = 100%

Large house and townhouse:

P[collapse | complete]: unknown, because collapse was not modeled for these index buildings, and no simulations were modeled as having reached the complete damage state.

Apartment:

P[collapse | extensive] = 100%
P[collapse | complete] = 100%

HAZUS Data Item 6, Mean Repair Costs

Table 5-9 presents average repair cost per square foot by index building, variant, and damage state. Figures are in 2001 dollars. Because these costs are in 2001 dollars, they will quickly become outdated; however, these are the terms required by HAZUS. To recalculate them at a future date, multiply each figure by the historic cost factor appropriate for 2001. For example, if in 2011, costs are 50% higher than they are in 2001, multiply each figure by 1.50. Historic cost factors are calculated on an ongoing basis by several sources, e.g., RS Means Co Inc. (2001). Similarly, location and union status affect the figures in the table, which are calculated for nonunion labor in Santa Monica, CA.

See Appendix F for a discussion of the cost to perform the same work using union labor, or in a different location. Note also that Appendix F (cost data sheet 9) contains the cost estimator's very approximate estimate of the cost to jack the collapsed small house back onto its foundation, viz., $39,000 to $51,000, which amounts to between 29% and 38% of the replacement cost of the house, or between $32.50 and $42.50 per square foot. Because the jacking cost is taken as an uncertain (random) variable in each simulation, the sample average repair cost per square foot for the small house, extensive damage state, is not exactly $37.50 per square foot.

Table 5-9:
Repair Cost per Square Foot Conditioned on HAZUS Damage State

Index Building, Variant	Slight	Moderate	Extensive	Complete
Small house, poor	$2.92		$37.69	
Small house, typical	$2.75		$37.23	
Small house, superior	$2.27	$7.75		
Small house, braced	$2.68	$6.61	$37.73	
Large house, poor	$2.03	$8.49	$15.96	
Large house, typical	$1.94	$7.06	$16.76	
Large house, superior	$1.93	$6.57	$16.24	
Large house, waist wall	$2.01	$7.38	$15.72	
Large house, IO	$1.94	$5.58		
Large house, rigid diaphragm	$2.07	$7.69	$16.27	
Townhouse, poor	$1.83	$7.02	$17.29	
Townhouse, typical	$1.85	$6.27		
Townhouse, superior	$1.84	$5.95		
Townhouse, limited drift	$1.65	$5.45		
Apartment, poor	$1.43	$3.91		$56.00
Apartment, typical	$1.40	$3.90		$56.00
Apartment, superior	$1.33	$3.76		$56.00
Apartment, steel frames	$1.42	$4.37		
Apartment, shearwall	$1.24	$4.43		$56.80

Blank: no data available for these damage states

It is assumed that repair materials are purchased in modest quantities and that therefore no volume discounts are available. The figures in Table 5-9 neglect possible regional post-earthquake increases in labor or material costs that could result from demand-driven cost inflation (usually called demand surge). Demand surge must be addressed considering regional economic effects.

The figures neglect any insurance effects that might cause loss adjusters to pay more or less than is required to repair earthquake-induced damage, e.g., paying for pre-existing damage not caused by the earthquake, or failing to pay for actual earthquake damage. Finally, the figures neglect ground-failure effects such as cracked slabs, as ground failure was not modeled.

Chapter 6. Risk Illustration: Benefits of Mitigation

The Importance of a Risk Study

To understand whether a particular retrofit or redesign measure is cost-effective, one must consider its cost and calculate the degree to which it reduces future costs relative to the as-is case. This reduction is often referred to as the benefit of the measure, although strictly speaking the benefit in a benefit-cost analysis is supposed to represent a positive income stream, not the reduction in a negative one.

Because the future losses are uncertain, we must consider the difference between as-is and what-if cases in terms of risk. Risk is a relationship between the likelihood of an event and the severity of loss if the event occurs. It can be plotted on a chart with severity of loss on the vertical axis and likelihood on the horizontal. Seismic risk is analogous to seismic hazard in that respect. In the case of seismic hazard, the severity is that of ground shaking, for risk, it is that of economic loss, fatalities, or some other measure of an undesirable outcome.

The present study addresses only the level of loss if strong shaking occurs, for various quality levels, retrofit and redesign measures. (It also quantifies the cost of these measures; see Appendix F for detail.) This study was not intended to examine the likelihood of various levels of shaking, and so cannot include a thorough assessment of the benefits of these measures and quality levels.

Nonetheless, we can list some important questions about the benefits of risk mitigation, present a methodology for answering them, and illustrate with a few examples. A separate risk study that pursues these questions in details for sites all over California and other seismic regions could provide valuable information to aid property owners and others in making risk-management decisions.

To illustrate such a study, this chapter presents an analysis of the economic costs and benefits of each index building and variant for a particular hypothetical site. It also presents an assessment of the likelihood that some these buildings would be red-tagged in a strong earthquake, or during a reasonable future period of time.

Some Important Benefits Questions

A risk study could answer several questions. (Many of these can be addressed using HAZUS, as supplemented by this study, while some require additional analytical tools.) Important questions include:

1. What is the expected present value of future earthquake damage for each index building and variant, for various stakeholders, locations, and soil conditions?

2. To what degree does a quality level, or a retrofit or redesign measure, reduce expected future earthquake repair costs and fatalities relative to some typical case?
3. Under what conditions (location, soil conditions) is a risk-mitigation measure cost-effective for a risk-neutral decision-maker?
4. What is the probability that a loss will exceed some specified amount during a given period of time? For example, what is the chance that loss will exceed the deductible on an insurance policy, during the insured's ownership period?
5. For which index buildings, mitigation measures, locations, and soil conditions is the potential for life-threatening damage most severe?
6. How does risk attitude in the decision-maker affect the decision to seek a particular mitigate measure? Most people are risk averse to some degree, and risk attitude should be considered for decisions with high stakes and substantial uncertainty. (The theory of decision analysis deals with this principle.)
7. Given a future large earthquake how would homes with a given quality, retrofit, or redesign fare compared with the typical case?

For illustrative purposes, we will answer some of these questions for a single location and decision-maker and briefly discuss some important issues associated with answering the others. The approach illustrated here requires six pieces of information:

1. Replacement cost of the building, such as shown in Appendix F. Let the replacement cost for new construction of the building be denoted by *RCN*.
2. Mean seismic vulnerability function, such as those presented in the previous chapter. Let the seismic vulnerability function be denoted by $\mu_{Y|Sa}$, which gives the mean damage factor as a function of spectral acceleration.
3. Seismic hazard, which is a measure of how often the site will experience ground motion of a certain shaking intensity. This is often expressed as the mean annual frequency of exceedance of spectral acceleration S_a versus S_a. This relationship depends on site location, soil conditions, structure fundamental period, and damping ratio. Let the frequency form of the seismic hazard function be denoted by $G_{Sa}(s)$, i.e., the annual frequency of shaking of $S_a \geq s$. Let $g_{Sa}(s)$ denote the negative of the first derivative of $G_{Sa}(s)$, i.e., the annual frequency of shaking of intensity $s \leq S_a < s+\mathrm{d}s$.
4. The decision-maker's planning period, t.
5. The decision-maker's discount rate, r. This is typically taken as the risk-free discount rate, after tax and inflation.
6. The probability of collapse or of life-threatening damage, given a certain level of ground shaking (i.e., the red-tag fragility function).

Sample Risk Studies

The seismic vulnerability functions presented in Chapter 5 can be used to answer these questions, when combined with knowledge of the seismic hazard (the likelihood of various levels of shaking) and knowledge of the decision-maker.

Benefit-cost Analysis

Let us begin with questions 1 through 3, which deal with the expected value of earthquake damage. Some math is required. Let the average yearly earthquake damage, often called expected annualized damage, be denoted by *EAD*, and defined by Equation 6-1. Let the present value of that damage be denoted by *PV*[*D*] and defined by Equation 6-2. The equation reflects the assumption that the decision-maker perceives no benefit of the redesign after the planning period *t*, perhaps because the decision-maker plans to sell the building at that time and does not expect the buyer to pay extra because of the retrofit or redesign measure.

We will refer to the difference between the as-is *PV*[*D*] and the what-if value, as the benefit, as shown in Equation 6-3. We will refer to the difference between the what-if and as-is construction costs as the cost of the measure (Equation 6-4). In the case of a retrofit, the cost is simply the up-front cost one must pay the contractor to perform the retrofit. The cost of a higher quality level is the cost to pay for more inspections during construction, and any added costs that the contractor passes on to the owner to meet more closely the plans and specifications.

$$EAD = \int_0^\infty RCN \cdot y(s) g_{Sa}(s) ds \tag{6-1}$$

$$PV[D] = \frac{1 - \exp(-rt)}{r} EAD \tag{6-2}$$

$$Benefit = PV[D]_{as\text{-}is} - PV[D]_{what\text{-}if} \tag{6-3}$$

$$Cost = RCN_{what\text{-}if} - RCN_{as\text{-}is} \tag{6-4}$$

Let us now consider the implications of these equations and the vulnerability functions presented in the previous chapter for a single sample site and a single decision maker. Consider a hypothetical site in California, whose hazard function for 0.2-sec period, 10% damping (appropriate for the townhouse and apartment building) is given by Figure 6-1. The curve is based on Leyendecker, 2001, for a San Jose site (37.3N x 121.9W) with soil of NEHRP category D, 0.2-sec. period, and 5% damping. The hazard curve would somewhat overstate the hazard for 10% viscous damping (as in the case of these index buildings), but is reasonable for illustration purposes.

Figure 6-1:
Seismic Hazard at Hypothetical Site in California.

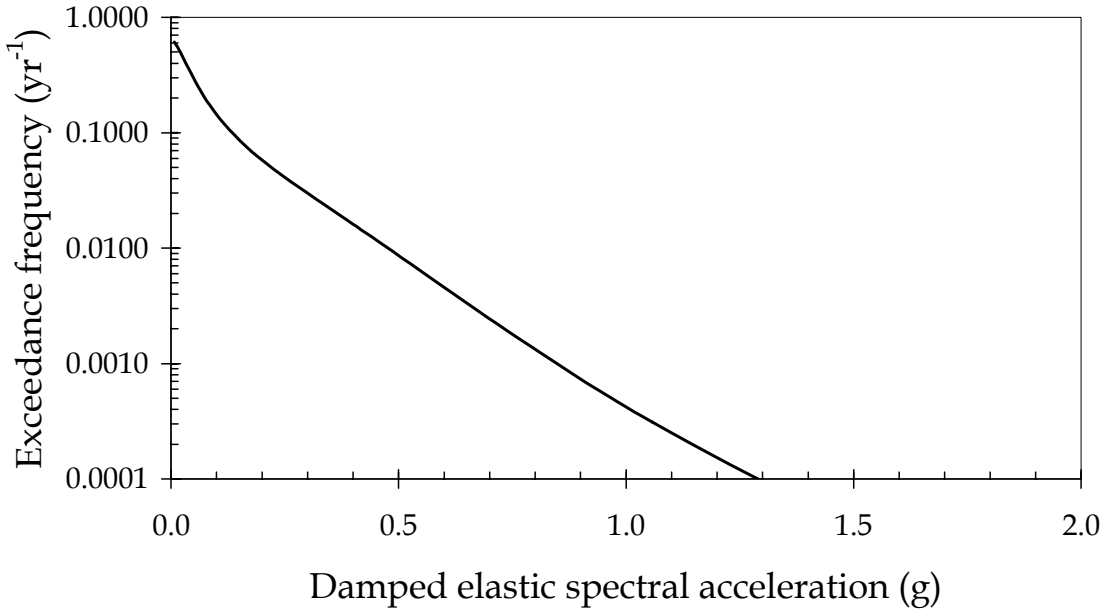

This frequency form of the hazard function, denoted here by $G_{Sa}(s)$, over the range of interest, from about 0.1 to about 1.3g, is approximated by Equation 6-5. Its negative first derivative, denoted by $g_{Sa}(s)$, in this range is approximated by Equation 6-6. (The hazard function for the small house and the large house would be different, because their periods are different from 0.2 sec, but we will use this same hazard function here for illustrative purposes.) Also consider a hypothetical decision-maker whose risk-free discount rate r, after tax and inflation, is 3%, and whose planning period t is 30 yr, a reasonable period when considering a new design. Our hypothetical decision-maker is also risk neutral at the loss levels treated here, a simplification that allows us to ignore utility functions in evaluating the desirability of quality levels and retrofit and redesign options. The reader interested in risk-averse decision-making is referred to Beck *et al.* (2002).

$$G_{Sa}(s) \approx \exp(-6.05s - 1.68) \tag{6-5}$$

$$g_{Sa}(s) \approx 6.05\exp(-6.05s - 1.68) \tag{6-6}$$

Table 6-1 gives results for this site and decision-maker, for each of the index buildings and variants. It shows that quality makes a big difference in future earthquake damage. Poor-quality construction and maintenance increases estimated future costs by up to 3 times relative to the typical case, while superior-quality reduces future costs up to 50%. (Recall that the superior-quality small house is superior primarily because is has a different foundation, not merely better materials and installation. This must be taken into

account to understand the 99% reduction.) The retrofit and redesign measures reduce future earthquake repair costs by 16 to 75% compared with the typical case. The apparent negative "benefits" associated with waist-wall nailing and rigid-diaphragm redesign appear to reflect simple statistical variability; they appear merely be insignificantly different from the typical-quality variant.

After considering the up-front cost of retrofit or redesign, some of the measures are cost effective (have a benefit-to cost ratio $B/C > 1$) and some are not ($B/C < 1$), when one considers only the structural and architectural savings. For the case of the San Jose site, the small house retrofit (bolts and bracing) and the townhouse redesign (limited drift), are both cost-effective. The measures for the large house and apartment building are not cost effective.

This is interesting, especially the contrast between the immediate-occupancy redesign and the townhouse limited-drift design. An Element-3 manager who participated in the design of both measures writes (Cobeen, 2002): "These are both based on the same concept of adding structure to reduce damage. The large house used the FEMA 273 methodology throughout. The townhouse used a shoot-from-the-hip approach that singled out one level and one direction as being most critical." The explanation probably lies in the fact that the large house is fairly rugged to begin with: the typical-quality variant has an EAD of $28, which leaves enough room for the IO redesign to provide only $22 per year of improvement. By contrast, the townhouse has farther to go: from $83 to $28 per year for all three units, at substantially lower up-front cost: $1,700 for the limited-drift measure vs. $7,500 for the IO measure.

These findings will of course differ for another site or decision-maker. Regions of higher seismicity will make the retrofits (other than the rigid-diaphragm and waist-wall) more beneficial, without a substantial change in cost. Decision-makers with higher discount rates and shorter planning periods will find the retrofits less desirable. Benefit-to-cost ratios will increase when one accounts for some important benefits not considered here, including:

- Reduction in fatality risk;
- Reduction in future additional living expenses while repairs are completed;
- Reduced earthquake insurance premiums, if incentives are offered; and
- Intangibles such as peace of mind, sentimental value, etc.

Before moving on, let us consider whether the figures in Table 6-1 are reasonable. Chapter 5 found reasonable agreement between the underlying seismic vulnerability functions and experience in the Northridge, Coalinga, and San Fernando earthquakes.

An additional check is possible of the aggregate risk. In 2000, there were 12.2 million housing units in California (U.S. Census Bureau, 2002), and approximately 1.25 housing

units per residential structure (U.S. Census Bureau, 2000), or approximately 9.8 million residential structures in California. A recent study using HAZUS (Federal Emergency Management Agency, 2000) estimated that the average annualized structure damage in California is $3.3 billion, of which approximately $2.6 billion is attributable to property damage (buildings and contents). If 50% to 70% of this figure is attributable to residential buildings (reasonable, since 70% of total building value is residential, and residential buildings tend to be more rugged than the average building), and 60% of the residential property loss is associated with the building (vs. contents, per insurance-industry practice), then one would expect annualized building repair costs of $80 to $110 per residential structure per year in California. The average damage for the four typical-quality variants at the sample site is $105 per year—fairly good agreement.

Of course, the risk figures calculated here are for relatively simple structures whose seismic vulnerability is acknowledged probably to underestimate that of more complex structures, and the risk figures are calculated only for the hypothetical site in San Jose, whose losses in the FEMA study were comparable to those of other Bay Area cities but somewhat higher than Los Angeles', as a fraction of building value. However, the order-of-magnitude agreement suggests that the figures of Table 6-1 are reasonable.

Table 6-1:
Sample Costs and Benefits of Quality, Retrofit, and Redesign

Index building, variant	Building replacement cost new, *RCN*	Expected annualized damage, *EAD*	Present value of damage, *PV[D]*	Benefit[1]	Cost[2]	Benefit-to-cost ratio, *B/C*	PV[D], % of typical
Small house, poor	$136,641	$612	$20,400	$(13,365)			290%
Small house, typical	$136,641	$211	$7,035	$-			100%
Small house, superior	$136,641	$1	$47	$6,988			1%
Small house, braced	$137,979	$78	$2,610	$4,425	$1,338	3.31	37%
Large house, poor	$221,430	$99	$3,289	$(2,357)			353%
Large house, typical	$221,430	$28	$932	$-			100%
Large house, superior	$221,430	$13	$442	$490			47%
Large house, waist wall	$221,692	$30	$1,001	$(69)	$262	-0.26	107%
Large house, IO	$228,919	$6	$193	$739	$7,489	0.10	21%
Large house, rigid diaphragm	$221,702	$34	$1,148	$(216)	$272	-0.79	123%
Townhouse, poor	$497,583	$211	$7,017	$(4,253)			254%
Townhouse, typical	$497,583	$83	$2,764	$-			100%
Townhouse, superior	$497,583	$55	$1,819	$945			66%
Townhouse, limited drift	$499,278	$28	$929	$1,835	$1,695	1.08	34%
Apartment, poor	$797,197	$136	$4,520	$(1,163)			135%
Apartment, typical	$797,197	$101	$3,357	$-			100%
Apartment, superior	$797,197	$62	$2,066	$1,291			62%
Apartment, steel frames	$826,201	$24	$808	$2,549	$29,004	0.09	24%
Apartment, shearwall	$808,524	$32	$1,071	$2,286	$11,327	0.20	32%

(1) Reduction in present value of future loss, relative to typical
(2) Cost of different quality levels is hard to determine and has not been estimated here.

Probability that Loss will Exceed a Specified Amount

One can express future earthquake repair costs via a relationship between the probability or frequency that loss would exceed a certain amount, as a function of that amount. The risk can be calculated from the hazard and the seismic vulnerability function as follows. Let $G_Y(y)$ denote the mean annual frequency of events causing the damage factor Y to exceed a given value y. It can be calculated as follows:

$$G_Y(y) = \int_0^\infty \left(1 - F_{Y|Sa}(y \mid s)\right) g_{Sa}(s)\, ds \tag{6-7}$$

where

$F_{Y|Sa}(y|s)$ = probability that $Y \le y$ given that $S_a = s$

$$\approx \Phi\left(\frac{y - \mu_{Y|Sa}}{\sigma_{Y|Sa}}\right)$$

$\Phi(\cdot)$ = cumulative standard normal distribution evaluated at the term in parentheses

$\mu_{Y|Sa}$ = mean damage factor at S_a

$\sigma_{Y|Sa}$ = standard deviation of damage factor at S_a

Chapter 5 provides estimates of $\mu_{Y|Sa}$ and $\sigma_{Y|Sa}$ for the index buildings. Table 6-2 presents results of Equation 6-7 for each of the variants examined here, at the hypothetical San Jose site.

Figure 6-2:
Seismic Risk at the Hypothetical Site in California.

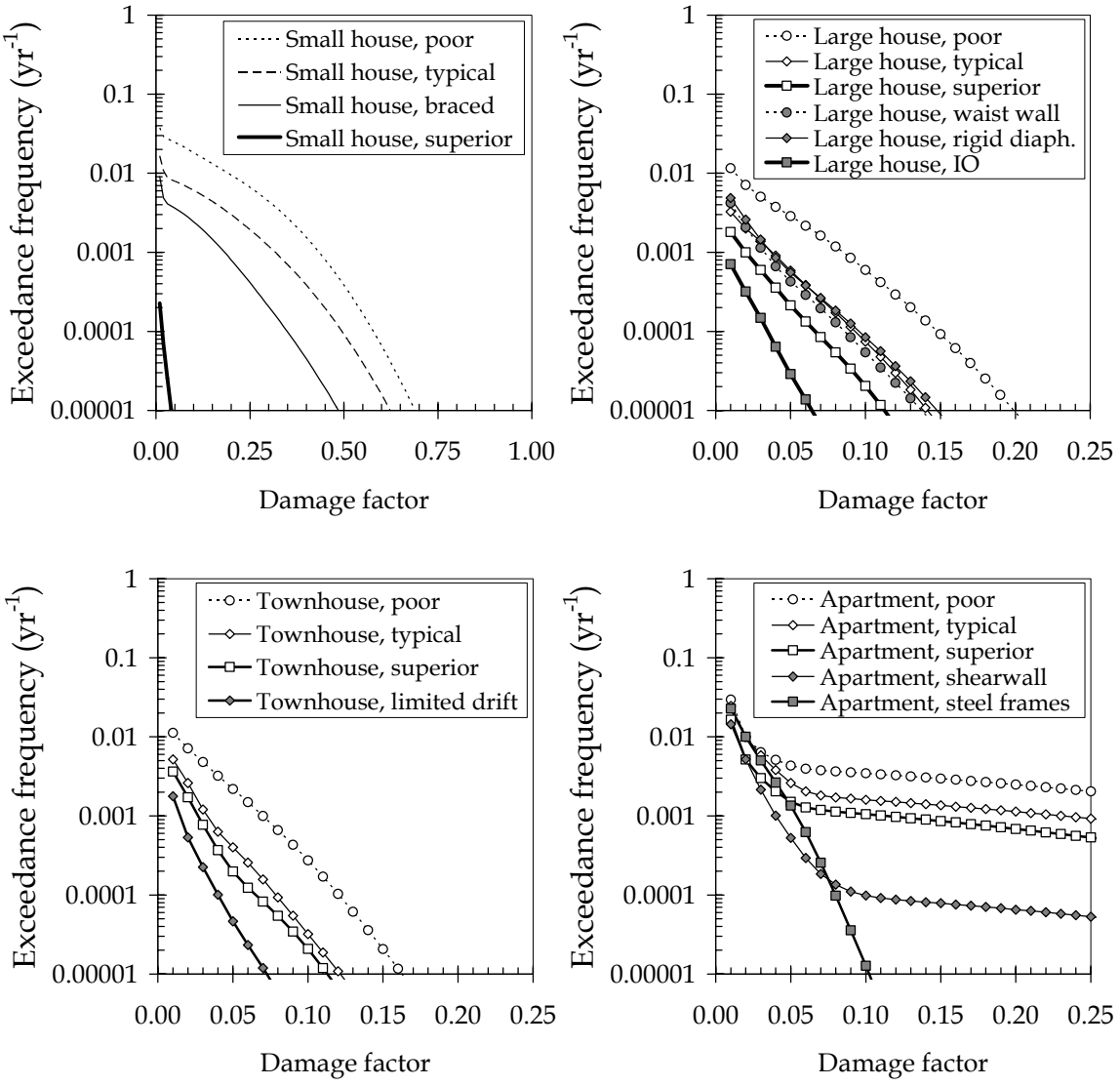

These figures are informative in several ways. For example, they can be used to answer question 4 on page 104, which asked what the chances were that loss would exceed a certain amount in a given period of time. Let f denote the exceedance frequency of that loss amount, e.g., from Figure 6-2. Let t denote the time period of interest. If we assume Poisson arrivals of losses (a common simplification), the probability that the loss would exceed that amount at least once ($N \geq 1$) during t is approximated by:

$$\begin{aligned} P[N \geq 1] &= 1 - \exp(-ft) \\ &\approx ft \quad \text{for } ft \leq 0.1 \end{aligned} \tag{6-8}$$

Probability that an insurance policy would pay off. Consider the owner of the typical-quality small house at the hypothetical San Jose site, who wants to know the likelihood that an insurance policy with a 15% deductible will pay off at least once during an ownership period of 10 years. From Figure 6-2, $f = 0.0044$, so $ft = 4.4\%$. That is, the chance that the policy will pay off once during the planning period is about 1 in 23. This fairly low probability might seem like a poor bet, but it is not the only basis for judging the desirability of an insurance policy.

Probability of ruin. Suppose the homeowner believes she can afford a loss up to $50,000; any more than that would be ruinous in some way, e.g., by forcing her to default on her mortgage. She is interested in buying earthquake insurance only if there is a significant probability of ruin during the next 10 years. The question then is: what is the probability that the loss will exceed $50,000/$137,000 = 36%, during the next 10 years? From Figure 6-2, $f = 0.00062$, so $ft = 0.62\%$. That is, there is a probability of approximately 1/160 that earthquake damage to her home would be so great that she could not afford to repair it, and would have to default on her mortgage. Depending on the decision-maker, this might well be an intolerably large probability, making the insurance policy desirable.

Probability of Life-Threatening Damage

Fatality risk is an important question, or rather the principle question, of seismic designed and performance, but it is also difficult to handle given our poor knowledge of the causal relationships between building damage and occupant death. A related and somewhat more tractable problem is to estimate the probability of life-threatening damage. We refer it to generically as red-tagging, in reference to the most familiar indicator of life-threatening damage: the red "unsafe" building-inspection tag sometimes produced by an ATC-20 safety evaluation of an earthquake-damaged building (Applied Technology Council, 1989).

Red-tagging is a different issue from repair cost: red-tagging concerns only structural damage, whereas repair costs reflect nonstructural as well as structural damage. When

considering the likelihood of a particular building being red-tagged, two questions of interest are:

1. What is the chance that the building will be red-tagged, given a particular level of ground shaking? The answer to this question is valuable to the homeowner and to emergency planners when planning for a worst-case scenario.
2. What is the chance that the building will be red-tagged during a reasonable planning period? This is a valuable question to answer when a homeowner or other decision-maker is assessing the probabilistic benefits of a seismic retrofit.

To model red-tagging thoroughly, a study should check physical damage in terms of ATC-20 safety tests (Applied Technology Council, 1989), which is the basis for most red-tagging procedures in California. The study must then produce the red-tag fragility function for each index building and variant. The fragility function would give the probability that one or more of the ATC-20 criteria for red-tagging are satisfied, as a function of shaking intensity. The fragility function can be used directly to answer the scenario question (number 1, above).

To answer the planning-period question (number 2), it is necessary also to consider the seismic hazard. The probability of red-tagging during a period t is given by

$$P = 1 - \exp\left(-t \int_0^\infty g(S_a) F(S_a) dS_a \right) \tag{6-9}$$

where P is the probability that the building will be red-tagged sometime during the planning period, $g(S_a)$ is the annual frequency of events with shaking intensity $S \le S_a < S + dS$, and $F(S_a)$ is the probability of red-tagging given an event of intensity S_a.

Let us illustrate the answer to these two questions using the variants of the small house and the hazard function shown in Figure 6-1. Let the scenario shaking level be 0.75g, which in Figure 6-1 corresponds to the 500-year earthquake, a common basis for earthquake scenario planning. (The nontechnical reader may wonder at the "500-year" level of shaking. This is another way to refer to an upper-bound shaking severity during the design life of a building. That is, this is the level of shaking that one would be 90% confident of not being exceeded during the next 50 years. Statistically, this level of shaking is actually estimated to occur once every 475 years, on average.)

To return to the problem, we are examining the probability of red-tagging, either assuming that an event occurs causing shaking severity of 0.75g, or allowing for uncertainty about whether and how strongly the ground will shake during a reasonable planning period, which we will take to be t = 10 years, as in the earlier examples. In the present study we did not explicitly examine the probability of red-tagging, but for illustrative purposes it is reasonable to assume that red-tagging of the small house is

caused predominantly by collapse of the cripple walls. Let $F(S_a)$ therefore be approximated by the cripple-wall collapse probability. Figure 6-3 shows the calculated probabilities of cripple-wall collapse in the poor, typical, and braced variants of the small house, produced by the ABV analysis. (The superior-quality variant has reinforced concrete stemwalls, and is therefore judged not to be significantly susceptible to collapse.) The figure also shows best-fit fragility functions for each data set, determined by least-squares, considering the data up to $S_a \leq 1.0$g. (The purpose of considering only $S_a \leq 1.0$g is to make the curves fit best at the lower, more-likely levels of shaking.)

Figure 6-3:
Cripple Wall Collapse Probability as a Function of S_a.

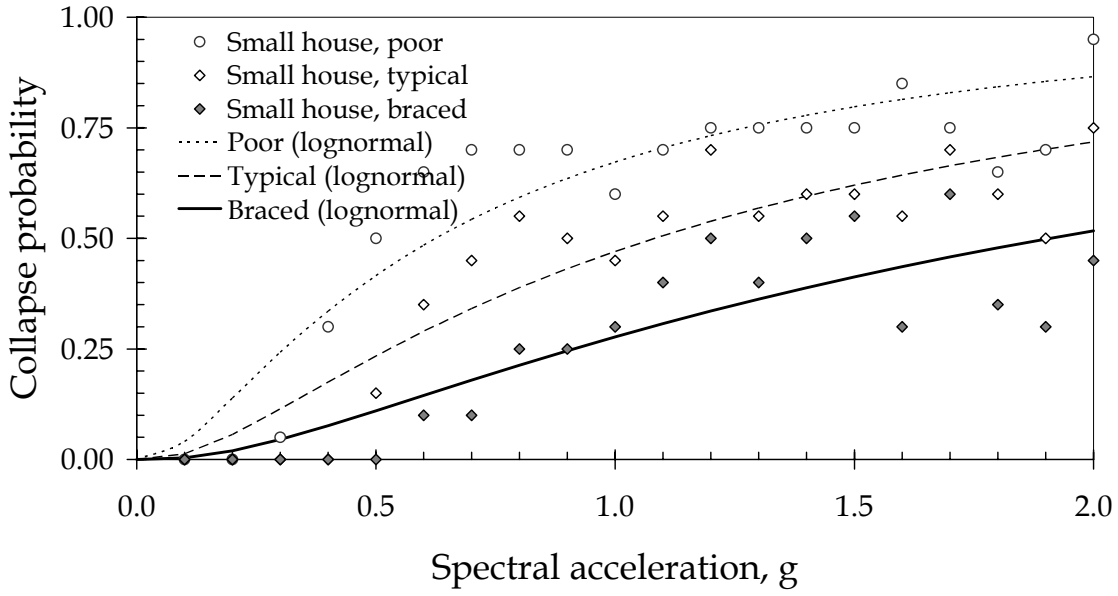

Each fragility function is in the form of a cumulative lognormal distribution on the value of S_a causing cripple-wall collapse. The parameters of the fragility functions are the median and logarithmic standard deviation, denoted by x_m and β, respectively. The parameters are presented in Table 6-2. Note that these fragility functions are different from the HAZUS-compatible curves presented in Chapter 5 because these are functions of S_a at the small-amplitude fundamental period of the building, rather than S_d at the intersection of the HAZUS pushover curve and the (S_d, S_a) response spectrum.

Table 6-2:
Parameters of Small-House Cripple-Wall Collapse Fragility Functions

	Poor	Typical	Braced
x_m	0.63	1.08	1.91
β	1.0	1.1	1.1

Before presenting the results of Equation 6-7 for the small house, a word of warning. A thorough study of red-tag probability of any particular building would not simply use a fragility function for the cripple-wall collapse as a proxy for red-tagging. In most cases the two conditions would not be so nearly equivalent, and given the detailed damage description provided by the ABV simulations, one would probably not need to resort to such a simplification.

This warning in mind, Figure 6-4 presents illustrative results of Equation 6-7 in terms of the probability that each small-house index building would be red-tagged in the planning scenario (i.e., given S_a = 0.75g of ground shaking), and the probability that each small-house index building would be red-tagged in a 10-year planning period. The table uses the hazard curve of Figure 6-1 and the collapse fragility functions of Figure 6-3. The number would be different for different locations, soil conditions, index buildings, potential for ground failure (an important contributor to red-tagging), and different modeling assumptions about the collapse of the small house.

The figure suggests an additional incentive for retrofitting unbraced cripple walls. The owner of the small house could reduce the probability that his or her home would suddenly be rendered unoccupiable by a strong earthquake by half. This intangible benefit is in addition to the economic benefits discussed in the previous section.

Figure 6-4:
Probability of Red-Tagging of Small House

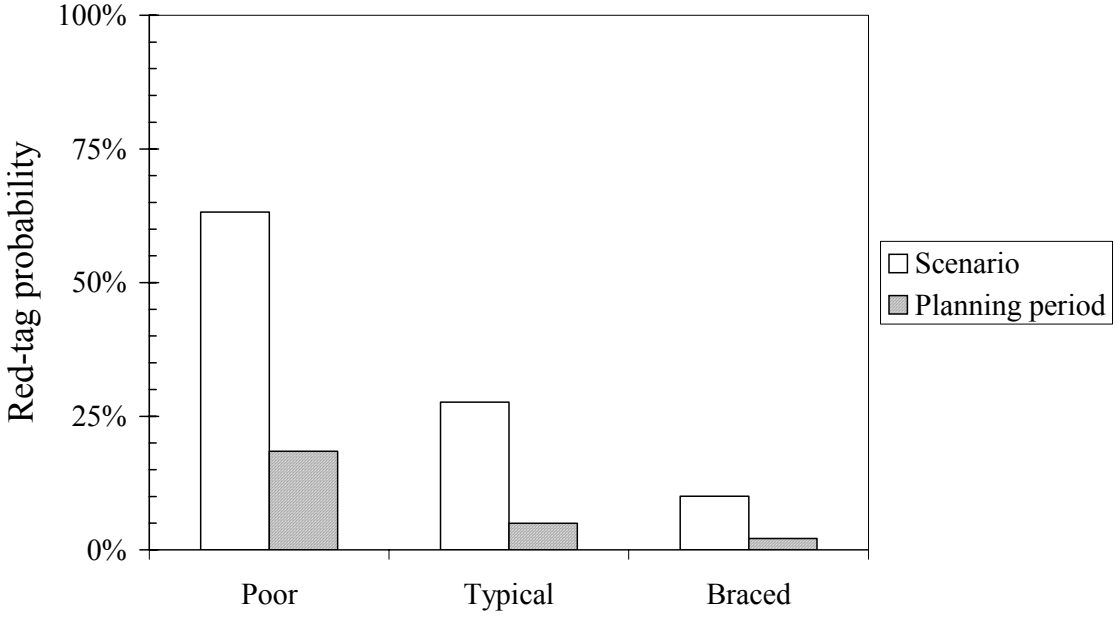

Conclusions Regarding Sample Risk Studies

These results are of course merely illustrative. They apply only at the hypothetical San Jose site, and to the decision-maker whose planning period and whose after-tax, after-inflation risk-free discount rate are 30 years and 3%, respectively. Other decision-makers and sites will have different results.

A thorough study would produce results such as shown in Table 6-1, would attempt to account for these additional benefits, and would present results calculated by geographic region such as ZIP Code, for various soil types, planning periods, and discount rates. If it were also desirable to account for risk attitude, one could use decision analysis and present results for a reasonable range of risk-tolerance values (e.g., see Beck *et al.*, 2002). The principles of decision analysis are unfamiliar to most people, so the study would provide a simple means for a decision-maker to assess his or her risk tolerance.

Such an analysis (with or without decision analysis) could inform the development of performance-based earthquake engineering standards or help decision-makers select their desired level of performance under performance-based design.

As these sample seismic risk studies show, it is practical and straightforward to assess the probabilistic benefits of the retrofit and redesign measures considered here. The assessment of benefits is novel in that, because of the nature of the ABV analysis, the

estimates are highly specific to the details of the risk-mitigation measure considered, they account for most important sources of uncertainty, and they largely avoid reliance on expert opinion. Such features tend to strengthen the defense of expensive risk-mitigation decisions, particularly decisions made in public forums such as building code committees, local jurisdictions, and state and federal legislatures.

Chapter 7. Conclusions and Recommendations

Conclusions

Creation of Building-Specific Motion-Damage Relationships. This project created building-specific motion-damage relationships for 19 particular woodframe buildings based on four floor plans: a small house, a large house, a three-unit townhouse, and a 10-unit apartment building. For each of these four buildings, three quality-level variants were assessed, plus a total of seven retrofit and redesign measures. For each building, the resulting motion-damage relationships include:

- *A probabilistic seismic vulnerability function*. A relationship is provided that relates shaking intensity and mean damage factor based on the cost to repair earthquake-induced damage. Shaking intensity is measured in terms of damped spectral acceleration, evaluated at the building's calculated small-amplitude fundamental period. It is found that a lognormal distribution approximately fits the damage factor at a given level of S_a for all but rare (S_a > 1.0g) shaking intensities.
- *Uncertainty*. Also provided is the residual coefficient of variation on damage factor, a measure of uncertainty in repair costs. This measure explicitly accounts for uncertainty in ground motion, structural characteristics, component damageability, and contractor repair costs. The methodology ensures that important uncertainties are accounted for and propagated through the analysis, and that correlations are preserved.
- *HAZUS-compatible fragility functions*. Four relationships per building are given that provide the probability of exceeding a threshold damage factor conditioned on shaking severity. Shaking severity is measured here in terms of the spectral displacement corresponding to the intersection of the damped elastic response spectrum and the idealized HAZUS pushover curve.
- *Damage by assembly category***.** The study examines the relative contribution to total repair cost from each of seven categories of woodframe building assembly (drywall, exterior nonstructural wall, exterior shearwall, interior shearwall, glazing, water heater, and paint). It is found that approximately half the total repair costs are attributable to painting, while the bulk of the remainder are attributable in approximately equal parts to drywall and exterior shearwall. This information can help to focus attention on the significant contributors to earthquake loss. Damage by assembly category is also provided in terms of fraction of assemblies damaged for a building in each HAZUS damage state.
- *Reusable assembly fragility functions*. The study provides a number of assembly fragility functions that are based on laboratory tests performed by CUREE-Caltech Woodframe project researchers. These fragility functions are highly specific, distinguishing for example between different types of woodframe wall based on structural sheathing and finish materials (gypsum wallboard or stucco)

and how they are fastened to the framing. These can be re-used in later studies, enhanced with further laboratory testing, and compiled into a library of standard assembly fragility functions.

- *Reusable repair-cost distributions*. For each assembly fragility function developed, repair efforts are described, including the labor and materials required to effect repairs, repair time required, and costs for each item involved. These repair efforts are calculated by a professional cost estimator and reflect current construction practice.

Quality, retrofit, and redesign make a difference in seismic vulnerability. It is shown that quality of construction and post-construction maintenance makes a substantial difference in the seismic vulnerability of an index building. The degree of this difference varies by level of shaking intensity, but it is shown that construction quality can raise or lower mean damage factor by a factor of 2 or more. Quality is described in terms of adequacy of nailing, degradation of construction materials, etc., and is parameterized in terms of the strength and stiffness of building elements relative to a high-quality laboratory test specimen. The implication is that vigorous, frequent inspections during construction can be highly beneficial in reducing future earthquake losses.

It is also shown that the retrofits and redesigns are generally at least as effective in reducing vulnerability as ensuring superior quality construction and maintenance. Especially beneficial are the FEMA 273 immediate occupancy redesign of the large house, and the limited-drift redesign of the townhouse. The steel-frame and shearwall measures for the apartment building are both quite effective. The exceptions are the waist-wall and rigid-diaphragm measures for the large house, which seem to produce seismic vulnerability functions and risk relationships that are indistinguishable from the typical-quality case. The cost of waist-wall nailing is very modest, however, and the additional effort is probably worthwhile.

It is shown how the vulnerability functions can be used to calculate the direct economic benefit of quality, retrofit, and redesign for a given site and decision maker. This approach is illustrated for a sample site to show how poor-quality construction and maintenance increases future costs up to 3 times, relative to the typical case, while superior-quality construction reduces future costs up to 50%. For convenience, these results are copied to Table 7-1.

Table 7-1 also shows that the retrofit and redesign measures reduced future earthquake repair costs up to 80% compared with the typical case. In the table, *EAD* refers to expected annualized damage (i.e., average yearly repair cost); *PV*[*D*] gives the present value of this figure for a 30-year planning period and 3% risk-free discount rate after taxes and inflation; benefit measures the reduction in *PV*[*D*] relative to the typical case, cost is the cost of construction, relative to the typical case; *B/C* is the benefit-to-cost ratio; and damage reduction is the fractional reduction in damage relative to typical.

Note that some validation is provided at two points in this study: Chapter 5 compares the calculated seismic vulnerability functions with experience in the Northridge, Coalinga, and San Fernando earthquakes, and finds general agreement. Chapter 6 compares the annualized damage given by the figures Table 7-1 with a recent estimate of statewide earthquake losses in California by the Federal Emergency Management Agency (2000), and also finds general agreement.

Table 7-1:
Sample Costs and Benefits of Quality, Retrofit, and Redesign

Index building, variant	Building replacement cost new, *RCN*	Expected annualized damage, *EAD*	Present value of damage, *PV[D]*	Benefit[1]	Cost[2]	Benefit-to-cost ratio, *B/C*	PV[D], % of typical
Small house, poor	$136,641	$612	$20,400	$(13,365)			290%
Small house, typical	$136,641	$211	$7,035	$-			100%
Small house, superior	$136,641	$1	$47	$6,988			1%
Small house, braced	$137,979	$78	$2,610	$4,425	$1,338	3.31	37%
Large house, poor	$221,430	$99	$3,289	$(2,357)			353%
Large house, typical	$221,430	$28	$932	$-			100%
Large house, superior	$221,430	$13	$442	$490			47%
Large house, waist wall	$221,692	$30	$1,001	$(69)	$262	-0.26	107%
Large house, IO	$228,919	$6	$193	$739	$7,489	0.10	21%
Large house, rigid diaphragm	$221,702	$34	$1,148	$(216)	$272	-0.79	123%
Townhouse, poor	$497,583	$211	$7,017	$(4,253)			254%
Townhouse, typical	$497,583	$83	$2,764	$-			100%
Townhouse, superior	$497,583	$55	$1,819	$945			66%
Townhouse, limited drift	$499,278	$28	$929	$1,835	$1,695	1.08	34%
Apartment, poor	$797,197	$136	$4,520	$(1,163)			135%
Apartment, typical	$797,197	$101	$3,357	$-			100%
Apartment, superior	$797,197	$62	$2,066	$1,291			62%
Apartment, steel frames	$826,201	$24	$808	$2,549	$29,004	0.09	24%
Apartment, shearwall	$808,524	$32	$1,071	$2,286	$11,327	0.20	32%

(1) Reduction in present value of future loss, relative to typical
(2) Cost of different quality levels is hard to determine and has not been estimated here.

Quality, retrofit, and redesign affect safety and post-earthquake habitability. It is also shown that quality and retrofit can impact the probability that a house will be rendered unsafe to occupy some time during its lifetime because of earthquake damage. An analysis presented in Chapter 6 estimates red-tagging probability for the small house under rare, strong shaking, and in terms of the probability of red-tagging over a 10-year period, for the sample site. For convenience, those results are copied to Figure 7-1. The calculation of these probabilities for other buildings and other sites would require additional analysis, as discussed in Chapter 6.

Figure 7-1:
Probability of Red-Tagging of Small House

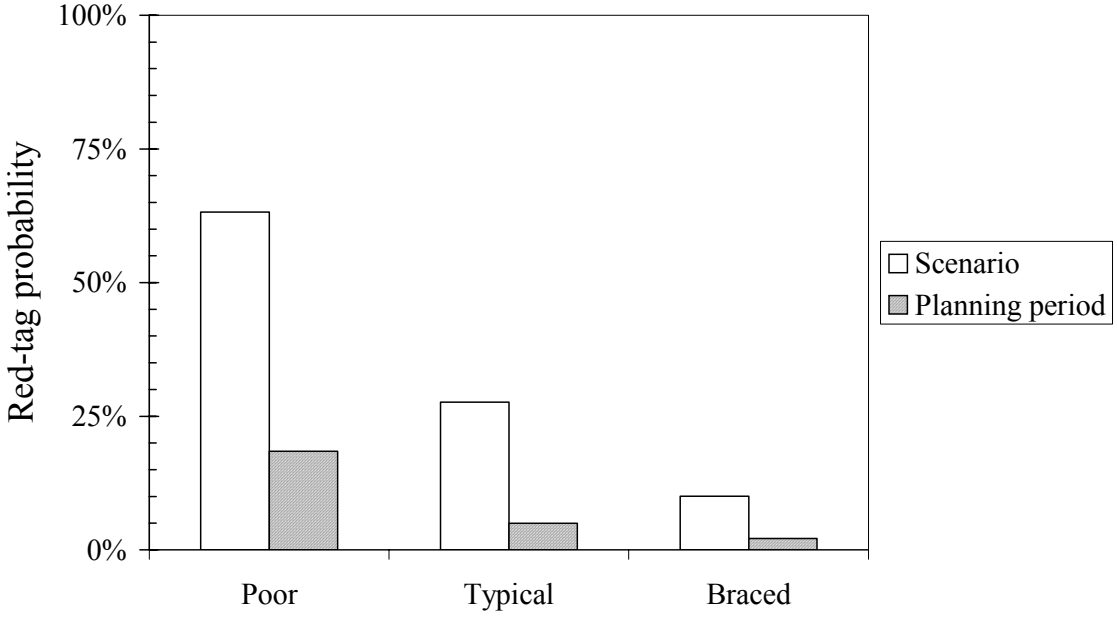

Probabilistic expressions of risk can provide addition decision-making information. By expressing risk as a relationship between loss level and exceedance frequency, one can inform decisions that are driven by probability of loss exceeding some ruinous or other threshold level. In Chapter 6, it was shown that, for a hypothetical San Jose site, one could answer two interesting questions for a decision-maker who was considering the purchase of earthquake insurance for her typical-quality small house:

1. ***Probability of the policy paying a claim.*** In the example, it was estimated that the probability of reaching a 15% deductible on an insurance policy during a 10-year period was less than 1 in 20.
2. ***Probability of ruin.*** It was estimated that the probability that, without insurance, the owner would have to pay more than $50,000 to repair earthquake damage during the coming 10-year period is approximately 1 in 160.

Future Work and Recommendations for Use of this Study

This study represents an effort to improve loss estimation for woodframe buildings. The information presented here is only valuable insofar as it increases the value of future risk-mitigation decisions. Therefore, we offer the following recommendations for using this study to inform and improve future risk-mitigation efforts by various stakeholders and decision-makers. Many of these efforts can be facilitated using HAZUS.

1. **Use these results to support risk-mitigation incentives.** Incentives offered by earthquake insurers to mitigate seismic damage are often based largely on judgment. These incentives could be informed and improved by validating them in terms of reduction in expected annualized insurance loss. Governmental and nongovernmental organizations sometimes consider tax incentives and subsidies to encourage seismic risk mitigation. The debate on the nature, magnitude, and value of these incentives could be informed based on probabilistic risk studies that use the vulnerability functions developed here.

2. **Examine additional index buildings.** A limited set of index buildings is examined here; far more diversity exists among the actual building stock of California and elsewhere. It is therefore recommended that similar studies be performed to examine other common types, such as the Craftsman style homes characteristic of the 1910s, 1920s and 1930s, Eichler homes of the 1950s and 1960s, Victorians with their distinctive shiplap siding, homes with brick veneer, houses on slopes, and the recent trend of very large (greater than 4,000 sf) houses with adventuresome or complex configurations. Furthermore, the additional index buildings should include more-complex features than those considered here, including split-level construction, brick chimneys, reentrant corners, vertical setbacks, soil or foundation problems, and other irregularities that tend to increase the amount of actual physical damage. Meaningful categories of woodframe buildings could be defined, and a statistically significant number of examples of each category could be analyzed, in order to create category-based seismic vulnerability functions from rigorous, detailed, building-specific engineering analysis. These categories could be defined in terms of building age, size, wall material, building configuration, and other parameters that are readily observable to a non-engineer.

3. **Perform probabilistic seismic risk assessments.** The project results provide researchers with necessary tools for performing probabilistic seismic risk assessments. By combining the vulnerability functions developed here with seismic hazard and decision-maker parameters, one can evaluate the economic benefits of risk mitigation, in terms of both economic performance and seismic safety. Chapter 6 illustrates such a methodology. It is recommended that the seismic vulnerability functions developed here be combined with seismic hazard information to show, by geographic location, discount rate, and planning period, results of the type shown in Table 7-1. Such risk assessments, if compiled by category of dwelling and packaged in convenient maps for use by lay readers, would benefit homeowners wishing to understand the quantitative benefits of seismic retrofit, building code authors who wish to evaluate the benefit of code changes, building inspectors wishing to determine the value of more frequent inspections, and legislators considering risk-mitigation incentives and subsidies.

4. **Study the installation quality and force-deformation-damage behavior of existing construction.** As noted in Chapter 4, little empirical data exist on the material strength and construction quality of various building elements such as stucco walls, shearwall nailing, etc., outside of the laboratory. It is shown here that the seismic risk of the index buildings is highly sensitive to quality of construction and post-construction maintenance. It would therefore be worthwhile to compile data on these characteristics as they exist in the field, e.g., through destructive testing of portions of buildings that are being renovated or demolished.

5. **Examine risk-communication issues.** It is important what one says to motivate decision-makers to mitigate risk, but it can be equally important how one says it. The present study was intended to inform the *what*, but did not focus on the *how*. It is recommended that a future study examine various ways of communicating risk, cost and benefit to decision-makers, and determine which means communicate best. Possibilities include photographs of actual damage, maps showing locations where the risk is greatest, maps showing locations where the risk-mitigation measure is most cost effective, case studies of successful risk-mitigation, etc. Such a study could build on the efforts of the California Seismic Safety Commission (1999). It would be of primary value to earthquake insurers, government agencies, consumer advocates, and similar entities who wish to influence others to mitigate their risk. Maragakis (2002) for example suggests a map showing for a given seismic event, the level of damage one might expect from a strengthened home vs. non-retrofitted structure, considering seismic hazard and the seismic vulnerability of homes by geographic location.

6. **Create red-tag fragility functions.** Post-earthquake safety inspections depend largely on observations of physical damage, the same type of physical damage modeled by the ABV approach. This was not a focus of the present study, but the data developed here could be reexamined and compared with ATC-20 safety-inspection protocols (Applied Technology Council, 1989) to relate probability of red-tagging to shaking intensity. Such fragility functions could be added to HAZUS to inform emergency planning decisions by local, state, and federal emergency responders. They could also be used by code writers to evaluate building-code efficacy and by other decision-makers to assess nonstructural benefits such as additional living expenses and intangibles such as peace of mind. We do not mean to imply this study or a derivative of it would replace ATC-20. The two products serve two different purposes: the former estimates future safety, the latter judges present safety given observable damage.

7. **Examine code enforcement issues.** It was shown in this study that quality of construction makes a significant difference in future earthquake performance. Maragakis (2002) observes that "despite new standards, outreach, codes, workshops and seminars, workmen in the field are making the same mistakes

Northridge was supposed to correct." He suggests that CUREE consider a partnership with the Contractors State License Board to mitigate these problems, using the results of the present study and ones like it to motivate the partnership. Since high-quality code enforcement impacts city budgets today, whereas the costs of poor enforcement are not seen until an uncertain future date, building inspection budgets represent an attractive target to budget cutters. Building departments would find it valuable to quantify the cost-effectiveness of inspections. Questions that should be addressed include the following: How frequently does an inspector have to visit a house under construction to ensure high-quality construction? What field tests are most effective in improving future seismic performance? How does the cost of additional or different inspections compare with the benefits obtained in terms of better seismic performance? Cobeen (2002) recommends that owners be informed of the benefits of more-frequent inspection, as motivation to contract additional inspections by design professionals and special inspectors.

8. **Quantify the effects of claims-adjustment practice.** This study does not account for insurance claims-adjustment practices, which can lead to insurance payment for non-earthquake-related damage. Research into the effects of loss adjustment practice would help to understand better how to use insurance loss data to develop seismic vulnerability functions with more general application. Related research is underway, under the sponsorship of the California Earthquake Authority. This research will attempt to establish claims-adjustment guidelines to reduce the mistaken attribution of preexisting damage with earthquake-related damage, and to reduce the potential for adjusters to confuse superficial damage with more substantial structural damage. However, additional study is called for to characterize the probability of such errors, as opposed to prescriptive guidelines to avoid them. These results would help insurers to estimate, and indirectly to control, their future losses. In addition, this information could inform state and federal planning for the financial consequences of future earthquakes.

9. **Validate inexpensive inspection protocols that rely heavily on judgment.** Several risk-screening procedures provide seismic inspection checklists of building features that affect seismic performance, and assign a risk score or letter grade based on judgmentally-assigned scores for each feature, notably ATC-21 (Applied Technology Council, 1988), ATC-50, (Applied Technology Council, 2000), and insurance-industry rating classes used to set premiums. ATC-21 is intended to estimate a collapse probability in a future rare earthquake for a variety of building types. The ATC-50 grades are intended to reflect ranges of future upper-bound losses for woodframe buildings in particular. Such procedures represent inexpensive means of assessing seismic risk. By encouraging or requiring the disclosure of such assessments in ownership transfers, local and state jurisdiction can cause seismic risk to become a decision variable in real estate transactions, and thus to provide incentives for mitigation. However, these

procedures rely heavily on expert opinion, which can open them to attack as unscientific. This apparent deficiency can be mitigated by validating the procedures using ABV. It is recommended that a number of buildings be examined in detail using ABV and ATC-50, to assure that letter grades accurately reflect future losses. The comparison could also improve ABV models, by highlighting important features recognized by ATC-50 that are not considered here.

10. **Check drift limits in performance-based design guidelines.** FEMA 273 (Federal Emergency Management Agency, 1997) provides limits on peak transient drift that are intended to provide high probability of meeting certain fairly detailed limits of physical damage. These limits are described qualitatively. The relationship between drift and probability or performance levels could be validated and the performance descriptions made quantitative, as shown in Chapter 5, using the present approach (see also Porter and Kiremidjian, 2001c). Quantification of performance levels would greatly enhance the value of these procedures.

11. **Identify the most important sources of uncertainty.** While this study quantified and included in the analysis uncertainty associated with ground motion, mass, damping, stiffness, etc., it did not examine the relative contribution from each source. It is recommended that these contributions be evaluated. This would enable engineers to focus more attention on major contributors and less on minor ones, simplifying the analysis and providing direction for future research to reduce the remaining uncertainty. Such an effort would be of particular value for code-writing authorities who wish to minimize the effort involved in analysis and design. (Such a study was recently performed for a real highrise reinforced-concrete building; see Porter *et al.*, ND.)

12. **Revisit these index buildings after research currently under way is completed.** A number of studies currently in progress can help to inform and improve the vulnerability functions developed here. A study by Pardoen and Waltman (in progress) can be used to inform shearwall fragility functions developed here. Work in progress by Osteraas (2002), a CUREE project for the California Earthquake Authority to produce guidelines for evaluation and repair of earthquake damage, can be used to improve the stucco elements of the structural models. A software product that is intended for use in three-dimensional nonlinear time-history structural analyses is being developed by CUREE-Caltech Woodframe researchers, under Task 1.5.1 (Consortium of Universities for Research in Earthquake Engineering, 2001); such software could be used to improve the structural analyses performed here by properly accounting for P-Δ effects and so better estimate collapse probability.

13. **Refine post-earthquake loss-data collection efforts.** The fragility functions reported here are based on controlled testing in university laboratories, and in some cases are based on theoretical considerations. These tests and theories can be greatly supplemented by careful collection of actual post-earthquake damage data. This will be a particularly challenging problem. As noted in Chapter 5, post-earthquake data collection has been addressed in several extensive projects by highly experienced engineers and architects. These researchers have faced the difficulties of determining seismic excitation; distinguishing earthquake-related damage and repair costs from prior damage and other costs; determining structure value; collecting representative samples; eliminating ambiguity from reporting forms; ensuring that survey forms are completely filled out; and generally collecting data both in great detail and from a large number of buildings. Every attempt yields new lessons about how to improve the data-collection process. The present study highlights the value of gathering field data on assembly fragility (damage as a function of structural deformation, as opposed to shaking severity) and on the distribution of repair costs, using a standard and detailed taxonomic system.

Chapter 8. References

Ang, A.H.S., and W. H. Tang, 1990, *Probability Concepts in Engineering Planning and Design, Vol. II—Decision, Risk, and Reliability,* New York, NY: John Wiley & Sons, 562 pp.

Applied Technology Council, 1985, *ATC-13: Earthquake Damage Evaluation Data for California,* Redwood City, CA, 492 pp.

Applied Technology Council, 1988, *ATC-21*, *Rapid Visual Screening of Buildings for Potential Seismic Hazards: A Handbook,* Redwood City, CA.

Applied Technology Council, 1989, *ATC-20, Post-Earthquake Safety Evaluation of Buildings,* Redwood City, CA.

Applied Technology Council, 2001, *ATC-50, Seismic Rehabilitation Guidelines for Wood-Frame Houses, 1/9/01 Draft,* Redwood City, CA

Applied Technology Council, in press, *ATC-38: Database on the Performance of Structures Near Strong-Motion Recordings,* Redwood City, CA

Beck, J.L., A. Kiremidjian, S. Wilkie, A. Mason, T. Salmon, J. Goltz, R. Olson, J. Workman, A. Irfanoglu, and K. Porter, 1999, *Decision Support Tools for Earthquake Recovery of Businesses, Final Report, CUREe-Kajima Joint Research Program Phase III,* Consortium of Universities for Earthquake Engineering Research, Richmond, CA

Beck, J.L., K.A. Porter, R.S. Shaikhutdinov, T. Moroi, Y. Tsukada, M. Masuda, 2002, *Impact of Seismic Risk on Lifetime Property Values, Final Report, CUREE-Kajima Joint Research Program Phase IV,* Consortium of Universities for Earthquake Engineering Research, Richmond, CA

Behr, R.A., A. Belarbi, and C.J. Culp, 1995, "Dynamic Racking Tests of Curtain Wall Glass Elements with In-Plane and Out-of-Plane Motions," *Earthquake Engineering and Structural Dynamics,* 24, New York: J. Wiley & Sons, Inc., 1-14.

Behr, R.A., and C.L. Worrell, 1998, "Limit States for Architectural Glass Under Simulated Seismic Loadings" *Proceedings [of the] Seminar on Seismic Design, Retrofit, and Performance of Nonstructural Components (ATC-29-1), San Francisco, Jan. 22-23, 1998.* Redwood City, CA: Applied Technology Council, 229-240.

California Seismic Safety Commission, 1999, *Earthquake Risk Management: A Toolkit for Decision-Makers,* Sacramento, CA, 198 pp.

Camelo, V.S., J.L. Beck, and J.F. Hall, 2001, *Dynamic Characteristics of Woodframe Structures,* Richmond, CA: Consortium of Universities for Research in Earthquake Engineering, 68 pp.

Carr, A.J., 1998, *Ruaumoko - Inelastic Dynamic Analysis Program*, Christchurch, New Zealand: Department of Civil Engineering, University of Canterbury

Chai, R.Y.H., Hutchinson, T.C., Sluis, B., & Vukazich, S.M., 2001, "CUREE-Caltech Woodframe Project Task 1.4.3, Seismic Behavior of Cripple Walls," *Proc. CUREE-Caltech Woodframe Project Element 1 – Research Meeting, January 12-13, 2001, University of California, San Diego*, Richmond, CA: Consortium of Universities for Research in Earthquake Engineering

Comerio, M.C., 1995, *Northridge Housing Losses,* Berkeley, CA: Center for Environmental Design Research, 100 pp.

Consortium of Universities for Research in Earthquake Engineering, 2001, *Task 1.5.1 – Development of a Seismic Analysis Software for Woodframe Construction,* http://www.curee.org/projects/woodframe_project/element1/task_summaries/task_1_5_1.html

CUREE-Caltech Woodframe Project, 1999, *Proceedings of the Invitational Workshop on Seismic Testing, Analysis and Design of Woodframe Construction (CUREE W-01)*, Richmond, California, 1999.

CUREE-Caltech Woodframe Project Element 3, in progress, *Recommendations for Earthquake Resistance in the Design and Construction of Woodframe Buildings,* Richmond, California: Consortium of Universities for Research in Earthquake Engineering

Czarnecki, 1973, Earthquake Damage to Tall Buildings, Structures Publication 359, Cambridge, MA: Massachusetts Institute of Technology, 125 pp.

Dalkey, N., B. Brown, and S. Cochrane, 1970, "Use of Self-Ratings to Improve Group Estimates," *Technological Forecasting: An International Journal,* 1 (3), American Elsevier Publishing, New York, NY, 283-291

Ellingwood, B., Galambos, T.V., MacGregor, J.G., and Cornell, C.A., 1980, *Development of a Probability Based Criterion for American National Standard A58,* Washington, DC: Special Publication 577, National Bureau of Standards, 222 pp.

EQE International and the GIS Group of the California Governor's Office of Emergency Services, 1995, *The Northridge Earthquake of January 17, 1994: Report of Data Collection and Analysis, Part A: Damage and Inventory Data*, EQE International, Oakland, CA.

Federal Emergency Management Agency (FEMA), 1997, *NEHRP Guidelines for the Seismic Rehabilitation of Buildings, FEMA 273,* Washington, DC.

Federal Emergency Management Agency (FEMA), 1999, *HAZUS 99,* Washington, DC.

Federal Emergency Management Agency (FEMA), 2000, *FEMA 366, HAZUS99 Estimated Annualized Earthquake Losses for the United States,* Washington, DC, 40 pp.

Folz, B., and A. Filiatrault, 2001, "Cyclic Analysis of Wood Shear Walls", *ASCE Journal of Structural Engineering*, 127(4).

Freeman, J.R., 1932, *Earthquake Damage and Earthquake Insurance,* McGraw-Hill Book Company, Inc., New York, NY, 904 pp.

Hachem, M.M., 2000, *BiSpec Version 1.1.2,* University of California, Berkeley, California.

International Conference of Building Officials, 1964, *Uniform Building Code*, Whittier, CA.

International Conference of Building Officials, 1988, *Uniform Building Code*, Whittier, CA.

International Conference of Building Officials, 1997, *Uniform Code for Building Conservation*, Whittier, California

Ishiyama, Y., 1983, "Motions of Rigid Bodies and Criteria for Overturning by Earthquake Excitation," *Proc., 3rd South Pacific Regional Conference on Earthquake Engineering, Wellington, May 1983*

Isoda, H., B. Folz, and A. Filiatrault, 2001, *Seismic Modeling of Index Woodframe Buildings on Research Task 1.5.4.,* Richmond, California: Consortium of Universities for Research in Earthquake Engineering, 144 pp.

Kircher, C., 1999, *Draft Procedures for Developing HAZUS-Compatible Building-Specific Damage and Loss Functions,* Washington, D.C.: Federal Emergency Management Agency

Kustu, O., 1986, "Earthquake Damage Prediction for Buildings Using Component Test Data," *Proc. Third U.S. National Conference on Earthquake Engineering, Aug 24-28, 1986, Charleston, SC,* El Cerrito, CA: Earthquake Engineering Research Institute, pp. 1493-1504

Kustu, O., D.D. Miller, and S.T. Brokken, 1982, *Development of Damage Functions for Highrise Building Components, San* Francisco: URS/John A Blume & Associates for the US Department of Energy

Leyendecker, E.V., 2001, *Uniform Hazard Response Spectra and Seismic Hazard Curves for the United States,* Denver, CO: U.S. Geological Survey

Mahaney, J.A., T.F. Paret, B.E. Kehoe, *et al.*, 1993, "The Capacity Spectrum Method for Earthquake Response During the Loma Prieta Earthquake," *Proc. 1993 U.S. National Earthquake Conference, Memphis TN, May 2-5, 1993,* Memphis, TN: Central United States Earthquake Consortium, 1993, Volume II, pp. 501-510

Makris, N., and D. Konstantinidis, 2001, *The Rocking Spectrum and the Shortcomings of Design Guidelines,* PEER 2001/07, Richmond, CA: Pacific Earthquake Engineering Research Center, 63 pp.

Maragakis, S., 2002, personal communication.

Martel, R.R., 1964, "Earthquake Damage to Type III Buildings in Long Beach, 1933," *Earthquake Investigations in the Western United States 1931-1964, Publication 41-2,* Washington, DC: U.S. Department of Commerce, Coast and Geodetic Survey.

McClure, F.E., 1973, *Performance of Single-Family Dwellings in the San Fernando Earthquake of February 9, 1971,* U.S. Department of Housing and Urban Development, Washington, DC, 95 pp.

McMullin, K.M., and Merrick, D., 2001, *Seismic Performance of Gypsum Walls – Experimental Test Program, d*Richmond, CA: Consortium of Universities for Research in Earthquake Engineering, 141 pp.

National Institute of Building Sciences and Federal Emergency Management Agency, 1999, *HAZUS Earthquake Loss Estimation Methodology: Technical Manual, I and II,* Washington, DC: Federal Emergency Management Agency

National Institute of Building Sciences and Federal Emergency Management Agency, 1997, *HAZUS Earthquake Loss Estimation Methodology: Technical Manual, Volumes I, II, and III, NIBS Document Number 5201,* Washington, DC: Federal Emergency Management Agency

National Institute of Building Sciences, 2000, http://www.nibs.org/hazus4a.htm.

Osteraas, J., 2002 (expected; in progress), *Evaluation and Repair of Earthquake Damage to Residential Construction*, Consortium of Universities for Research in Earthquake Engineering

Pardoen, G., and A. Waltman, in progress, *CoLA Shearwall Tests,* Irvine, CA: University of California

Porter, K.A. and A.S. Kiremidjian, 2001c, "Verifying Performance-Based Design Objectives Using Assembly-Based Vulnerability" *Structural Safety and Reliability, ICOSSAR 2001, Newport Beach, California, USA, June 17-22 2001,* Lisse, the Netherlands: A.A. Balkema.

Porter, K.A., 2000, *Assembly-Based Vulnerability of Buildings and Its Uses in Seismic Performance Evaluation And Risk-Management Decision-Making, Doctoral Dissertation,* Stanford, CA: Stanford University, 196 pp.

Porter, K.A., A.S. Kiremidjian, and J.S. LeGrue, 2001b, "Assembly-based Vulnerability of Buildings and Its Use in Performance Evaluation," *Earthquake Spectra,* 17 (2), Oakland, CA: Earthquake Engineering Research Institute, 291-312.

Porter, K.A., and A.S. Kiremidjian, 2001a, *Assembly-based Vulnerability and its Uses in Seismic Performance Evaluation and Risk-Management Decision-Making,* Stanford, CA: John A. Blume Earthquake Engineering Center, 214 pp.

Porter, K.A., J.L. Beck, and R.V. Shaikhutdinov, ND, "Sensitivity of Building Loss Estimates to Major Uncertain Variables," submitted to *Earthquake Spectra*, Earthquake Engineering Research Institute, Oakland, CA, March 2002

R.S. Means Co., Inc., 1994, *Means Square Foot Costs,* Kingston, MA, 442 pp.

R.S. Means Co., Inc., 2001, *Assemblies Cost Data,* Kingston, MA, 575 pp.

Scawthorn, C., 1982, "Optimum Seismic Design of Mid-Rise Buildings," *Proceedings of the Seventh European Conference on Earthquake Engineering, Athens, Greece, Sept. 1982,* Vol. 3, 511-520

Scawthorn, C.R., H. Iemura, and Y. Yamada, 1981, "Seismic Damage Estimation for Low- and Mid-rise Buildings in Japan," *Earthquake Engineering and Structural Dynamics, vol. 9,* John Wiley & Sons, 93-115

Schierle, G.G., 2000, *Northridge Earthquake Field Investigations: Statistical Analysis of Woodframe Damage, CUREE Publication No. W-02,* Richmond, CA: Consortium of Universities for Research in Earthquake Engineering

Schmidt., B., J. Kariotis and G. Dick, ND, *Extreme Earthquake Hazard in Certain Wood-framed Residential Structures with Tuck-under Parking*, Draft August 21, 2000, unpublished.

Scholl, R.E., and O. Kustu, 1981, *Procedures and Data Bases for Earthquake Damage Predictions and Risk Assessment,* US Geological Survey Open-File Report 81-437, US Geological Survey, Menlo Park, CA, 248 pp.

Somerville, P., N. Smith, S. Punyamurthula, and S. Sun, 1997, *Development of Ground Motion Time Histories for Phase 2 of the FEMA/SAC Steel Project,* SAC Joint Venture, Background Document Report No. SAC/BD-97/04.

Steinbrugge, K.V., and S.T. Algermissen, 1990, *Earthquake Losses to Single-Family Dwellings: California Experience,* Bulletin 1939, U.S. Geological Survey, Washington, DC

Steinbrugge, K.V., F.E. McClure, and A.J. Snow, 1969, *Studies in Seismicity and Earthquake Damage Statistics*, US Coast and Geodetic Survey, Washington, DC

Structural Engineers Association of California, 1996, *Recommended Lateral Force Requirements and Commentary, Sixth Edition,* Sacramento, California

Sucuoglu, H., and C.V.G. Vallabhan, 1997, "Behavior of Window Glass Panels During Earthquakes," *Engineering Structures* 19(8), Aug. 1997, 685-694.

U.S. Census Bureau, 2000, *American Housing Survey National Tables: 1999*, Washington, D.C., http://www.census.gov/hhes/www/housing/ahs/ahs99/ahs99.html

U.S. Census Bureau, 2002, *State and County QuickFacts,* Washington, D.C., http://quickfacts.census.gov/qfd/states/06000.html

U.S. Coast and Geodetic Survey, 1969, *Studies in Seismicity and Earthquake Damage Statistics,* Washington, D.C.

U.S. Department of Housing and Urban Development, 1994, *Assessment of Damage to Residential Buildings Caused by the Northridge Earthquake,* Washington, DC, 110 pp.

U.S. Geological Survey, 2001a, *TriNet Instrumental Intensity Map for San Fernando Earthquake,* http://www.trinet.org/shake/San_Fernando/intensity.html

U.S. Geological Survey, 2001b, *TriNet Peak Acceleration Map (in %g) for San Fernando Earthquake,* http://www.trinet.org/shake/San_Fernando/intensity.html

Von Neumann, J., and O. Morgenstern, 1944, *Theory of Games and Economic Behavior,* Princeton, NJ: Princeton University Press, 641 pp.

Wald, D.J., V. Quitoriano, T.H. Heaton, and H. Kanamori, 1999, "Relationships between Peak Ground Acceleration, Peak Ground Velocity and Modified Mercalli Intensity in California," *Earthquake Spectra*, 15 (3), Earthquake Engineering Research Institute, Oakland, CA, 557-564

Chapter 9. Glossary

Assembly	A part of a building treated as a single entity for analysis and cost purposes. An example is a wood stud wall with ½-in. gypsum wallboard on two sides, nailed to the studs at 6 in centers with cooler nails.
Cripple wall	A carpenter's term indicating a woodframe wall of less than full height, usually built without bracing.
Critical damping	The level of viscous damping such that free vibration of a structure will cease after one cycle in the fundamental mode of vibration.
Damage	Physical degradation. Also often used interchangeably with reduction in value because of unwanted events. In the earthquake context, damage is typically equated with repair cost.
Damage factor	Cost to repair damage as a fraction of building replacement cost (new).
Damage state	One of several descriptive categories of damage such as slight, moderate, extensive, complete.
Damping	Represents the energy lost in the process of material deformation.
Fault	A zone of the earth's crust within which the two sides have moved. Faults may be hundreds of miles long, and generate earthquakes as deep as 20 miles. Some earthquakes occur at much greater depth, in places where oceanic lithosphere sinks back into the mantle.
FEMA	Federal Emergency Management Agency
Fragility	Probability of an undesirable event as a function of some input excitation. In the context of earthquake damage, typically refers to the probability of a structure or component reaching or exceeding a given damage state as a function of some earthquake response such as acceleration, deformation, or force.
HAZUS	A standardized, nationally applicable earthquake loss estimation methodology, implemented through PC-based geographic information system (GIS) software. (Developed by NIBS and funded by FEMA.)
IBV	Index-building variant. Each index building was modeled here several ways, with IBVs representing poor-quality construction, typical quality, and superior quality, and with seismic retrofit or redesign measures.

Index building	Basic building type. Four were used for analysis in this study: the small house, the large house, the townhouse, and the apartment building.
Intensity	A measure of the effect, or the strength, of an earthquake hazard at a specific location, commonly measured on qualitative scales such as MMI, MSK and JMA. Some researchers also refer to instrumental intensity, based on quantitative measurements such as peak ground acceleration, spectral acceleration, etc.
Lateral force-resisting system	A structural system for resisting horizontal forces that result, for example, from earthquake or wind (as opposed to the vertical force-resisting system, which supports self-weight, contents, and other superimposed weights).
Magnitude	A unique measure of an individual earthquake's release of strain energy, measured on a variety of scales, of which the moment magnitude Mw (derived from seismic moment) is often preferred.
Modified Mercalli Intensity (MMI)	A I-to-XII scale that qualitatively describes earthquake effects at a particular site, based on apparent effects.
NIBS	National Institute of Building Sciences
Peak ground acceleration (PGA)	The maximum amplitude of recorded acceleration (also termed the ZPA, or zero period acceleration)
Peak horizontal acceleration (PHA)	The maximum amplitude of recorded acceleration in the horizontal plane
Pounding	The collision of adjacent buildings during an earthquake because of insufficient lateral clearance.
Response spectrum	A plot of maximum amplitudes (acceleration, velocity or displacement) of a single degree of freedom (SDOF) oscillator, as the natural period of the oscillator is varied across a spectrum of engineering interest. (Typically calculated for natural periods from 0.03 to 3.0 or more sec., or frequencies of 0.3 to 30+ Hz).
Seismic hazards	The phenomena or expectation of an earthquake-related agent of damage, such as fault rupture, vibratory ground motion (i.e., shaking), inundation (e.g., tsunami, seiche, dam failure), various kinds of permanent ground failure (e.g. liquefaction), fire or hazardous materials release. "Seismic hazard" is often used to refer only to ground shaking.
Seismic risk	The relationship between various levels of loss and the probability of those loss levels.

Shaking severity	As used here a generic term to refer to a measure of shaking at a particular site.
Simulation	Mathematical modeling of a stochastic process via repeated trials in which selected variables are treated probabilistically. A common form of simulation is *Monte Carlo simulation*.
Soft story	A story of a building significantly less stiff than adjacent stories. That is, the lateral stiffness is 70% or less than that in the story above, or less than 80% of the average stiffness of the three stories above (Structural Engineers Association of California, 1996).
Spectrum amplification factor	The ratio of a response spectral parameter (acceleration, velocity or displacement) to the corresponding ground motion parameter.
Spectral acceleration	An instrumental measure of shaking severity at a particular site. Technically and as used here, it is the peak value of absolute acceleration experienced by a single-degree-of-freedom, linear elastic, viscously damped oscillator, when subjected to a particular acceleration time-history.
Stochastic	Involving chance or probability.
Taxonomy	A categorization system.
Uniform hazard spectra	Response spectra with the attribute that the probability of exceedance is the same at all spectral frequencies.
Vulnerability	The amount of damage or loss given a specified value of a hazard parameter.
Vulnerability function	Damage or loss as a function of earthquake shaking severity, typically given in the form of a curve or table.
Waist wall	A spandrel, i.e., a short wall above and below windows and doors, or alternatively “waste wall,” in reference to the scrap materials used as sheathing.